**Project No. 037005**

# CECILIA

**Central and Eastern Europe Climate Change Impact and Vulnerability Assessment**

Specific targeted research project

1.1.6.3.I.3.2: Climate change impacts in central-eastern Europe

# D 5.4: The evaluation of climate change impacts on simulated monthly river flow and the description, sensitivity analysis and uncertainty analysis of the „atmosphere-river network-reservoir" modelling system for hydrology and water quality simulations

Due date of deliverable: 1$^{st}$ December 2007

Actual submission date: 20$^{th}$ December 2009

Start date of project: 1$^{st}$ June 2006                    Duration: 36 months

Lead contractor for this deliverable: **Institute of Atmospheric Physics, Prague, Czech Republic (IAF)**

| Project co-funded by the European Commission within the Sixth Framework Programme (2002-2006) | | |
|---|---|---|
| Dissemination Level | | |
| **PU** | Public | X |
| **PP** | Restricted to other programme participants (including the Commission Services) | |
| **RE** | Restricted to a group specified by the consortium (including the Commission Services) | |
| **CO** | Confidential, only for members of the consortium (including the Commission Services) | |

CONTENTS

# Part A
# Impacts of climate change on simulated monthly river flow along a Bohemia/Moravia/Slovakia/Romania geographic gradient

## 1. Introduction

The first part of this deliverable provide the research of WP5 partners (IAP, CHMI, FRI and NIHWM) with the aim to evaluate impacts of the predicted climate change on the hydrology in selected catchments of the Czech Republic, Slovakia and Romania (Fig. 1.1). The modelling was accomplished with the previously calibrated models, *i.e.* HSPF, BILAN, KVKH, and WATBAL at the Vltava, Dyje, Hron, and Buzău/Ialomiţa basins, respectively (see CECILIA Project Deliverables D5.2 and D5.3).
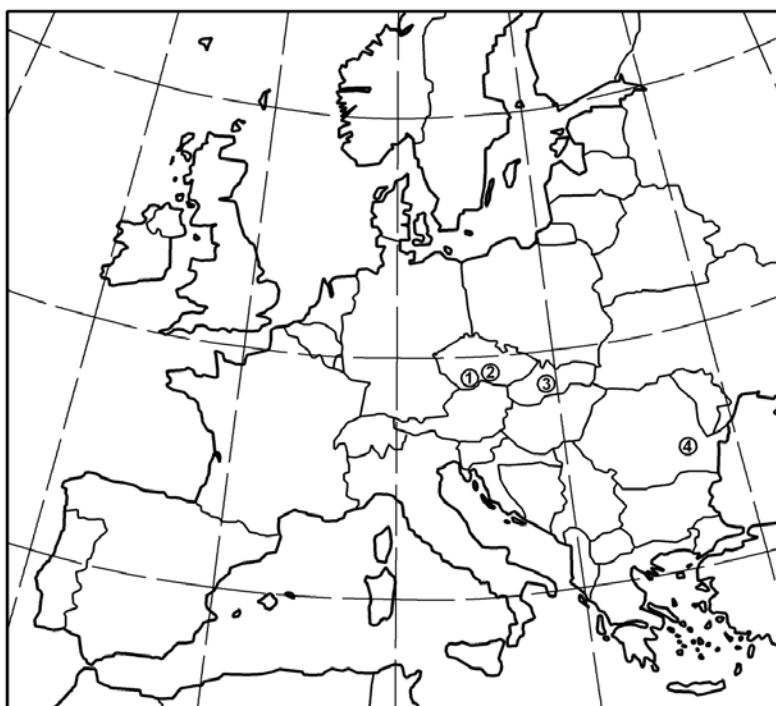


*Figure 1.1. A situation drawing with position of basins included impacts studies of climate change on stream hydrology: 1 – Vltava, 2 – Dyje, 3 – Hron, 4 – Buzău/Ialomiţa*

The scenarios of climate change were developed using the pattern scaling techniques from (i) outputs of 3 global climate models (GCMs) together with representative scenarios for the development of emissions of greenhouse gases and aerosols and for a range of the climatic sensitivity to the emissions and (ii) outputs of 2 regional models with high spatial resolution, i.e., ALADINE (10 km grid) and RegCM (25 km grid).

## 2. Climate change scenarios

*2.1 Methods*

The site-specific scenarios of GCM-based climate change were prepared using the pattern scaling method described in Dubrovsky et al. (2005). In this method, the standardised scenario, that relates the climate variable responses to a 1°C rise in global mean temperature ($T_G$), is multiplied by the predicted change ($\Delta T_G$). The standardised scenarios were determined from GCM runs and $\Delta T_G$ values that were calculated by the simple climate model MAGICC (Harvey et al. 1997, Hulme et al. 2000) for 3 combinations of conditions that were selected from representative emission scenarios and climatic sensitivities.

The climate change scenarios were based on the transient simulations with three GCMs (Tab. 2.1.) available from the IPCC-DDC (http://ipcc-ddc.cru.uea.ac.uk) at the beginning of 2001. The following variables were used from the GCM outputs in a daily step: daily mean temperature (*TAVG*), minimum and maximum daily temperatures, precipitation (*PREC*), solar radiation (*SRAD*), vapour pressure (*VAPO*), and wind speed (*WIND*). Since *SRAD* was not available from HadCM, cloudiness was used as a surrogate for determining changes in solar radiation. The data from the GCM runs were geographically interpolated to the central points of the target basin areas, *i.e.* the Vltava basin (14.467 E; 49.180 N), the Dyje basin (16.083 E; 49.133 N), the Hron basin (19.300 E; 48.717 N), and the Buzău/Ialomiţa basins (26.717 E; 45.96 N).

*Table 2.1. GCM simulations used in the determination of standardised scenarios (according to Dubrovsky et al. 2005)*

| Model | Acronym | Atmospheric resolution | Emission scenario |
|-------|---------|-----------------------|-------------------|
| ECHAM4/OPYC3 | ECHAM | 2.8×2.8° | 1860–1989: historic CO2; 1990–2099: IS92a |
| HadCM2 | HadCM | 2.5×3.75° | 1860–1989: historic CO2; 1990–2099: 1% compound increase |
| NCAR DOE-PCM | NCAR | 2.8×2.8° | Until 1999: historic CO2; 2000–2099: 'business as usual' scenario (~IS92a) |

The emission scenarios SRES A1, A2, B1, and B2 from the IPCC Third Assessment Report (IPCC 2001) were used in the estimation of future global temperature increase together with the most likely range of the values for the climate sensitivity factor, *i.e.* an increase of global temperature by 1.5–4.5 °C per a doubling of the atmospheric $CO_2$ concentration (IPCC 2001). To reduce the number of scenarios for the hydrology modelling, the values of global temperature increase for the used emission scenarios were compared for the low, middle, and high estimates of the climate sensitivity factor and 3 scenarios, i.e. the most optimistic, middle, and most pessimistic, were selected for the requested time instants (Tab. 2.2)

*Table 2.2. The increase of global temperature (relative to the period 1971–2000) corresponding to three values of climate sensitivity factor (low/mid/high: 1.5, 2.5, 4.5 K) and to four major emission scenarios (SRES-A1, -A2, -B1, -B2). The lowest line (Selection) gives the low (optimistic), middle, and high (pessimistic) estimate of the $\Delta T_G$.*

| Time instant | 2025 | 2050 | 2100 |
|---|---|---|---|
| Climate sensitivity factor | low / middle / high | low / middle / high | low / middle / high |
| Emission scenarios: SRES-A1 | 0.60 / 0.85 / 1.17 | 1.02 / 1.47 / 2.07 | 1.49 / 2.21 / 3.24 |
| SRES-A2 | 0.56 / 0.80 / 1.10 | 1.03 / 1.48 / 2.08 | 2.06 / 3.00 / 4.29 |
| SRES-B1 | 0.49 / 0.70 / 0.98 | 0.76 / 1.11 / 1.57 | 1.17 / 1.74 / 2.57 |
| SRES-B2 | 0.53 / 0.75 / 1.05 | 0.84 / 1.22 / 1.73 | 1.33 / 1.97 / 2.88 |
| **Selection** | **0.49 / 0.78 / 1.17** | **0.76 / 1.35 / 2.08** | **1.17 / 2.09 / 4.29** |

High-resolution regional climate modelling projections were developed using the pattern scaling techniques from the outputs of 2 regional models of different spatial resolution, i.e., ALADINE (10 km grid) and RegCM (25 km grid), that are both using the A1B scenario for the development of emissions of greenhouse gases and aerosols.

*2.2 Predicted climate change at target basins*

The predicted mean ± optimistic/pessimistic changes in temperature, precipitation, solar radiation, and wind speed with three GCMs in 2025, 2050, and 2100 are in Fig. 2.1; the seasonal changes for the 2050 period are shown in Fig. 2.2.

A temperature increase was predicted by all models in all target basins with mean increments of 0.7–1.0°C, 1.3-2.1°C, and 2–3°C in 2025, 2050, and 2100, respectively. The optimistic predictions were lower by ~50 % than these mean values but the pessimistic predictions were higher by up to ~100 %. There was a consistent increase in temperature change along the geographic transect from the Vltava to Buzău/Ialomița basins in all three models (Fig. 2.1). The seasonal pattern of temperature changes (Fig. 2.2) were characterised by higher temperature increases in summer and autumn months compared to winter and spring months. The results of ECHAM and HadCM were mutually comparable; the results of NCAR showed slightly lower temperature increases (by ca 25 %) than the other two models.

The long-term precipitation amounts decreased in all model predictions except for the NCAR outputs at the Czech basins (Vltava and Dyje), where a slight increase (up to 1.5 %) was obtained (Fig. 2.1). There was a consistent decreasing trend in precipitation depths from the Vltava to Buzău/Ialomița basins. Larger differences among the models could be seen in the seasonal distribution of precipitation (Fig. 2.2). The ECHAM outputs predicted minimum seasonal changes but the HadCM and NCAR results indicated an increased precipitation activity in winter and spring and precipitation deficits in summer and autumn.

The solar radiation change showed almost a mirror pattern compared to the precipitation both in the long-term averages and the seasonality.

The predicted wind speed changes were relatively small and differed among the models. The ECHAM outputs showed a decrease in wind speed, especially in summer months. The HadCM

and NCAR outputs indicated similarly positive long-term changes but differed in seasonal patterns (cf. Figs. 2.1 and 2.2).
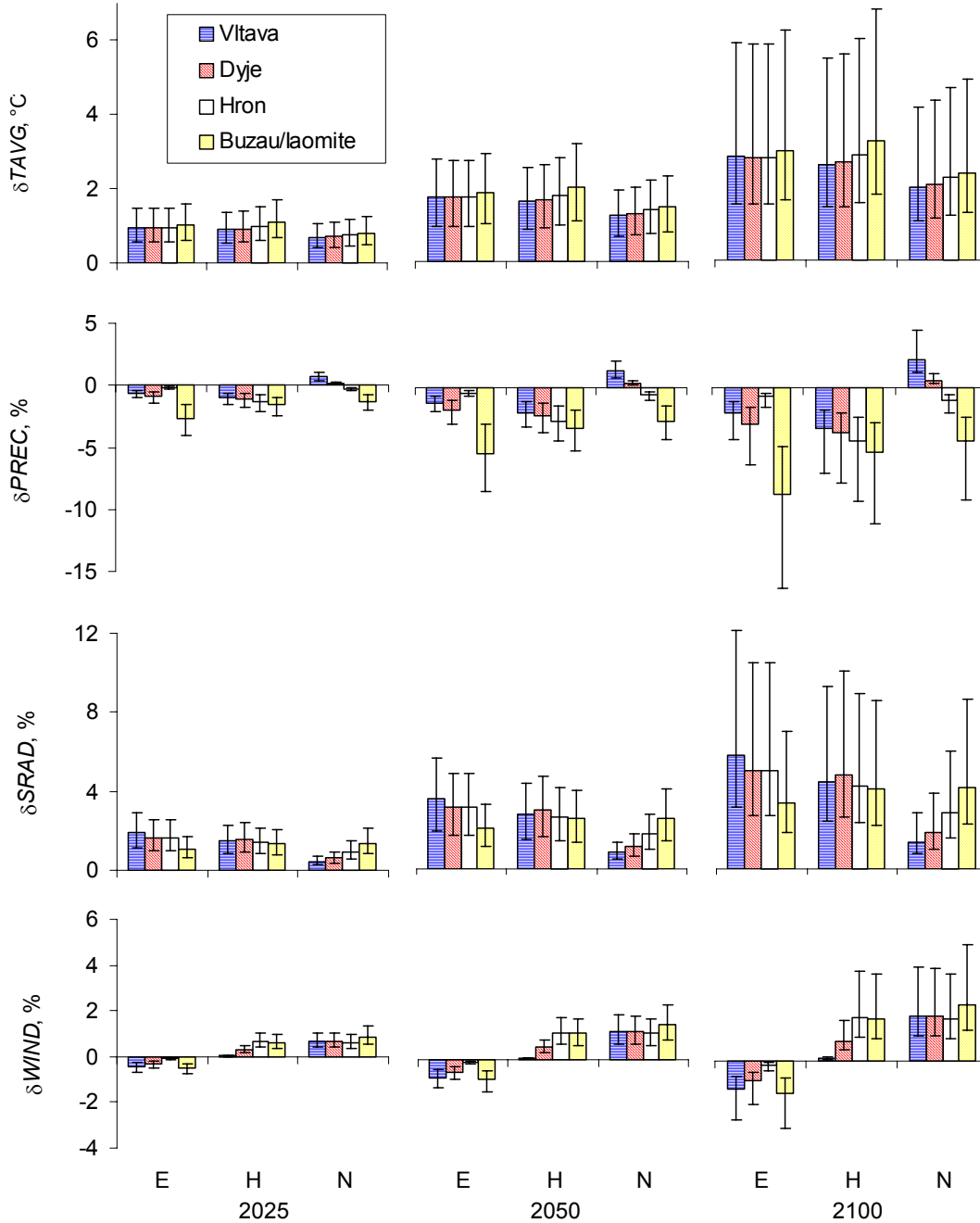


*Figure 2.1. Mean changes of temperature, precipitation, solar radiation and wind speed that were simulated by three GCMs (E – ECHAM, H – HadCM, N –NCAR) for middle ± optimistic/ pessimistic (vertical lines) climate change scenarios at the target river basins (Vltava, Dyje, Hron, Buzău/Ialomiţa) in three time periods (2025, 2050, 2100) compared to 1971-2000*
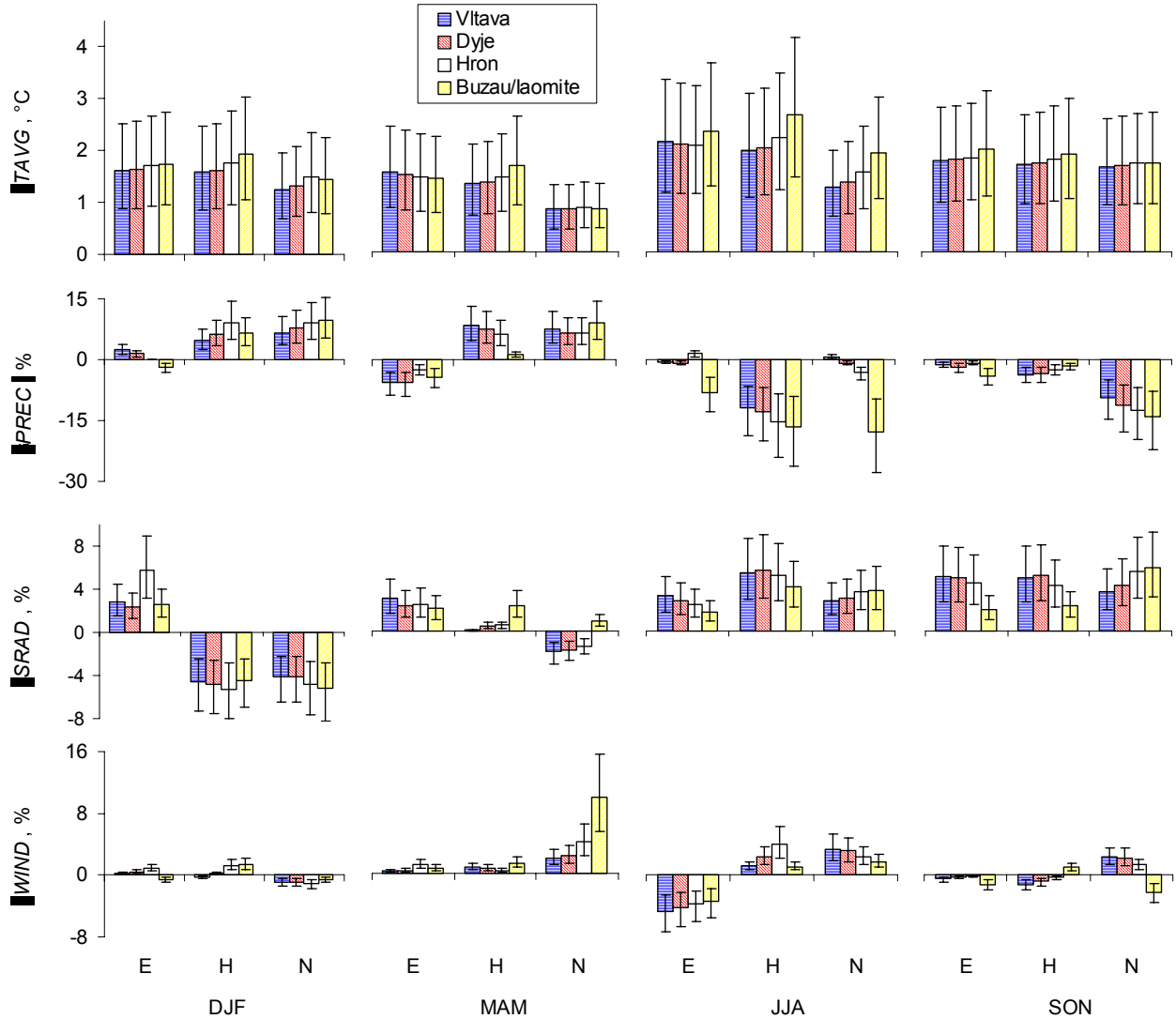
*Figure 2.2. Seasonal changes of temperature, precipitation, solar radiation and wind speed simulated by three GCMs (E – ECHAM, H – HadCM, N –NCAR) for middle ± optimistic/ pessimistic (vertical lines) climate change scenarios at the target river basins (Vltava, Dyje, Hron, Buzău/Ialomiţa) in four time periods (DJF – December to February, MAM – March to May, JJA – June to August, SON – September to November) in 2050 compared with measured data from 1971-2000*

The above-described trends in meteorological variables indicate a possibility of substantial impacts on river hydrology. The largest effects might occur especially in summer and autumn periods when increased temperatures go congruently with increased solar radiation and decreased precipitation, which can result in significant decrease in stream flow. The increases in precipitation and temperature in the winter/spring period can slightly increase stream flow and modify the timing of snowmelt runoff events, however, as precipitation in Central and Eastern Europe is typical with a seasonal minimum in winter, the increase of relative amounts of

precipitation in this period would have much less positive effect on stream flow than would be the negative effect of numerically comparable values of precipitation in summer months.

The high-resolution regional climate modelling projections derived from the ALADIN and RegCM models showed an increased temperature with mean increments of 0.8–1.5 °C and 2.8–3.1 °C in the 2021–2050 and 2071–2100 periods, respectively. There was a consistent increase in the temperature change along the geographic transect from the Vltava to Buzău/Ialomița basins in the regional climate model outputs, similarly to the results obtained previously with the outputs of GCMs. Seasonal pattern of temperature changes featured higher temperature increases in the summer and autumn months than in the winter and spring months. The precipitation amounts decreased in most model predictions except for the RegCM outputs at the Czech river basins, where a slight increase was predicted for the far future period of 2071–2100. A decreasing trend in precipitation depths could be noticed from the Vltava towards the Buzău/Ialomița basins. Notable differences existed between the two regional models in the seasonal distribution of precipitation. The ALADIN outputs predicted small seasonal changes in the near future period of 2021–2050 and a significant drop in summer precipitation activity in the far future period of 2071–2100 by contrast to the RegCM outputs that had an increased precipitation activity in winter and spring months but deficits in the summer and autumn.

*2.3 References*

Dubrovsky M., Nemesova I., Kalvova J. (2005): Uncertainties in climate change scenarios for the Czech Republic. Climate Research, 29, 139–156.

Harvey L. D. D., Gregory J., Hoffert M., Jain A. and 5 others (1997): An introduction to simple climate models used in the IPCC Second Assessment Report. IPCC Tech Paper 2, Intergovernmental Panel on Climate Change, Geneva.

Hulme M., Wigley T. M. L., Barrow E. M., Raper S. C..B., Centella A., Smith S., Chipanshi A. C. (2000): Using a climate scenario generator for vulnerability and adaptation assessments: MAGICC and SCENGEN Version 2.4 Workbook. Climatic Research Unit, Norwich.

IPCC (2001): Climate Change 2001: The Scientific Basis. Contribution of Working Group I to the Third Assessment Report of the Intergovernmental Panel on Climate Change [Houghton, J.T.,Y. Ding, D.J. Griggs, M. Noguer, P.J. van der Linden, X. Dai, K. Maskell, and C.A. Johnson (eds.)]. Cambridge University Press, Cambridge, United Kingdom and New York, NY, USA, 881 pp.

## 3. The Vltava River basin

*3.1 Introduction and methods*

The anticipated impacts of GCM-based climate change projections on river flow in the Vltava basin were evaluated for three different profiles with the aim to describe the development of hydrological conditions from the upper parts of the basin towards the lowlands (Fig. 3.1). The Římov and Hluboká n/V. stations represented mountainous and highland region with by ca 150 m higher mean altitude, 6% higher precipitation depth, and 30% higher runoff compared to the whole Vltava basin with the closing profile at Vrané n/V. For main characteristics of respective catchments see Tab. 3.1.
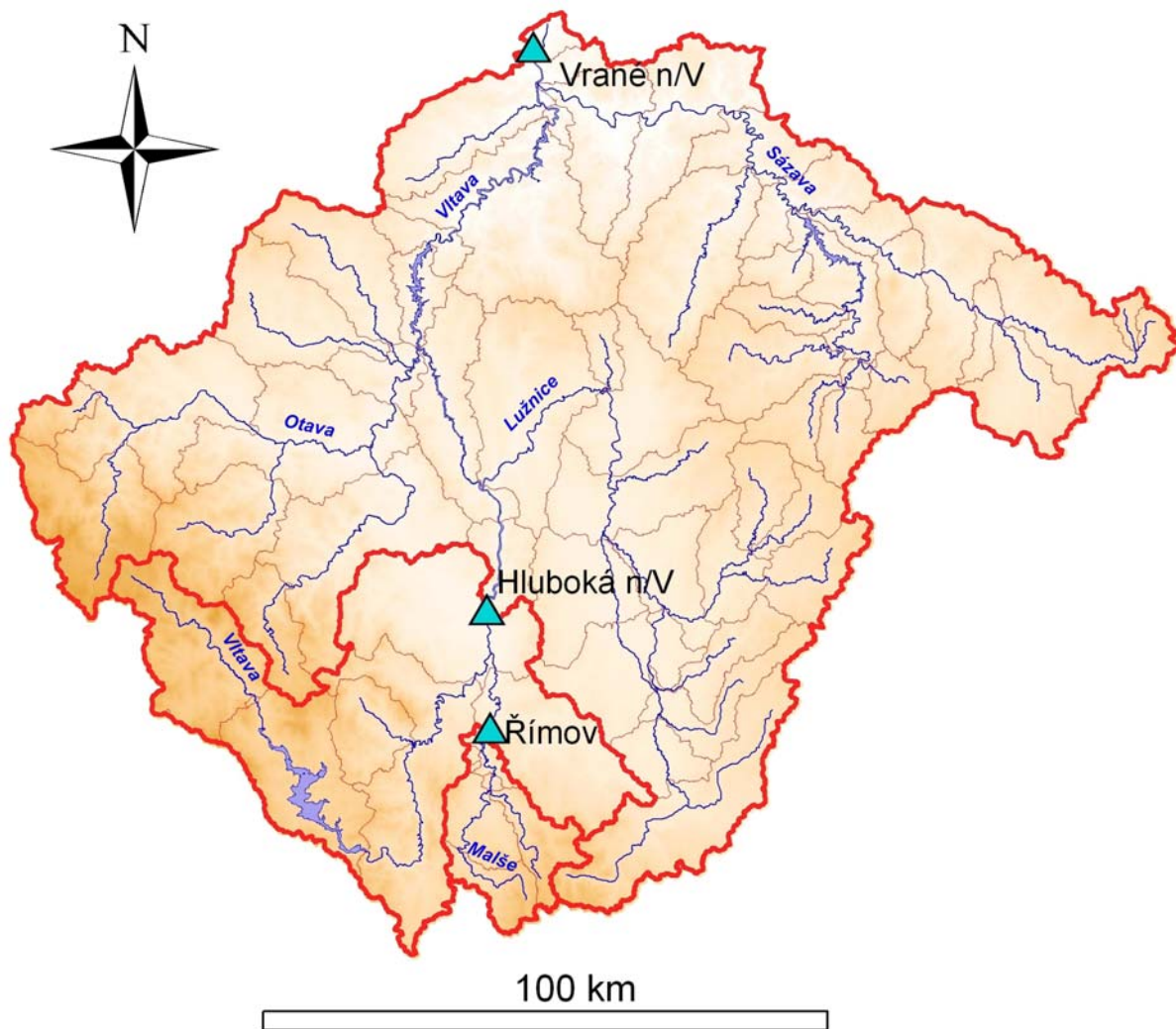


*Figure 3.1. The upper part of the Vltava basin with its main rivers and profiles employed in the predictions of climate change on river flow (blue triangles). Thin brown lines delineate subcatchmens that were used as basic units in the HPSF modelling of flow.*

*Table 3.1. Main characteristics of subcatchments in the Vltava basin used in the climate-change scenario-modelling study*

| Characteristic | Římov | Hluboká n/V. | Vrané n/V. |
|---|---|---|---|
| Catchment area, km$^2$ | 488 | 3395 | 17,780 |
| Altitude, m a.s.l.* | 713 (430-1,111) | 678 (365-1,372) | 553 (188-1,372) |
| Precipitation 1971-2000, mm/yr | 702 | 695 | 658 |
| Runoff, mm/year | 269 | 261 | 184 |
| Runoff coefficient | 0.38 | 0.38 | 0.28 |

\* Average values with a minimum-maximum range in parenthesis

The hydrology of Vltava basin was simulated with the HSPF model (Bicknell et al. 2001) that was run with a daily time step. The model setup and calibration with data from a 1961-2004 period is described in detail in a previous CECILIA project report (Deliverable D5.2). The efficiency of model in the simulations of river flow at the evaluated profiles during in the 1971-2000 period is showed in Fig. 3.2, Tab. 3.2, and Tab. 3.3. The agreement between the simulated and observed values was acceptable in all profiles with differences that were approximately evenly distributed along the seasonal course. The values of mean error (Table 3.3) ranged between -7 % at Římov station and +2 % at Vrané n/V. station. Mean error was typically zero in calibration periods that, however, varied in length at different stations within a range between 9 and 44 years according to the availability of data. The Nash-Sutcliffe coefficient ranged between 0.68 and 0.76 (Tab. 3.3), which is slightly better than the range obtained for the whole calibration period 1961-2004 (i.e. 0.51 to 0.77; Deliverable D5.2).
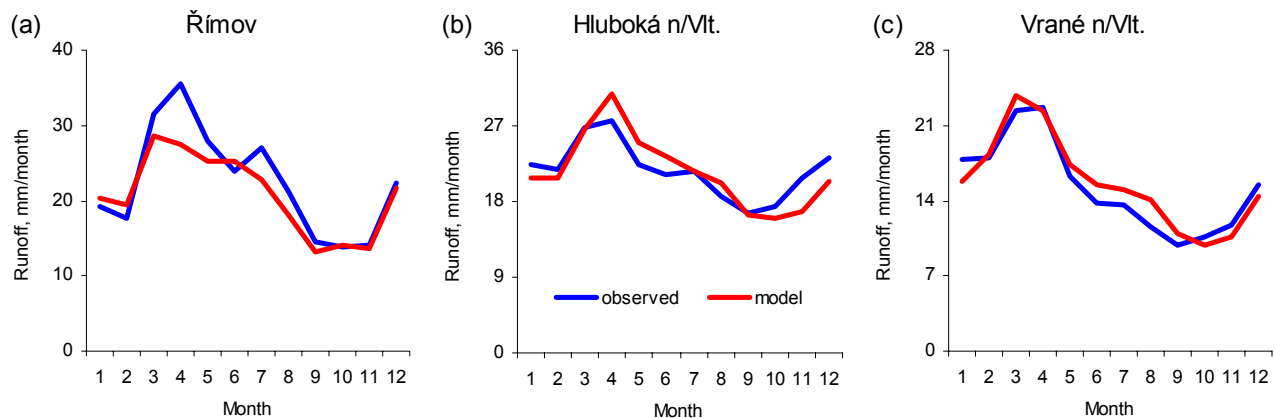


*Figure 3.2. Comparison of monthly mean observed and simulated runoff values at stations Římov (a), Hluboká n/V. (b), and Vrané n/V. (d) during the period of 1971-2000 that were used in the scenario modelling study of climate change impacts on river flow*

*Table 3.2. Results of calibration the HSPF model: the comparison of monthly mean observed and modelled runoff values in the subcatchments of the Vltava basin during 1971-2000. (The deviation between observed and modelled runoff was calculated by equation: dev.=100\*(RM-R)/R [%], where R is observed runoff and RM is modelled runoff.)*

| Month | Římov | | | Hluboká n/V. | | | Vrané n/V. | | |
|---|---|---|---|---|---|---|---|---|---|
| | runoff, mm | | dev., % | runoff, mm | | dev., % | runoff, mm | | dev., % |
| | observed | model | | observed | model | | observed | model | |
| 1 | 19.2 | 20.1 | 6.2 | 22.4 | 20.8 | -7.1 | 17.8 | 15.8 | -11.0 |
| 2 | 17.6 | 20.9 | 9.8 | 21.8 | 20.8 | -4.7 | 18.1 | 18.3 | 1.3 |
| 3 | 31.6 | 28.1 | -9.8 | 26.9 | 26.6 | -1.0 | 22.3 | 23.7 | 6.3 |
| 4 | 35.5 | 28.0 | -22.5 | 27.7 | 30.9 | 11.6 | 22.7 | 22.3 | -1.6 |
| 5 | 28.0 | 24.9 | -9.4 | 22.3 | 25.0 | 11.9 | 16.3 | 17.4 | 7.2 |
| 6 | 23.8 | 25.6 | 5.5 | 21.2 | 23.4 | 10.6 | 13.8 | 15.4 | 12.0 |
| 7 | 27.1 | 22.4 | -16.1 | 21.5 | 21.6 | 0.2 | 13.6 | 15.0 | 10.6 |
| 8 | 21.3 | 17.9 | -14.9 | 18.7 | 20.2 | 8.3 | 11.5 | 14.1 | 22.6 |
| 9 | 14.5 | 13.4 | -9.5 | 16.7 | 16.5 | -1.2 | 9.9 | 10.9 | 11.0 |
| 10 | 13.9 | 13.8 | 0.4 | 17.5 | 15.9 | -9.0 | 10.7 | 9.9 | -7.5 |
| 11 | 14.2 | 13.9 | -3.6 | 20.8 | 16.8 | -19.2 | 11.8 | 10.6 | -9.7 |
| 12 | 22.3 | 21.3 | -3.0 | 23.1 | 20.4 | -11.9 | 15.5 | 14.4 | -7.1 |

*Table 3.3. Statistics of differences between monthly mean observed and modelled runoff values in subcatchments of the Vltava basin during 1971-2000. R - observed runoff, RM - modelled runoff, ME - mean error, MAE - mean absolute error, RMSE - root mean squared error, NS - Nash-Sutcliffe's Model Efficiency (Nash, Sutcliffe 1970)*

| Profile | R, mm/month | RM, mm/month | ME, mm/month | MAE, mm/month | RMSE, mm/month | NS |
|---|---|---|---|---|---|---|
| Římov | 22.4 | 20.8 | -1.6 | 5.4 | 7.9 | 0.76 |
| Hluboká n/V. | 21.7 | 21.6 | -0.1 | 4.1 | 5.8 | 0.68 |
| Vrané n/V. | 15.3 | 15.7 | 0.4 | 3.1 | 4.8 | 0.76 |

The calibrated HSPF model was used for simulation of runoff in the Vltava basin with boundary conditions changed according to the scenarios of climate change described in Chapter 2. The procedure included: (i) simulation of the reference runoff using original input climate data from the period of 1971−2000; (ii) modification of the input climate data series from the reference period (precipitation, air temperature, and potential evapotranspiration) according to the climate change scenarios for the middle, pessimistic, and optimistic prediction of climate change with the ECHAM, HadCM, and NCAR model outputs and for the time horizons of 2025, 2050 and 2100 or with the ALADIN and RegCM model outputs for the periods of 2021–2050 and 2071–2100; (iii) simulation of the runoff series with the changed input data series and the parameters of the HSPF model from the calibration; (iv) comparison of differences between the average and seasonal runoff distribution for the individual scenarios and time horizons.

## 3.2 Scenario modelling

The simulation results of the development of precipitation, potential evapotranspiration, runoff and runoff coefficient in the Vltava basin during the 21st century according to the GCM-predicted climate change are given in Fig. 3.3 and Tab. 3.4.



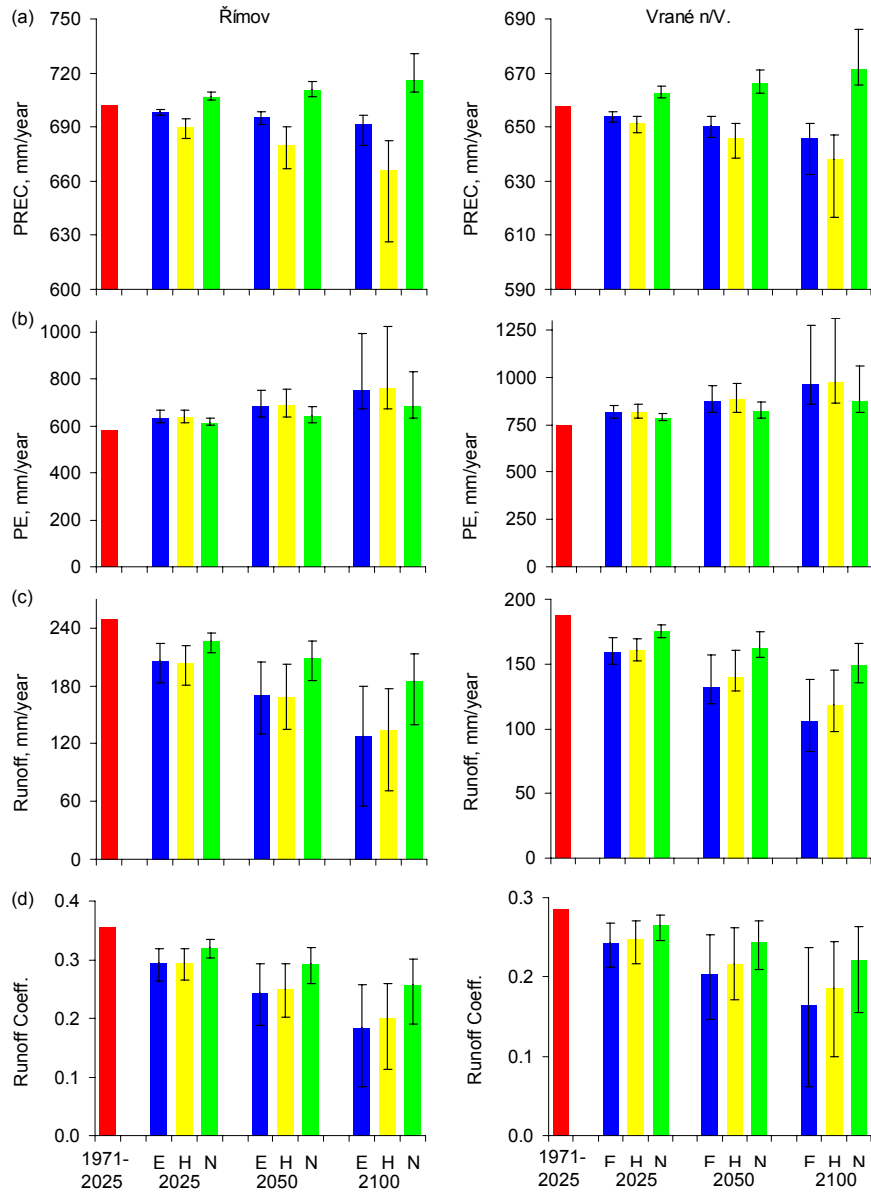*Figure 3.3. Comparison of precipitation (PREC), potential evapotranspiration (PE), runoff (R), and runoff coefficient (RC = R/PREC) in the reference period 1971-2000 and in the future time horizons for the climate change scenarios at two river profiles of the Vltava basin. GCMs: E - ECHAM, H - HadCM, N – NCAR; vertical lines show uncertainty of prediction for middle ± optimistic/ pessimistic climate change scenarios*

10

*Table 3.4. Precipitation (PREC), potential evapotranspiration (PE), runoff (R) and runoff coefficient (RC = R/PREC) in the scenario simulations of effects of climate change for three river profiles of the Vltava basin. GCMs: E - ECHAM, H - HadCM, N - NCAR.*

| Quantity | 1971-2000 | Type of change | Scenario simulation | | | | | | | | |
|---|---|---|---|---|---|---|---|---|---|---|---|
| | | | 2025 | | | 2050 | | | 2100 | | |
| | | | E | H | N | E | H | N | E | H | N |
| *Římov:* | | | | | | | | | | | |
| PREC, mm/yr | 702 | middle | 699 | 690 | 707 | 696 | 680 | 711 | 692 | 666 | 716 |
| | | low | 700 | 695 | 705 | 699 | 690 | 707 | 696 | 682 | 710 |
| | | high | 697 | 684 | 709 | 692 | 667 | 716 | 680 | 626 | 731 |
| PE, mm/yr | 584 | middle | 636 | 638 | 615 | 685 | 689 | 644 | 754 | 763 | 685 |
| | | low | 615 | 616 | 603 | 637 | 639 | 615 | 671 | 675 | 636 |
| | | high | 666 | 670 | 633 | 750 | 759 | 683 | 997 | 1026 | 830 |
| R, mm/yr | 250 | middle | 206 | 204 | 227 | 170 | 169 | 208 | 128 | 134 | 184 |
| | | low | 224 | 222 | 235 | 205 | 203 | 227 | 180 | 177 | 213 |
| | | high | 184 | 181 | 215 | 130 | 135 | 186 | 56 | 71 | 139 |
| RC | 0.36 | middle | 0.29 | 0.29 | 0.32 | 0.24 | 0.25 | 0.29 | 0.18 | 0.20 | 0.26 |
| | | low | 0.32 | 0.32 | 0.33 | 0.29 | 0.29 | 0.32 | 0.26 | 0.26 | 0.30 |
| | | high | 0.26 | 0.27 | 0.30 | 0.19 | 0.20 | 0.26 | 0.08 | 0.11 | 0.19 |
| *Hluboká n/V.:* | | | | | | | | | | | |
| PREC, mm/yr | 695 | middle | 691 | 688 | 700 | 687 | 682 | 704 | 682 | 674 | 709 |
| | | low | 692 | 691 | 698 | 691 | 688 | 700 | 688 | 684 | 703 |
| | | high | 688 | 684 | 702 | 683 | 675 | 709 | 668 | 651 | 725 |
| PE, mm/yr | 606 | middle | 660 | 662 | 638 | 710 | 715 | 668 | 783 | 791 | 711 |
| | | low | 638 | 639 | 625 | 661 | 663 | 639 | 697 | 701 | 660 |
| | | high | 691 | 695 | 657 | 779 | 787 | 708 | 1035 | 1064 | 861 |
| R, mm/yr | 259 | middle | 233 | 240 | 254 | 200 | 215 | 238 | 163 | 188 | 219 |
| | | low | 248 | 242 | 260 | 232 | 239 | 253 | 208 | 221 | 242 |
| | | high | 212 | 220 | 244 | 165 | 189 | 220 | 92 | 127 | 181 |
| RC | 0.37 | middle | 0.34 | 0.35 | 0.36 | 0.29 | 0.32 | 0.34 | 0.24 | 0.28 | 0.31 |
| | | low | 0.36 | 0.35 | 0.37 | 0.34 | 0.35 | 0.36 | 0.30 | 0.32 | 0.34 |
| | | high | 0.31 | 0.32 | 0.35 | 0.24 | 0.28 | 0.31 | 0.14 | 0.20 | 0.25 |
| *Vrané n/V.* | | | | | | | | | | | |
| PREC, mm/yr | 658 | middle | 654 | 651 | 663 | 650 | 646 | 666 | 646 | 638 | 671 |
| | | low | 656 | 654 | 661 | 654 | 651 | 663 | 651 | 647 | 665 |
| | | high | 652 | 648 | 665 | 646 | 639 | 671 | 633 | 616 | 686 |
| PE, mm/yr | 746 | middle | 813 | 815 | 786 | 875 | 881 | 823 | 964 | 975 | 875 |
| | | low | 786 | 788 | 770 | 814 | 817 | 787 | 858 | 863 | 813 |
| | | high | 852 | 856 | 809 | 959 | 970 | 872 | 1275 | 1311 | 1061 |
| R, mm/yr | 188 | middle | 159 | 161 | 175 | 132 | 140 | 163 | 106 | 119 | 149 |
| | | low | 170 | 169 | 180 | 157 | 160 | 175 | 138 | 145 | 166 |
| | | high | 141 | 146 | 167 | 108 | 119 | 149 | 62 | 79 | 124 |
| RC | 0.29 | middle | 0.24 | 0.25 | 0.26 | 0.20 | 0.22 | 0.24 | 0.16 | 0.19 | 0.22 |
| | | low | 0.26 | 0.26 | 0.27 | 0.24 | 0.25 | 0.26 | 0.21 | 0.22 | 0.25 |
| | | high | 0.22 | 0.22 | 0.25 | 0.17 | 0.19 | 0.22 | 0.10 | 0.13 | 0.18 |

A monotonous, approximately linear decrease of runoff with time between the reference period 1971-2000 and the end of the 21$^{st}$ century was predicted for all GCMs and at all stations (Fig. 3.3c, Tab. 3.4). The slopes of the runoff decrease rates with time differed both among the GCMs and the stations. The ECHAM and HadCM model outputs gave approximately two times larger runoff decreases than the NCAR modelling output did. For example, the ECHAM and HadCM decreases in 2100 for the middle scenarios were on average 32-48 % while the comparable NCAR decreases were on average 15-26 %. The largest and smallest responsiveness of runoff upon the climate change were obtained at the Římov and Hluboká n/V. stations, respectively, whereas intermediate values were obtained for the closing profile of the whole Vltava basin at Vrané n/V.

The runoff coefficient decreased in a close correlation to runoff, which reflects the fact that the increase in temperature and evapotranspiration was the main cause of the runoff decreases while the precipitation changes were relatively little and of a less importance. Most of the runoff variability could be explained by the differences among the GCMs in potential evapotranspiration (cf. Figs. 3.3c vs. Figs. 3.3b). The highest increase of potential evapotranspiration was predicted by the ECHAM and HadCM modelling outputs, which, together with the decrease in precipitation, explains coherently the reason for the runoff decrease in comparison with the NCAR modelling outputs that were characterised by a lesser increase in potential evaporation together with a slight absolute increase in precipitation.

The seasonal patterns of runoff are summarised for all stations and GCMs in Fig. 3.4 and the data are given in Tabs. 3.5-3.10. The climate change impacts on flow conditions were seasonally different. In the winter and spring period, only a small decrease or, eventually, an increase in runoff was predicted in contrast to the summer and autumn period when a significant drop was modelled.

The ECHAM predictions of winter and spring runoff were most adverse among of the GCMs outputs, which was apparently caused by a tiny increase in precipitation in winter but a substantial decrease in precipitation in spring (compared to the reference period 1971-2000) in this model. The HadCM and NCAR model scenarios had increased precipitation amounts in winter and spring (Fig. 2.2) but an increased runoff occurred only at the Hluboká n/V and mostly only in the closest perspective (2025). The summer and autumn runoff predictions were lowest in the case of the HadCM scenarios that featured a combination of high temperature increase together with the lowest precipitation prediction from all three models. The agreement of the three GCMs in the runoff predictions was better in the summer to autumn than in the winter to spring periods.

In addition to the general drop in runoff, the predicted climate change induced also amplification in the seasonal fluctuation of flow. This seasonal flow inequality can be expressed as the coefficient of variation (CV; the ratio of standard deviation and mean) calculated from average monthly runoff values. For the middle scenarios in all GCMs and all three profiles CV increased during 1971-2000, 2025, 2050, and 2100 in the sequence of 0.20-0.28, 0.30-0.39, 0.30-0.40, and 0.31-0.58, respectively. The largest increase in the seasonal flow inequality was obtained at the Římov station, which suggests that this phenomenon can be of an increasing importance for small catchments.
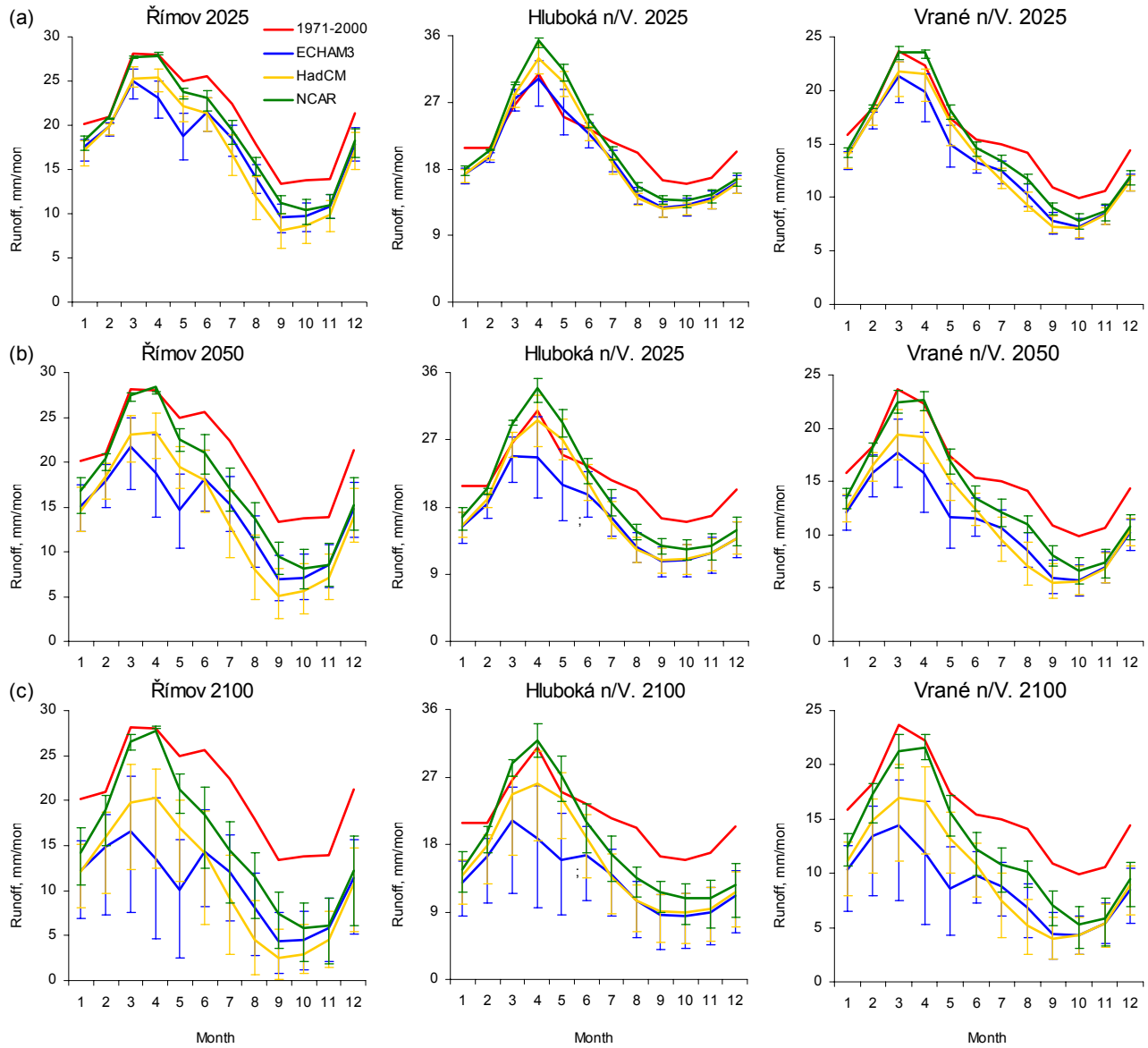
*Figure 3.4. Comparison of simulated runoff 1971-2000 with GCM scenarios for time periods 2025 (top), 2050 (middle), and 2100 (bottom) and middle +/- optimistic/pessimistic (error bars) global change scenarios at the stations of Římov (left), Hluboká n/V. (middle), and Vrané n/V. (right).*

The uncertainty in the runoff predictions increased with time and in the time horizon of 2100 it occupied a very wide range of runoff values (Fig. 3.4). Especially in the winter and spring periods the zone of uncertainty spread to the range of decreases from about 0 % to 60-90 %, which makes the applicability of these results problematic. In the summer and autumn months

13

this uncertainty belt was narrower because the results of the three models were more coincident and the decrease in runoff seems to be doubtless.

*Table 3.5. Simulated mean monthly runoff (mm) at the gauging station Římov in the reference period 1971-2000 and in time horizons of 2025, 2050 and 2100 for all considered climate change scenarios*

| Period | Model/ type of change | | Month | | | | | | | | | | | |
|---|---|---|---|---|---|---|---|---|---|---|---|---|---|---|
| | | | 1 | 2 | 3 | 4 | 5 | 6 | 7 | 8 | 9 | 10 | 11 | 12 |
| 1971-2000 | - | - | 20.1 | 20.9 | 28.1 | 28.0 | 24.9 | 25.6 | 22.4 | 17.9 | 13.4 | 13.8 | 13.9 | 21.3 |
| 2025 | E | high | 15.9 | 18.7 | 23.0 | 20.8 | 16.1 | 19.4 | 16.5 | 12.2 | 7.9 | 8.0 | 9.4 | 15.9 |
| | | low | 18.4 | 20.2 | 26.3 | 25.0 | 21.3 | 23.1 | 20.0 | 15.6 | 11.0 | 11.3 | 12.1 | 19.7 |
| | | middle | 17.5 | 19.8 | 25.0 | 23.1 | 18.7 | 21.4 | 18.5 | 14.1 | 9.6 | 9.8 | 10.8 | 17.9 |
| | H | high | 15.4 | 18.9 | 24.3 | 23.8 | 20.4 | 19.3 | 14.3 | 9.3 | 6.0 | 6.6 | 8.0 | 15.0 |
| | | low | 18.3 | 20.1 | 26.6 | 26.3 | 23.3 | 23.1 | 18.9 | 14.1 | 10.1 | 10.5 | 11.4 | 19.2 |
| | | middle | 17.2 | 19.8 | 25.3 | 25.4 | 22.1 | 21.4 | 16.8 | 11.9 | 8.2 | 8.7 | 9.8 | 17.2 |
| | N | high | 17.1 | 20.7 | 27.6 | 28.2 | 23.0 | 21.6 | 17.9 | 14.3 | 10.0 | 8.8 | 9.4 | 16.3 |
| | | low | 18.8 | 20.8 | 27.8 | 28.0 | 24.2 | 24.0 | 20.5 | 16.4 | 12.0 | 11.6 | 12.1 | 19.6 |
| | | middle | 18.3 | 20.9 | 27.7 | 27.8 | 23.7 | 23.1 | 19.4 | 15.6 | 11.2 | 10.4 | 10.9 | 18.3 |
| 2050 | E | high | 12.3 | 14.9 | 16.9 | 13.8 | 10.4 | 14.6 | 12.3 | 8.2 | 4.5 | 4.7 | 6.0 | 11.6 |
| | | low | 17.4 | 19.8 | 25.0 | 23.0 | 18.7 | 21.4 | 18.4 | 14.0 | 9.5 | 9.7 | 10.8 | 17.7 |
| | | middle | 15.0 | 17.8 | 21.7 | 18.7 | 14.6 | 18.2 | 15.4 | 11.2 | 7.0 | 7.1 | 8.6 | 14.8 |
| | H | high | 12.2 | 15.9 | 20.0 | 20.3 | 17.1 | 14.4 | 9.3 | 4.6 | 2.6 | 3.1 | 4.7 | 11.0 |
| | | low | 17.1 | 19.8 | 25.2 | 25.4 | 21.8 | 21.3 | 16.7 | 11.8 | 8.1 | 8.6 | 9.7 | 17.1 |
| | | middle | 14.6 | 18.3 | 23.0 | 23.3 | 19.4 | 18.0 | 12.9 | 7.9 | 5.0 | 5.6 | 7.1 | 13.8 |
| | N | high | 14.2 | 19.1 | 26.8 | 27.7 | 21.3 | 18.6 | 14.5 | 11.6 | 7.5 | 5.9 | 6.2 | 12.4 |
| | | low | 18.3 | 20.9 | 27.7 | 27.8 | 23.8 | 23.0 | 19.4 | 15.5 | 11.1 | 10.3 | 10.9 | 18.3 |
| | | middle | 16.8 | 20.4 | 27.4 | 28.4 | 22.5 | 21.0 | 17.1 | 13.7 | 9.4 | 8.1 | 8.6 | 15.2 |
| 2100 | E | high | 7.0 | 7.3 | 7.6 | 4.7 | 2.5 | 8.2 | 6.6 | 2.8 | 0.8 | 1.2 | 2.1 | 5.2 |
| | | low | 15.6 | 18.4 | 22.7 | 20.3 | 15.7 | 19.0 | 16.1 | 11.9 | 7.6 | 7.7 | 9.1 | 15.7 |
| | | middle | 12.2 | 14.8 | 16.6 | 13.6 | 10.1 | 14.4 | 12.1 | 8.0 | 4.3 | 4.6 | 5.8 | 11.5 |
| | H | high | 8.1 | 9.6 | 12.4 | 12.5 | 11.1 | 6.2 | 2.9 | 0.6 | 0.2 | 0.8 | 1.5 | 5.4 |
| | | low | 15.2 | 18.7 | 24.0 | 23.5 | 20.1 | 18.9 | 13.9 | 8.9 | 5.7 | 6.3 | 7.7 | 14.7 |
| | | middle | 12.1 | 15.9 | 19.8 | 20.2 | 17.0 | 14.2 | 9.2 | 4.5 | 2.5 | 3.0 | 4.6 | 10.8 |
| | N | high | 10.7 | 14.9 | 25.7 | 28.0 | 18.6 | 12.5 | 8.7 | 6.9 | 3.6 | 2.1 | 1.8 | 6.1 |
| | | low | 17.1 | 20.6 | 27.4 | 28.3 | 23.0 | 21.5 | 17.7 | 14.1 | 9.8 | 8.6 | 9.2 | 16.0 |
| | | middle | 14.2 | 18.9 | 26.6 | 27.7 | 21.2 | 18.5 | 14.4 | 11.5 | 7.4 | 5.8 | 6.1 | 12.2 |

*Table 3.6. Percentage changes of the simulated mean monthly runoff at the gauging station Římov for all considered climate change scenarios in comparison with the reference period of 1971-2000*

| Period | Model/ type of change | | Month | | | | | | | | | | | |
|---|---|---|---|---|---|---|---|---|---|---|---|---|---|---|
| | | | 1 | 2 | 3 | 4 | 5 | 6 | 7 | 8 | 9 | 10 | 11 | 12 |
| 1971-2000 | - | - | 0 | 0 | 0 | 0 | 0 | 0 | 0 | 0 | 0 | 0 | 0 | 0 |
| 2025 | E | high | -21 | -11 | -18 | -26 | -35 | -24 | -26 | -32 | -41 | -42 | -32 | -25 |
| | | low | -9 | -3 | -6 | -11 | -15 | -10 | -10 | -13 | -18 | -18 | -13 | -8 |
| | | middle | -13 | -5 | -11 | -18 | -25 | -16 | -18 | -21 | -28 | -29 | -22 | -16 |
| | H | high | -23 | -10 | -13 | -15 | -18 | -25 | -36 | -48 | -55 | -52 | -42 | -30 |
| | | low | -9 | -4 | -5 | -6 | -7 | -10 | -15 | -21 | -25 | -24 | -18 | -10 |
| | | middle | -15 | -5 | -10 | -9 | -11 | -16 | -25 | -33 | -39 | -37 | -29 | -19 |
| | N | high | -15 | -1 | -2 | 1 | -8 | -15 | -20 | -20 | -25 | -36 | -32 | -24 |
| | | low | -7 | -1 | -1.0 | 0.0 | -3 | -6 | -8 | -8 | -11 | -16 | -13 | -8 |
| | | middle | -9 | 0 | -1 | -0.6 | -5 | -10 | -13 | -13 | -17 | -25 | -21 | -14 |
| 2050 | E | high | -39 | -29 | -40 | -51 | -58 | -43 | -45 | -54 | -67 | -66 | -57 | -46 |
| | | low | -13 | -6 | -11 | -18 | -25 | -16 | -18 | -21 | -29 | -29 | -23 | -17 |
| | | middle | -25 | -15 | -23 | -33 | -41 | -29 | -31 | -37 | -48 | -48 | -38 | -30 |
| | H | high | -39 | -24 | -29 | -27 | -31 | -44 | -58 | -74 | -81 | -78 | -66 | -48 |
| | | low | -15 | -5 | -10 | -9 | -13 | -17 | -25 | -34 | -40 | -38 | -30 | -20 |
| | | middle | -27 | -12 | -18 | -17 | -22 | -30 | -42 | -56 | -62 | -59 | -49 | -35 |
| | N | high | -29 | -9 | -5 | -1.1 | -15 | -27 | -35 | -35 | -44 | -57 | -56 | -42 |
| | | low | -9 | 0 | -1 | -0.5 | -5 | -10 | -13 | -13 | -17 | -25 | -22 | -14 |
| | | middle | -17 | -3 | -2 | 2 | -10 | -18 | -23 | -23 | -30 | -41 | -38 | -28 |
| 2100 | E | high | -65 | -65 | -73 | -83 | -90 | -68 | -70 | -84 | -94 | -91 | -85 | -76 |
| | | low | -23 | -12 | -19 | -27 | -37 | -26 | -28 | -33 | -43 | -44 | -34 | -26 |
| | | middle | -39 | -29 | -41 | -51 | -59 | -44 | -46 | -55 | -68 | -67 | -58 | -46 |
| | H | high | -60 | -54 | -56 | -55 | -56 | -76 | -87 | -97 | -99 | -95 | -89 | -75 |
| | | low | -25 | -11 | -15 | -16 | -19 | -26 | -38 | -50 | -57 | -54 | -45 | -31 |
| | | middle | -40 | -24 | -29 | -28 | -32 | -44 | -59 | -75 | -81 | -78 | -67 | -49 |
| | N | high | -47 | -29 | -9 | 0 | -26 | -51 | -61 | -61 | -73 | -84 | -87 | -71 |
| | | low | -15 | -2 | -2 | 1 | -8 | -16 | -21 | -21 | -27 | -37 | -34 | -25 |
| | | middle | -30 | -10 | -5 | -1.0 | -15 | -28 | -36 | -36 | -45 | -58 | -56 | -43 |

*Table 3.7. Simulated mean monthly runoff (mm) at the gauging station Hluboká n/V. in the reference period 1971-2000 and in time horizons of 2025, 2050 and 2100 for all considered climate change scenarios*

| Period | Model/ type of change | | Month | | | | | | | | | | | |
|---|---|---|---|---|---|---|---|---|---|---|---|---|---|---|
| | | | 1 | 2 | 3 | 4 | 5 | 6 | 7 | 8 | 9 | 10 | 11 | 12 |
| 1971-2000 | - | - | 20.8 | 20.8 | 26.6 | 30.9 | 25.0 | 23.4 | 21.6 | 20.2 | 16.5 | 15.9 | 16.8 | 20.4 |
| 2025 | E | high | 16.0 | 18.9 | 25.9 | 26.5 | 22.6 | 20.7 | 17.6 | 13.3 | 11.5 | 11.6 | 12.6 | 14.7 |
| | | low | 18.1 | 20.1 | 28.7 | 32.6 | 28.7 | 24.3 | 20.5 | 15.5 | 13.6 | 14.0 | 15.0 | 17.2 |
| | | middle | 17.3 | 19.6 | 27.4 | 30.2 | 26.0 | 22.8 | 19.2 | 14.5 | 12.7 | 13.0 | 14.0 | 16.2 |
| | H | high | 16.1 | 19.2 | 26.4 | 29.2 | 26.4 | 21.7 | 17.2 | 13.0 | 11.5 | 11.7 | 12.6 | 14.7 |
| | | low | 18.0 | 20.6 | 28.1 | 33.0 | 29.7 | 23.7 | 19.4 | 14.7 | 13.1 | 13.5 | 14.4 | 16.6 |
| | | middle | 17.3 | 19.8 | 28.1 | 31.3 | 28.4 | 23.6 | 18.8 | 14.0 | 12.5 | 12.9 | 13.8 | 16.0 |
| | N | high | 17.1 | 20.4 | 29.4 | 34.4 | 29.9 | 23.5 | 19.2 | 15.0 | 13.2 | 12.8 | 13.3 | 15.6 |
| | | low | 18.5 | 20.6 | 29.8 | 35.7 | 32.1 | 25.3 | 21.0 | 16.1 | 14.3 | 14.4 | 15.2 | 17.4 |
| | | middle | 18.0 | 20.6 | 29.4 | 35.4 | 31.4 | 24.6 | 20.3 | 15.7 | 13.8 | 13.7 | 14.5 | 16.7 |
| 2050 | E | high | 13.1 | 16.5 | 21.3 | 19.2 | 16.1 | 16.6 | 14.1 | 10.6 | 8.6 | 8.6 | 9.1 | 11.3 |
| | | low | 17.3 | 19.7 | 27.3 | 30.0 | 25.8 | 22.7 | 19.1 | 14.5 | 12.7 | 12.9 | 13.9 | 16.1 |
| | | middle | 15.3 | 18.4 | 24.8 | 24.6 | 20.9 | 19.6 | 16.7 | 12.6 | 10.8 | 10.9 | 11.8 | 13.8 |
| | H | high | 13.9 | 17.9 | 24.7 | 26.2 | 24.3 | 18.9 | 13.7 | 10.5 | 9.1 | 9.0 | 9.5 | 11.7 |
| | | low | 17.2 | 19.8 | 28.1 | 33.0 | 29.7 | 23.7 | 18.7 | 14.0 | 12.5 | 12.9 | 13.7 | 16.0 |
| | | middle | 15.6 | 19.1 | 26.7 | 29.6 | 27.0 | 21.4 | 16.1 | 12.2 | 10.9 | 11.1 | 11.8 | 13.8 |
| | N | high | 14.9 | 19.6 | 29.0 | 32.0 | 27.3 | 21.1 | 16.8 | 13.6 | 11.7 | 10.9 | 10.9 | 12.7 |
| | | low | 17.9 | 20.5 | 29.7 | 35.2 | 31.1 | 24.5 | 20.3 | 15.7 | 13.8 | 13.6 | 14.5 | 16.6 |
| | | middle | 16.7 | 20.4 | 29.2 | 33.9 | 29.3 | 23.0 | 18.6 | 14.7 | 12.9 | 12.4 | 12.7 | 14.9 |
| 2100 | E | high | 8.4 | 10.2 | 11.5 | 9.5 | 8.6 | 10.6 | 8.4 | 5.6 | 3.9 | 4.2 | 4.7 | 6.3 |
| | | low | 15.8 | 18.7 | 25.6 | 25.8 | 22.1 | 20.4 | 17.3 | 13.1 | 11.3 | 11.4 | 12.3 | 14.4 |
| | | middle | 13.0 | 16.4 | 21.2 | 18.8 | 15.9 | 16.5 | 14.0 | 10.5 | 8.5 | 8.4 | 9.0 | 11.1 |
| | H | high | 10.1 | 12.8 | 16.6 | 18.5 | 18.7 | 13.5 | 8.8 | 6.4 | 5.0 | 4.7 | 5.0 | 7.0 |
| | | low | 16.0 | 19.3 | 27.1 | 30.5 | 27.6 | 22.0 | 16.7 | 12.7 | 11.3 | 11.5 | 12.3 | 14.3 |
| | | middle | 13.8 | 17.9 | 24.6 | 26.1 | 24.3 | 18.9 | 13.6 | 10.4 | 9.1 | 8.9 | 9.4 | 11.6 |
| | N | high | 11.7 | 16.9 | 27.0 | 29.6 | 23.8 | 16.9 | 13.1 | 10.9 | 9.0 | 7.3 | 6.8 | 8.3 |
| | | low | 17.1 | 20.4 | 29.2 | 34.1 | 29.8 | 23.4 | 19.0 | 14.9 | 13.1 | 12.7 | 13.2 | 15.4 |
| | | middle | 14.7 | 19.6 | 28.9 | 31.9 | 27.3 | 21.0 | 16.7 | 13.5 | 11.6 | 10.8 | 10.9 | 12.6 |

*Table 3.8. Percentage changes of the simulated mean monthly runoff at the gauging station Hluboká n/V. for all considered climate change scenarios in comparison with the reference period of 1971-2000*

| Period | Model/ type of change | | Month | | | | | | | | | | | |
|---|---|---|---|---|---|---|---|---|---|---|---|---|---|---|
| | | | 1 | 2 | 3 | 4 | 5 | 6 | 7 | 8 | 9 | 10 | 11 | 12 |
| 1971-2000 | - | - | 0 | 0 | 0 | 0 | 0 | 0 | 0 | 0 | 0 | 0 | 0 | 0 |
| 2025 | E | high | -23 | -9 | -3 | -14 | -9 | -12 | -19 | -34 | -30 | -27 | -25 | -28 |
| | | low | -13 | -3 | 8 | 6 | 15 | 4 | -5 | -23 | -17 | -12 | -11 | -16 |
| | | middle | -17 | -6 | 3 | -2 | 4 | -3 | -11 | -28 | -23 | -18 | -17 | -21 |
| | H | high | -23 | -8 | -1 | -6 | 6 | -7 | -20 | -36 | -30 | -26 | -25 | -28 |
| | | low | -14 | -1 | 6 | 7 | 19 | 1 | -10 | -27 | -20 | -15 | -14 | -18 |
| | | middle | -17 | -5 | 6 | 1 | 14 | 1 | -13 | -31 | -24 | -19 | -18 | -21 |
| | N | high | -18 | -2 | 10 | 11 | 20 | 0 | -11 | -26 | -20 | -19 | -21 | -23 |
| | | low | -11 | -1 | 11.9 | 15.6 | 29 | 8 | -3 | -20 | -13 | -10 | -10 | -15 |
| | | middle | -14 | -1 | 11 | 14.7 | 26 | 5 | -6 | -22 | -16 | -14 | -14 | -18 |
| 2050 | E | high | -37 | -21 | -20 | -38 | -36 | -29 | -34 | -48 | -48 | -46 | -46 | -45 |
| | | low | -17 | -5 | 3 | -3 | 3 | -3 | -11 | -28 | -23 | -19 | -17 | -21 |
| | | middle | -27 | -12 | -7 | -20 | -16 | -16 | -23 | -38 | -34 | -31 | -30 | -32 |
| | H | high | -33 | -14 | -7 | -15 | -3 | -19 | -36 | -48 | -44 | -43 | -44 | -43 |
| | | low | -17 | -5 | 5 | 7 | 19 | 1 | -13 | -31 | -24 | -19 | -18 | -22 |
| | | middle | -25 | -8 | 0 | -4 | 8 | -9 | -26 | -39 | -34 | -30 | -30 | -32 |
| | N | high | -29 | -6 | 9 | 3.5 | 10 | -10 | -22 | -33 | -29 | -31 | -35 | -38 |
| | | low | -14 | -1 | 11 | 14.1 | 24 | 4 | -6 | -23 | -16 | -14 | -14 | -18 |
| | | middle | -20 | -2 | 10 | 10 | 17 | -2 | -14 | -27 | -22 | -22 | -24 | -27 |
| 2100 | E | high | -60 | -51 | -57 | -69 | -66 | -55 | -61 | -73 | -76 | -74 | -72 | -69 |
| | | low | -24 | -10 | -4 | -16 | -12 | -13 | -20 | -35 | -32 | -28 | -27 | -29 |
| | | middle | -38 | -21 | -21 | -39 | -36 | -30 | -35 | -48 | -48 | -47 | -47 | -45 |
| | H | high | -52 | -38 | -38 | -40 | -25 | -42 | -59 | -68 | -70 | -70 | -70 | -65 |
| | | low | -23 | -8 | 2 | -1 | 11 | -6 | -23 | -37 | -31 | -28 | -27 | -30 |
| | | middle | -34 | -14 | -8 | -16 | -3 | -19 | -37 | -48 | -45 | -44 | -44 | -43 |
| | N | high | -44 | -19 | 2 | -4 | -5 | -28 | -39 | -46 | -46 | -54 | -60 | -59 |
| | | low | -18 | -2 | 10 | 11 | 19 | 0 | -12 | -26 | -20 | -20 | -22 | -24 |
| | | middle | -29 | -6 | 9 | 3.4 | 9 | -10 | -23 | -33 | -29 | -32 | -35 | -38 |

*Table 3.9. Simulated mean monthly runoff (mm) at the gauging profile Vrané n/V. in the reference period 1971-2000 and in time horizons of 2025, 2050 and 2100 for all considered climate change scenarios*

| Period | Model/ type of change | | Month | | | | | | | | | | | |
|---|---|---|---|---|---|---|---|---|---|---|---|---|---|---|
| | | | 1 | 2 | 3 | 4 | 5 | 6 | 7 | 8 | 9 | 10 | 11 | 12 |
| 1971-2000 | - | - | 15.8 | 18.3 | 23.7 | 22.3 | 17.4 | 15.4 | 15.0 | 14.1 | 10.9 | 9.9 | 10.6 | 14.4 |
| 2025 | E | high | 12.7 | 16.4 | 18.9 | 17.1 | 12.8 | 12.3 | 11.2 | 9.2 | 6.6 | 6.2 | 7.4 | 10.6 |
| | | low | 14.3 | 18.0 | 22.7 | 21.5 | 16.8 | 14.5 | 13.4 | 11.2 | 8.6 | 8.1 | 9.2 | 12.2 |
| | | middle | 14.0 | 17.7 | 21.4 | 19.9 | 15.0 | 13.3 | 12.5 | 10.2 | 7.8 | 7.3 | 8.5 | 11.7 |
| | H | high | 12.7 | 16.7 | 19.4 | 19.0 | 14.9 | 12.6 | 10.9 | 8.8 | 6.6 | 6.3 | 7.5 | 10.6 |
| | | low | 14.2 | 18.1 | 22.7 | 22.0 | 17.5 | 14.5 | 12.7 | 10.5 | 8.3 | 7.9 | 9.0 | 12.1 |
| | | middle | 13.8 | 17.8 | 21.7 | 21.6 | 17.0 | 13.9 | 11.6 | 9.3 | 7.3 | 7.1 | 8.3 | 11.5 |
| | N | high | 13.8 | 18.3 | 22.9 | 23.0 | 17.3 | 13.8 | 12.5 | 11.2 | 8.4 | 7.0 | 7.8 | 11.2 |
| | | low | 14.7 | 18.6 | 24.1 | 23.8 | 18.7 | 15.1 | 13.9 | 12.1 | 9.5 | 8.4 | 9.4 | 12.4 |
| | | middle | 14.3 | 18.6 | 23.5 | 23.5 | 18.2 | 14.6 | 13.4 | 11.8 | 9.0 | 7.8 | 8.7 | 11.9 |
| 2050 | E | high | 10.4 | 13.6 | 14.5 | 12.1 | 8.7 | 9.8 | 8.9 | 6.9 | 4.5 | 4.3 | 5.5 | 8.5 |
| | | low | 13.6 | 17.5 | 20.8 | 19.7 | 14.8 | 13.4 | 12.3 | 10.3 | 7.7 | 7.2 | 8.4 | 11.4 |
| | | middle | 12.1 | 15.8 | 17.7 | 15.8 | 11.7 | 11.6 | 10.6 | 8.6 | 6.0 | 5.7 | 6.9 | 10.2 |
| | H | high | 11.2 | 15.0 | 17.0 | 16.7 | 13.3 | 10.8 | 7.5 | 5.2 | 4.1 | 4.3 | 5.4 | 9.0 |
| | | low | 13.8 | 17.8 | 21.7 | 21.6 | 17.0 | 13.9 | 11.6 | 9.3 | 7.3 | 7.1 | 8.3 | 11.5 |
| | | middle | 12.5 | 16.5 | 19.4 | 19.2 | 15.1 | 12.4 | 9.5 | 7.1 | 5.5 | 5.6 | 6.8 | 10.4 |
| | N | high | 12.4 | 17.4 | 21.4 | 21.7 | 15.7 | 12.3 | 10.8 | 10.2 | 7.1 | 5.4 | 5.9 | 9.6 |
| | | low | 14.3 | 18.6 | 23.6 | 23.5 | 18.1 | 14.5 | 13.3 | 11.7 | 9.0 | 7.8 | 8.7 | 11.9 |
| | | middle | 13.4 | 18.1 | 22.4 | 22.6 | 16.9 | 13.5 | 12.1 | 11.0 | 8.1 | 6.6 | 7.3 | 10.8 |
| 2100 | E | high | 6.5 | 7.9 | 7.5 | 5.3 | 4.2 | 7.3 | 6.1 | 4.0 | 2.1 | 2.6 | 3.5 | 5.4 |
| | | low | 12.5 | 16.2 | 18.6 | 16.6 | 12.4 | 12.0 | 11.0 | 9.0 | 6.4 | 6.0 | 7.3 | 10.5 |
| | | middle | 10.3 | 13.5 | 14.4 | 11.9 | 8.6 | 9.8 | 8.8 | 6.8 | 4.4 | 4.2 | 5.4 | 8.4 |
| | H | high | 7.9 | 10.0 | 11.1 | 11.8 | 10.1 | 7.9 | 4.1 | 2.5 | 2.1 | 2.5 | 3.2 | 6.2 |
| | | low | 12.9 | 16.9 | 20.0 | 19.9 | 15.6 | 12.8 | 10.0 | 7.6 | 6.0 | 6.0 | 7.2 | 10.7 |
| | | middle | 11.1 | 14.9 | 17.0 | 16.7 | 13.2 | 10.8 | 7.4 | 5.2 | 4.0 | 4.3 | 5.4 | 9.0 |
| | N | high | 10.6 | 14.7 | 19.7 | 20.5 | 13.4 | 9.8 | 8.2 | 8.7 | 5.2 | 3.0 | 3.3 | 7.0 |
| | | low | 13.7 | 18.3 | 22.8 | 22.8 | 17.2 | 13.7 | 12.4 | 11.2 | 8.3 | 6.9 | 7.7 | 11.1 |
| | | middle | 12.4 | 17.3 | 21.3 | 21.6 | 15.6 | 12.2 | 10.7 | 10.1 | 7.0 | 5.3 | 5.9 | 9.5 |

*Table 3.10. Percentage changes of the simulated mean monthly runoff at the gauging station Vrané n/V. for all considered climate change scenarios in comparison with the reference period of 1971-2000*

| Period | Model/ type of change | | Month | | | | | | | | | | | |
|---|---|---|---|---|---|---|---|---|---|---|---|---|---|---|
| | | | 1 | 2 | 3 | 4 | 5 | 6 | 7 | 8 | 9 | 10 | 11 | 12 |
| 1971-2000 | - | - | 0 | 0 | 0 | 0 | 0 | 0 | 0 | 0 | 0 | 0 | 0 | 0 |
| 2025 | E | high | -20 | -10 | -20 | -23 | -27 | -20 | -25 | -35 | -40 | -37 | -30 | -26 |
| | | low | -10 | -1 | -4 | -3 | -4 | -6 | -11 | -21 | -21 | -18 | -13 | -15 |
| | | middle | -12 | -3 | -10 | -11 | -14 | -13 | -17 | -28 | -29 | -27 | -20 | -18 |
| | H | high | -20 | -9 | -18 | -15 | -15 | -18 | -28 | -38 | -39 | -36 | -30 | -26 |
| | | low | -10 | -1 | -4 | -1 | 0 | -6 | -15 | -26 | -24 | -20 | -15 | -16 |
| | | middle | -13 | -3 | -8 | -3 | -2 | -10 | -22 | -34 | -33 | -28 | -22 | -20 |
| | N | high | -13 | 0 | -3 | 3 | -1 | -10 | -17 | -20 | -23 | -29 | -26 | -22 |
| | | low | -7 | 2 | 1.6 | 6.6 | 7 | -2 | -7 | -14 | -13 | -15 | -12 | -13 |
| | | middle | -9 | 2 | -1 | 5.5 | 4 | -5 | -11 | -17 | -17 | -21 | -18 | -17 |
| 2050 | E | high | -34 | -25 | -39 | -46 | -50 | -36 | -41 | -51 | -59 | -56 | -49 | -41 |
| | | low | -14 | -4 | -12 | -12 | -15 | -13 | -18 | -27 | -30 | -27 | -21 | -20 |
| | | middle | -24 | -14 | -25 | -29 | -33 | -25 | -29 | -39 | -45 | -43 | -35 | -29 |
| | H | high | -29 | -18 | -28 | -25 | -24 | -30 | -50 | -63 | -63 | -56 | -49 | -37 |
| | | low | -13 | -3 | -8 | -3 | -2 | -10 | -23 | -34 | -33 | -28 | -22 | -20 |
| | | middle | -21 | -9 | -18 | -14 | -13 | -19 | -37 | -50 | -49 | -43 | -36 | -28 |
| | N | high | -22 | -5 | -10 | -2.7 | -10 | -20 | -28 | -28 | -35 | -46 | -44 | -34 |
| | | low | -10 | 2 | -1 | 5.3 | 4 | -6 | -11 | -17 | -18 | -21 | -18 | -18 |
| | | middle | -15 | -1 | -5 | 2 | -3 | -13 | -20 | -22 | -26 | -33 | -31 | -25 |
| 2100 | E | high | -59 | -57 | -68 | -76 | -76 | -53 | -59 | -71 | -80 | -74 | -67 | -62 |
| | | low | -21 | -11 | -22 | -25 | -29 | -22 | -26 | -36 | -42 | -39 | -32 | -27 |
| | | middle | -35 | -26 | -39 | -47 | -51 | -37 | -41 | -52 | -60 | -57 | -49 | -41 |
| | H | high | -50 | -45 | -53 | -47 | -42 | -49 | -73 | -82 | -81 | -74 | -69 | -57 |
| | | low | -19 | -8 | -16 | -11 | -10 | -17 | -33 | -46 | -46 | -40 | -32 | -26 |
| | | middle | -30 | -19 | -28 | -25 | -24 | -30 | -50 | -63 | -63 | -57 | -49 | -38 |
| | N | high | -33 | -20 | -17 | -8 | -23 | -36 | -45 | -38 | -53 | -69 | -69 | -52 |
| | | low | -13 | 0 | -4 | 2 | -1 | -11 | -17 | -21 | -24 | -30 | -28 | -23 |
| | | middle | -22 | -6 | -10 | -3.1 | -10 | -21 | -28 | -28 | -36 | -46 | -45 | -34 |

Impacts of high-resolution climate modelling projections by the ALADIN 10×10 km and RegCM3 25×25 km regional models were studied at the Vltava River basin for the catchment of Římov. The changes in temperature and precipitation predicted with this model for this catchment (Tab. 3.11, Fig. 3.5) show consistent trends with the other Central European localities, i.e. Dyje and Hron catchments.

*Table 3.11. Precipitation (PREC), potential evapotranspiration (PE), runoff (R) and runoff coefficient (RC = R/PREC) in the scenario simulations of effects of climate change at the gauging station Římov with the outputs of ALADIN 10×10 km and RegCM3 25×25 km models*

| Quantity | Measured 1971-2000 | ALADIN | | RegCM3 | |
|---|---|---|---|---|---|
| | | 2021-2050 | 2071-2100 | 2021-2050 | 2071-2100 |
| PREC, mm/yr | 702 | 733 | 690 | 714 | 690 |
| PE, mm/yr | 584 | 634 | 830 | 637 | 830 |
| R, mm/yr | 250 | 237 | 127 | 209 | 127 |
| RC | 0.36 | 0.32 | 0.18 | 0.29 | 0.18 |
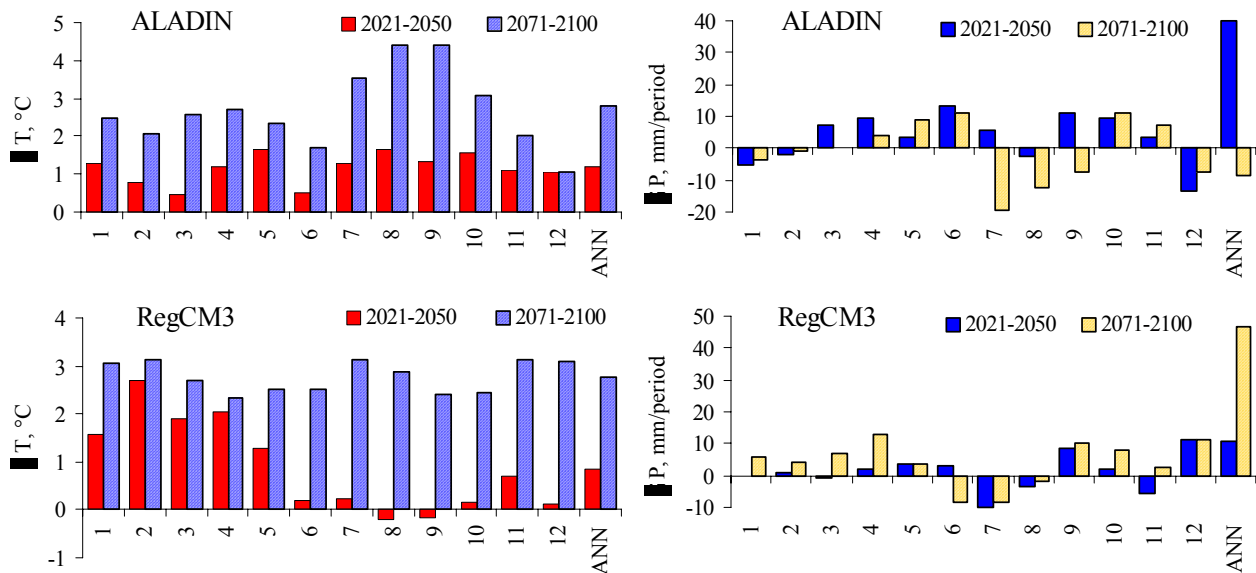


*Figure 3.5. Temperature and precipitation changes predicted with the ALADIN and RegCM3 regional high-resolution climatic models in the catchment of the gauging station Římov for the 2021–2050 and 2071-2100 periods*

The seasonal patterns of runoff and their difference changes are given in Fig. 3.6 and Tab. 3.12 and 3.13. The climate change impacts on flow conditions varied seasonally and significantly

differed for the near and far future periods. For the near future (2021−2050) period, a not very significant decrease was obtained for the mean annual runoff value and the runoff decrease was almost evenly distributed through the periods of year. For the far future (2071−2050) period, the mean runoff decreased by ca 50 % and a serious drop in the summer and autumn runoff values by up to ca 80 % was modelled.
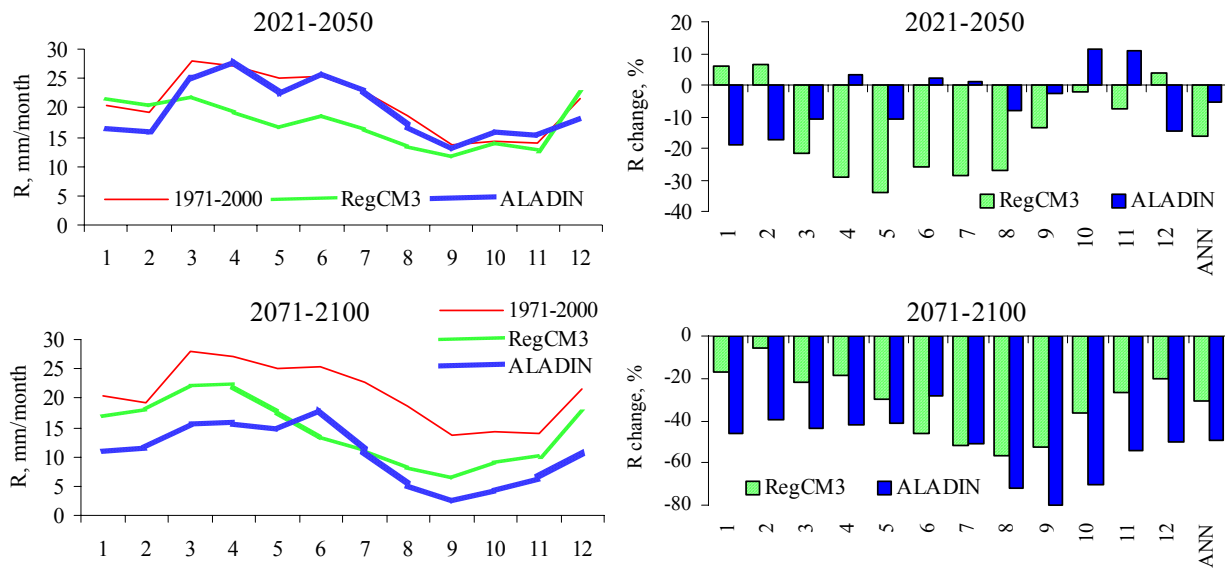


*Figure 3.6. The monthly and annual mean runoff values and their changes simulated at the gauging station Římov according to ALADIN 10×10 km and RegCM3 25×25 km climatic predictions for the time periods of 2021-2050 and 2071-2100*

*Table 3.12. Simulated mean monthly runoff (mm) at the gauging profile Římov in the reference period 1971-2000 and in the future periods of 2021−2050 and 2071−2100 for climate change scenarios predicted with the ALADIN 10×10 km a RegCM3 25×25 km regional models*

| Period | Model | Month | | | | | | | | | | | | ANN |
|---|---|---|---|---|---|---|---|---|---|---|---|---|---|---|
| | | 1 | 2 | 3 | 4 | 5 | 6 | 7 | 8 | 9 | 10 | 11 | 12 | |
| 1971−2000 | – | 20.4 | 19.2 | 28.1 | 27.0 | 25.1 | 25.2 | 22.9 | 18.5 | 13.6 | 14.4 | 14.0 | 21.7 | 250 |
| 2021−2050 | RegCM3 | 21.6 | 20.4 | 21.9 | 19.2 | 16.5 | 18.7 | 16.3 | 13.5 | 11.7 | 14.1 | 12.9 | 22.5 | 209 |
| | ALADIN | 16.5 | 15.9 | 25.0 | 27.9 | 22.4 | 25.8 | 23.2 | 17.0 | 13.3 | 16.0 | 15.5 | 18.5 | 237 |
| 2071−2100 | RegCM3 | 16.9 | 18.1 | 22.0 | 22.1 | 17.6 | 13.5 | 11.0 | 8.1 | 6.4 | 9.2 | 10.2 | 17.3 | 173 |
| | ALADIN | 11.0 | 11.6 | 15.8 | 15.8 | 14.7 | 18.0 | 11.1 | 5.2 | 2.8 | 4.3 | 6.4 | 10.8 | 127 |

*Table 3.13. Percentage changes of the simulated mean monthly runoff at the gauging station Římov with the ALADIN 10×10 km a RegCM3 25×25 km regional models in 2021–2050 and 2071–2100  in comparison with the reference period 1971-2000*

| Period | Model | \multicolumn{12}{c}{Month} | ANN |
| | | 1 | 2 | 3 | 4 | 5 | 6 | 7 | 8 | 9 | 10 | 11 | 12 | |
|---|---|---|---|---|---|---|---|---|---|---|---|---|---|---|
| 1971–2000 | – | 0 | 0 | 0 | 0 | 0 | 0 | 0 | 0 | 0 | 0 | 0 | 0 | 0 |
| 2021–2050 | RegCM3 | 6 | 6 | -22 | -29 | -34 | -26 | -29 | -27 | -14 | -2 | -8 | 4 | -16 |
| | ALADIN | -19 | -17 | -11 | 3 | -11 | 2 | 1 | -8 | -3 | 11 | 11 | -15 | -5 |
| 2071–2100 | RegCM3 | -17 | -6 | -22 | -18 | -30 | -46 | -52 | -56 | -53 | -36 | -27 | -20 | -31 |
| | ALADIN | -46 | -40 | -44 | -42 | -41 | -29 | -51 | -72 | -80 | -70 | -55 | -50 | -49 |

*3.3 References*

Bicknell B. R., Imhoff J. C., Kittle Jr. J. L., Jobes T. H., Donigian Jr. A. S. (2001): Hydrological Simulation Program–Fortran (HSPF). User's Manual for Release 12. U.S. EPA National Exposure Research Laboratory, Athens, GA, in cooperation with U.S. Geological Survey, Water Resources Division, Reston, VA.

Nash J. E., Sutcliffe J. V. (1970): River flow forecasting through conceptual models I: A discussion of principles. J. Hydrol. 10, 282–290.

# 4. The Dyje River basin

For simulation of monthly flow considering climate change on Dyje basin there have been chosen two catchments of the Jihlava River, namely the catchment to the gauge station Ptáčov (catchment area of 964 km$^2$) as the upper part of Jihlava basin and the catchment to the gauge station Ivančice (catchment area of 2,682 km$^2$), where the Jihlava River has already received its two most important tributaries, i.e. the Oslava River and the Rokytná River (Fig. 4.1). These two catchments have been also selected by the reason of examination divergences of the climate change impact on the upper part of the basin compared to the bottom basin. The flow was simulated with the model BILAN.

*4.1 Model BILAN*

*4.1.1 Basic information*

BILAN water balance model has been developed by the staff of the T. G. M. Water Research Institute in Prague for assessing water balance components of a catchment in a monthly step. It is structured as a system of relationships between these components on the land surface, in the soil zone of aeration, including the effect of vegetation cover, and in the groundwater aquifer. Air temperature is used as an indicator of energy conditions which affects significantly the equilibrium between the water balance components.
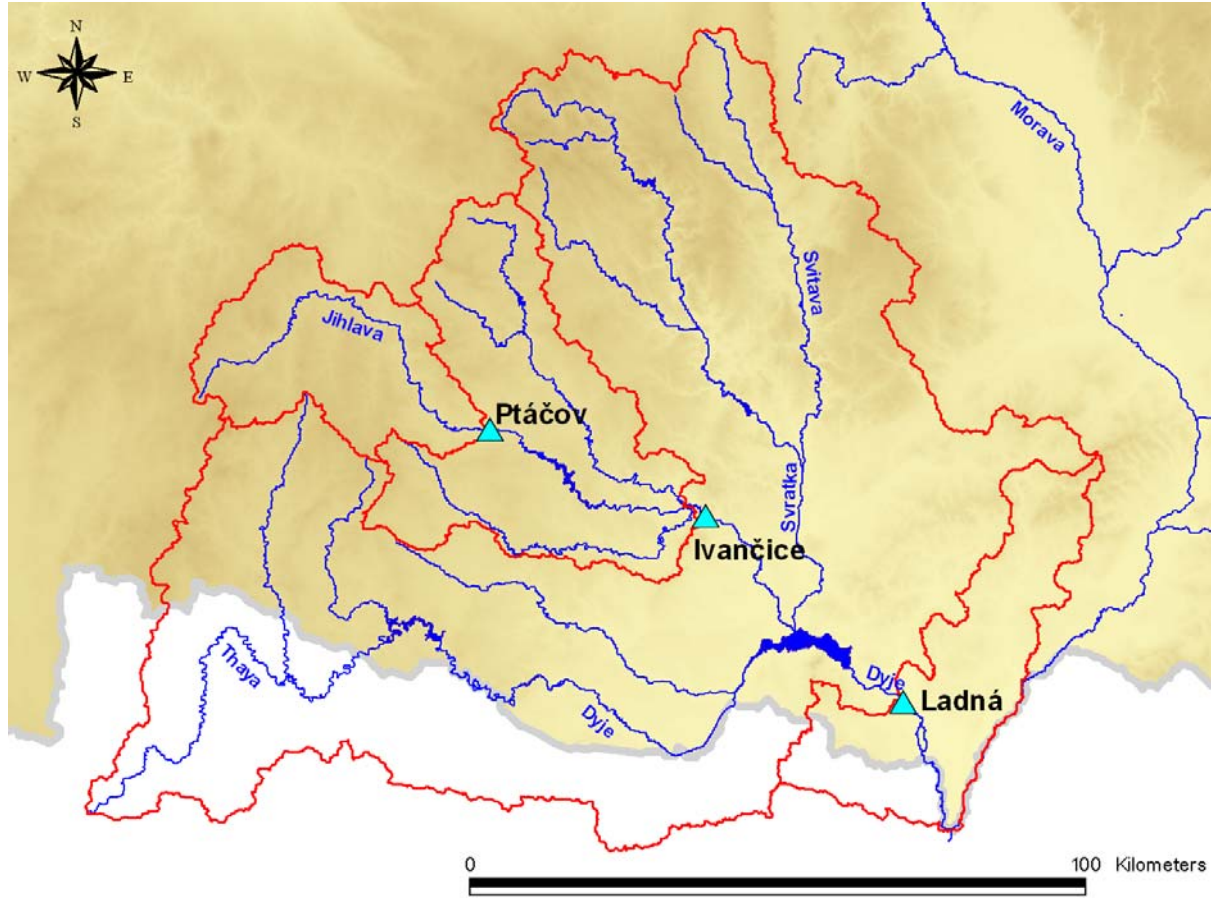
*Figure 4.1. Dyje basin with Jihlava River and its two catchments – to the gauge stations Ptáčov and Ivančice*

The entry data of the model are monthly series of basin precipitation *p* [mm/month], air temperature *t* [°C] and relative air humidity *h* [%]. To calibrate the parameters of the model, simulated and observed monthly runoff series *r* [mm/month] at the outlet from the basin are used.

Standard version of the model uses tables given in Rekomendatsii of Gidrometeoizdat (1976), where potential evapotranspiration *ep* [mm/month] is related to bioclimatic zones and catchment relative air humidity. The model embodies an interpolation algorithm that uses catchment long-term average air temperature for the interpolating between the bioclimatic zones (which is between particular tables) and relative air humidity for interpolating between neighbouring values. A detailed description of the method is presented in Krejčová et al. (1993). If a series of monthly potential evapotranspiration calculated by other method is available, it can be entered as an input.

The model generates monthly series of basin potential evapotranspiration, actual evaporation *e* [mm/month], infiltration *inf* [mm/month] to the zone of aeration, percolation *perc* [mm/month] of water towards the groundwater aquifer, recharge of groundwater storage *rech* [mm/month] and water storage components in the snow cover *sx* [mm], zone of aeration (soil moisture) *w* [mm]

23

and groundwater aquifer *rb* [mm]. The total runoff (simulated) *rv* [mm/month] consists of three components that include direct runoff *ds* [mm/month], interflow (amount of water exceeding soil moisture capacity) *dr* [mm/month] and base flow *bf* [mm/month].

The model has eight free parameters and its optimisation technique uses observed data for their calibration. The optimisation is aimed at attaining the best fit between the observed and simulated runoff series.

The model parameters include:

*Spa* – capacity of soil moisture storage [mm]
*Alf* – parameter of rainfall-runoff equation
*Dgm* – temperature/snow melting factor
*Dgw* – factor for calculating the quantity of liquid water available on the land surface under winter conditions
*Mec* – parameter to control distribution of percolation into interflow and groundwater recharge under conditions of snow melting
*Wic* – parameter to control distribution of percolation into interflow and groundwater recharge under winter conditions
*Soc* – parameter to control distribution of percolation into interflow and groundwater recharge under summer conditions
*Grd* – parameter controlling outflow from groundwater storage (base flow)

*4.1.2 Description of the model*

The internal structure of the BILAN model is given in Fig. 4.2 and individual algorithms are described in the text that follows.

**Type of regime:**

Several model algorithms are season dependent, i.e. applied dependably on conditions in a particular month. Taking into account mean monthly air temperature, the model distinguishes between summer and winter conditions. The summer conditions are assumed if the temperature

$$t(i) \geq 0, \tag{1}$$

where *i* signifies month index in a year.

If there is snow cover on the basin, a snow-melting algorithm is used instead of the summer algorithm.

**Components of total runoff:**

The model simulates the total runoff *rv(i)* as the sum ot three components

$$rv(i) = ds(i) + dr(i) + bf(i), \tag{2}$$

where $ds(i)$, $dr(i)$ and $bf(i)$ are direct runoff, interflow and base flow in given month, respectively.

The $ds(i)$ component of the total runoff includes summer direct runoff and that part of interflow that, together with the direct runoff, flows so rapidly that it neither affects water balance in the soil nor is significantly available for evaporation. Direct runoff in summer is caused by high intensity of rain.

Irrespective of the season, the interflow $dr(i)$ results from water balance as excess water in the soil zone of aeration. This runoff component is assumed to include also direct runoff if it occurs in winter or during the period when snow melts.

The base flow $bf(i)$, whose delay time in the basin is longer than that of other runoff components, is formed by outflow from the groundwater storage.

**Formation of direct runoff under summer conditions:**

Direct runoff occurring during the summer season consequently to a rainfall episode with high intensity is calculated as

$$ds(i) = Alf \cdot p(i)^2 \cdot (w(i\text{-}1) \, / \, Spa), \tag{3}$$

where $Alf$ is a parameter of quadratic rainfall-runoff relationship between direct runoff and rainfall, $p(i)$ is precipitation in month $i$, $w(i\text{-}1)$ is soil moisture in month $i$-1, and $Spa$ is a parameter expressing soil moisture capacity.

The precipitation reduced by the direct runoff

$$inf(i) = p(i) - ds(i) \tag{4}$$

becomes a component of water balance in the zone of aeration.

**Evaporation and water balance in the soil under summer conditions:**

If precipitation reduced by direct runoff, $inf(i)$, calculated by Eq. 4 equals or exceeds potential evapotranspiration, i.e. if

$$inf(i) \geq ep(i), \tag{5}$$

the basin evaporation is equal to the potential evapotranspiration

$$e(i) = ep(i) \tag{6}$$

and the excess water amounting $inf(i)$-$ep(i)$ is available to feed the soil moisture

$$w(i) = w(i\text{-}1) + inf(i) - ep(i) \tag{7}$$

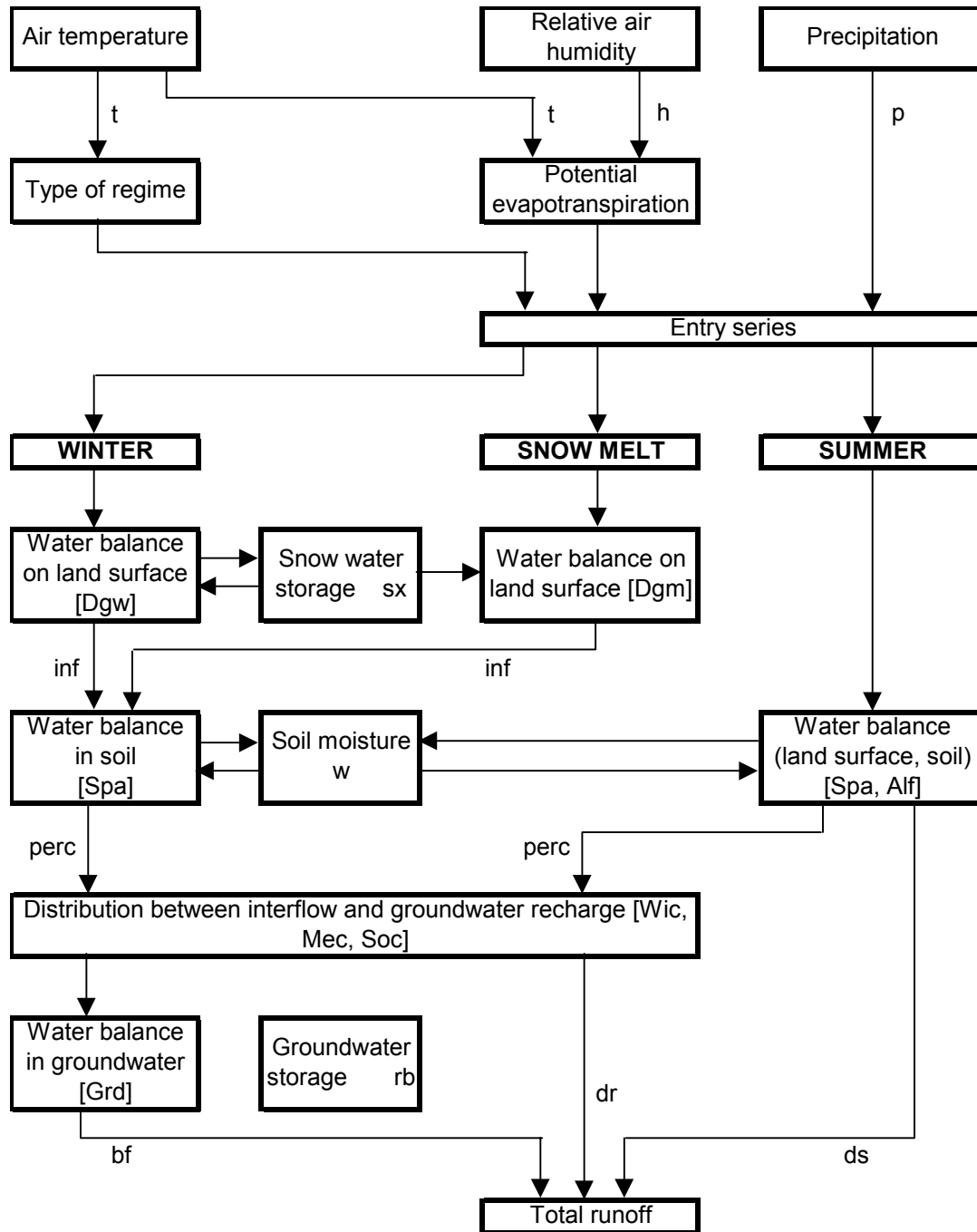and if capacity of the soil moisture storage is exceeded

$$w(i) > Spa, \tag{8}$$

*Figure 4.2. Internal structure of BILAN water balance model*

the remaining water percolates downwards

$$perc(i) = w(i) - Spa, \tag{9}$$

while the soil moisture storage *w(i)* is equal to *Spa* capacity.

If potential evapotranspiration exceeds the precipitation reduced by direct runoff, the basin evaporation is supplied from the soil moisture storage, which is being depleted

$$w(i) = w(i\text{-}1) \cdot \exp^{(inf(i)\text{-}ep(i))/Spa}, \qquad (10)$$

where exp is a base of hyperbolic logarithm.

The basin evaporation then equals the sum of the reduced precipitation and the soil moisture depletion

$$e(i) = inf(i) + w(i\text{-}1) - w(i) \qquad (11)$$

and no water is available for percolation.


**Evaporation and water balance on the land surface under winter conditions and during the period when snow melts:**

If the sum of precipitation and water storage in the snow cover in the given month exceeds potential evapotranspiration, it is assumed that the basin evaporation is equal to the potential evapotranspiration

$$e(i) = ep(i). \qquad (12)$$

The quantity of remaining water that is potentially available for infiltration (disposable water in the form of snow), is

$$akt(i) = sx(i\text{-}1) + p(i) - ep(i), \qquad (13)$$

where $sx(i\text{-}1)$ is water storage in the snow cover in month $i\text{-}1$.

However, the virtual quantity of water available for infiltration is limited by the heat capacity of the air to melt the snow cover in the given month, which is, under snow melting conditions, expressed as

$$pot(i) = t(i) \cdot Dgm + p(i), \qquad (14)$$

where $t(i)$ is the mean air temperature in month $i$ and $Dgm$ is a parameter expressing the rate of snowmelt in relation to the air temperature.

Under winter conditions, a part of precipitation is assumed to be formed by rainfall, or the existing snow cover melts partially, if the monthly air temperature exceeds a certain value set implicitly as $Tepk = \text{-}8\ °C$.

The amount of water that will be available in a liquid form is again determined by using the air temperature

$$pot(i) = (t(i) - Tepk) \cdot Dgw \qquad (15)$$

and controlled by *Dgw* parameter.

If the mean monthly air temperature is below the value specified as *Tepk*, the water balance on the land surface is described by the equation

$$sx(i) = sx(i\text{-}1) + p(i) - ep(i) \qquad (16)$$

and *inf(i)* = 0, that is no water infiltrates into the soil, and the difference between precipitation and potential evapotranspiration is added to the snow water storage.

Under both winter and snow melting conditions, if the disposable water *akt(i)* exceeds the limit *pot(i)*, the *akt(i)* is distributed into a part that infiltrates, *inf(i)*, and water that remains on the land surface as the snow cover. The following is, therefore, valid

$$inf(i) = pot(i), \qquad (17)$$

$$sx(i) = akt(i) - inf(i). \qquad (18)$$

If the limit *pot(i)* exceeds the quantity of the disposable water, this water is fully available for infiltration

$$inf(i) = akt(i) \qquad (19)$$

and water storage in the snow cover is exhausted.

The *akt(i)* value can exceptionally be negative, when the sum of precipitation and water storage in the snow cover in the given month is lower than potential evapotranspiration and thus

$$inf(i) = 0, \qquad (20)$$

$$sx(i) = 0, \qquad (21)$$

$$e(i) = p(i) + sx(i\text{-}1). \qquad (22)$$

Water balance in soil under winter and snow melting conditions:

Water calculated as infiltration *inf(i)* supplies the soil moisture (or zone of aeration), which is assumed to have its capacity given by *Spa* parameter. If the soil capacity is exceeded, the excess water, *perc(i)*, percolates downwards to feed the groundwater storage. In other words, if the sum of soil water storage from the preceding month, *w(i-1)*, and infiltration in the given month, *inf(i)*, exceeds the *Spa* parameter, the following is valid

$$perc(i) = w(i\text{-}1) + inf(i) - Spa, \qquad (23)$$

$$w(i) = Spa. \qquad (24)$$

Otherwise

$$perc(i) = 0, \qquad (25)$$

$$w(i) = w(i\text{-}1) + inf(i).$$ (26)

Distribution of percolation into interflow and groundwater recharge:

Percolation *perc(i)* is divided into runoff component *dr(i)* that reaches the stream channel in the given month and recharge *rech(i)* that replenishes the groundwater storage

$$dr(i) = c \cdot perc(i),$$ (27)

$$rech(i) = (1\text{-}c) \cdot perc(i).$$ (28)

In the above equations, *Wic* parameter is substituted for *c* under winter conditions, *Mec* parameter for snow melting and *Soc* parameter in summer.

**Water balance in groundwater and base flow:**

Groundwater storage *rb(i)* in month *i* is calculated as the sum of the storage in the preceding month and recharge *rech(i)*. The base flow represented by the outflow from the groundwater is proportional to its storage at the beginning of the given month and is controlled by *Grd* parameter

$$bf(i) = Grd \cdot rb(i\text{-}1).$$ (29)

Therefore, the groundwater storage at the end of the month is

$$rb(i) = rech(i) + (1\text{-}Grd) \cdot rb(i\text{-}1).$$ (30)

*4.1.3 Optimisation of parameters*

In the standard optimisation procedure, standard error of estimate (standard deviation between the observed and simulated runoff series) would normally be used as an optimisation criterion. A drawback of this criterion is in the fact that its application does not ensure good fit between the observed and simulated runoff series in the area of low flows. This can substantially be improved by using a sum of relative deviations between the observed and simulated runoff series („relative" means that individual deviations are divided by the mean runoff in identical month) instead of the standard error of estimate. However, this criterion frequently deteriorates the fit in terms of the mean runoff and, therefore, an optimisation procedure with combining these two criteria was developed.

The calibration of the parameters is executed in two steps. First, the standard error of estimate is used as the optimisation criterion to calibrate *Spa, Dgm, Dgw* and *Alf* parameters that affect significantly the mean runoff. Then, the remaining four parameters (*Mec, Wic, Soc, Grd*) affecting the runoff distribution into its individual components are calibrated by using the sum of relative deviations. This optimisation procedure is executed in number of 500 iterations.

It has been demonstrated by experimental calculations that this calibration procedure ensures mostly an acceptable fit in terms of both mean runoff and low flow runoff that is formed predominantly by base flow. For simulation of monthly runoff series considering the climate change the model is not working with the standard deviation between the observed and simulated runoff series, so that no iteration step (number of iterations is zero) enters the calculation and only the scenarios monthly series of basin precipitation, air temperature, relative air humidity and the eight calibrated parameters are used.

## 4.2 Scenario modelling

### 4.2.1 Calibration of BILAN for the Jihlava basin

The calibration results of the BILAN water balance model for the Jihlava basin were at both stations, Ptáčov and Ivančice, quite good (Tab. 4.1, Fig. 4.3). Major differences between observed and simulated runoffs at both stations occurred in spring months, *i.e.* March (11 and 27 %, respectively) and April (33 and 25 %, respectively), and a minor bias occurred in June, July and November.
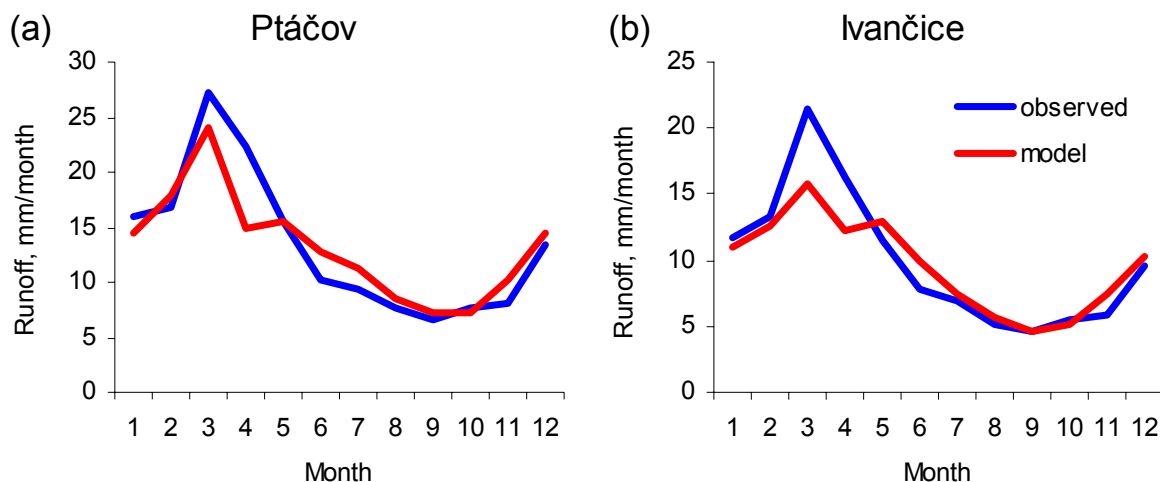
*Table 4.1. Comparison of monthly averages of observed and simulated runoffs at the stations Ptáčov and Ivančice during the calibration period 1971–2000. (The deviation between observed and simulated runoff is expressed by equation: dev.=100\*(RM-R)/R [%], where R is observed runoff and RM is simulated runoff.)*

| Month | Ptáčov | | | Ivančice | | |
|---|---|---|---|---|---|---|
| | Runoff [mm] | | dev. [%] | Runoff [mm] | | dev. [%] |
| | observed | model | | observed | model | |
| 1 | 15.9 | 14.5 | -8.5 | 11.6 | 10.9 | -6.0 |
| 2 | 16.8 | 17.9 | 6.7 | 13.3 | 12.7 | -5.0 |
| 3 | 27.2 | 24.1 | -11.4 | 21.5 | 15.7 | -26.8 |
| 4 | 22.3 | 15.0 | -32.8 | 16.3 | 12.2 | -25.2 |
| 5 | 15.6 | 15.4 | -1.0 | 11.6 | 12.9 | 11.5 |
| 6 | 10.3 | 12.7 | 23.6 | 7.8 | 9.9 | 26.9 |
| 7 | 9.4 | 11.3 | 19.9 | 6.9 | 7.5 | 9.0 |
| 8 | 7.6 | 8.6 | 13.2 | 5.1 | 5.7 | 11.6 |
| 9 | 6.6 | 7.2 | 8.9 | 4.6 | 4.6 | 0.8 |
| 10 | 7.6 | 7.2 | -6.5 | 5.5 | 5.1 | -7.6 |
| 11 | 8.1 | 10.3 | 26.4 | 5.9 | 7.4 | 26.2 |
| 12 | 13.4 | 14.5 | 8.6 | 9.6 | 10.3 | 7.8 |

*Figure 4.3. Comparison of monthly averages of observed and simulated runoffs at the stations Ptáčov and Ivančice during the calibration period 1971–2000*

*4.2.2 Runoff simulations considering the climate change*

The runoff simulations with considering the climate change were done for 27 scenarios – all combinations of 3 global climate models (ECHAM, HadCM, and NCAR), 3 types of global temperature change development (optimistic, mean and low emission scenarios) and 3 time periods (2025, 2050, and 2100) as described in Chapter 2.1. The differences in monthly average values of flow between the 1971–2000 simulation and the GCM scenarios for the time periods of 2025, 2050 and 2100 are shown in Fig. 4.4.

The runoff values for all GCM scenarios and all time periods are generally lower than the 1971-2000 simulation and monotonously decrease from the period of 2025 to 2100, whereas their runoff profiles are essentially relatively similar in the all time periods.

In the next we consider only the middle GCM scenarios runoff values. In the first half a year (from January to June) the ECHAM runoffs are for all time periods always lower then the other scenarios values. The HadCM runoffs are higher, but from July to December their values are similar to the ECHAM values. The NCAR scenarios give the highest runoff values till the October and then they are comparable with the other two GCM models.

The mean values of runoff coefficient at the Ptáčov station decreased in all GCM model scenarios of the future climate change when compared with the period 1971–2000 (Tab. 4.2, Fig. 4.5). The highest decrease was obtained for the outputs of the ECHAM model (from 19 % in 2025 to 46 % in 2100) while the NCAR model scenarios resulted in a minor decline (9.3 to 26 %). At the Ivančice station it was similar - the highest decrease occurred for the ECHAM model outputs (from 18 % in 2025 to 40 % in 2100) and the lowest decrease for the NCAR runoff coefficients (10 to 21 %).
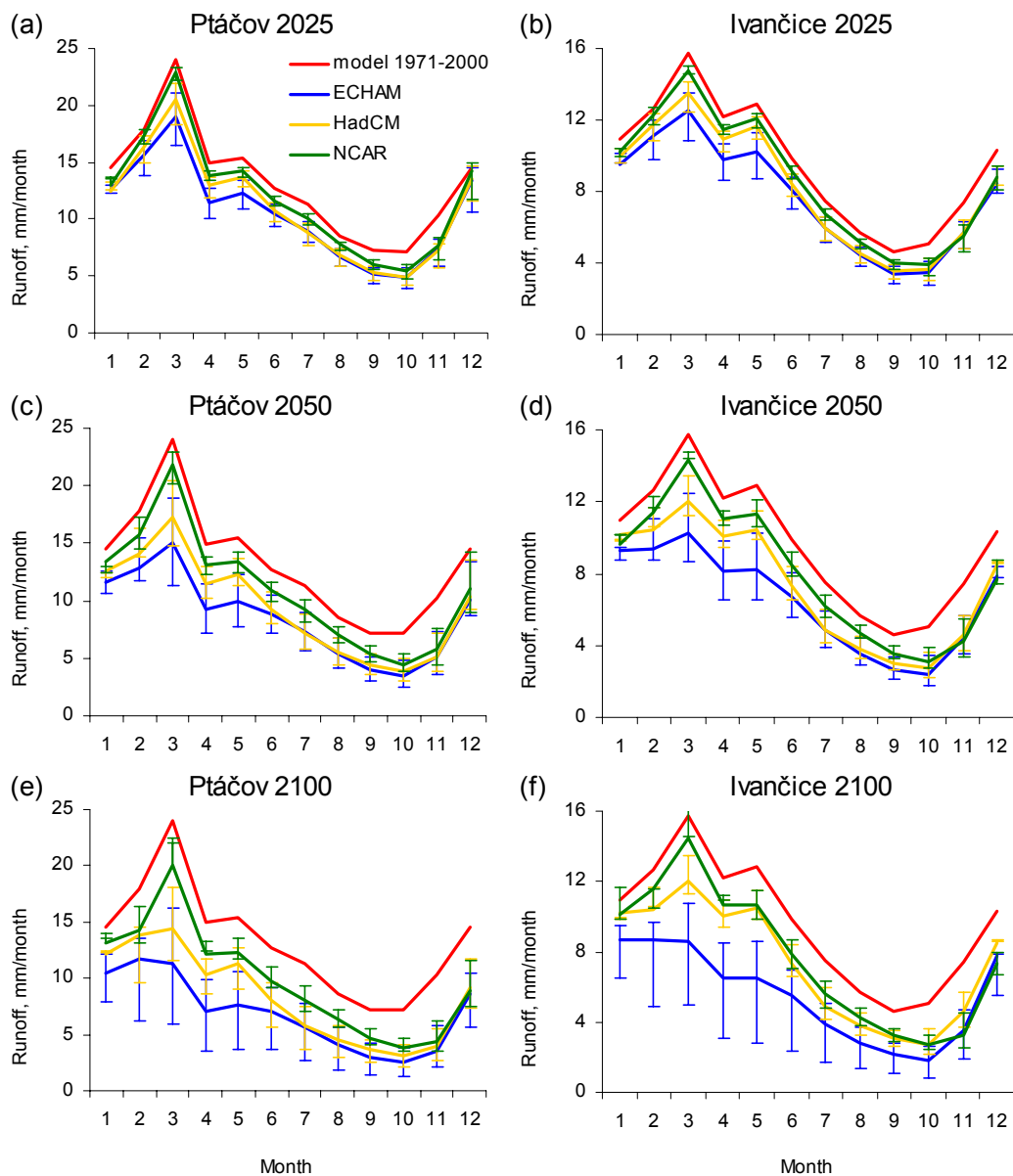
*Figure 4.4. Comparison of simulated runoff 1971–2000 with GCM scenarios for time periods 2025 (top), 2050 (middle), and 2100 (bottom) and middle +/- optimistic/pessimistic (error bars) global temperature change scenarios at the stations of Ptáčov (left) and Ivančice (right).*

*Table 4.2. Comparison of runoff coefficients simulated with BILAN for the period and for the GCM model scenarios in 2025, 2050, and 2100 with middle +/- optimistic/pessimistic (error bars) global temperature change development in the Jihlava basin at stations Ptáčov and Ivančice. (The deviation between the 1971–2000 period and the GCM scenarios is expressed by equation: dev.=100\*(RSc-RMc)/RMc [%], where RMc is runoff coefficient over the simulated period of 1971–2000 and RSc is the GCM runoff coefficient for middle scenario.)*

| Period | GCM model | Ptáčov | | | | Ivančice | | | |
|---|---|---|---|---|---|---|---|---|---|
| | | mid. | pes.(-) | opt.(+) | dev. [%] | mid. | pes.(-) | opt.(+) | dev. [%] |
| 1971–2000 | – | 0,248 | – | – | – | 0,200 | – | – | – |
| 2025 | ECHAM | 0,202 | 0,025 | 0,018 | -18 | 0,163 | 0,018 | 0,014 | -18 |
| | HadCM | 0,211 | 0,020 | 0,013 | -13 | 0,173 | 0,012 | 0,011 | -13 |
| | NCAR | 0,225 | 0,013 | 0,009 | -10 | 0,180 | 0,009 | 0,007 | -10 |
| 2050 | ECHAM | 0,164 | 0,030 | 0,037 | -31 | 0,138 | 0,018 | 0,024 | -31 |
| | HadCM | 0,182 | 0,018 | 0,029 | -21 | 0,157 | 0,008 | 0,015 | -21 |
| | NCAR | 0,204 | 0,021 | 0,020 | -17 | 0,165 | 0,006 | 0,015 | -17 |
| 2100 | ECHAM | 0,133 | 0,056 | 0,041 | -40 | 0,119 | 0,051 | 0,024 | -40 |
| | HadCM | 0,163 | 0,029 | 0,026 | -25 | 0,149 | 0,028 | 0,010 | -25 |
| | NCAR | 0,183 | 0,007 | 0,027 | -21 | 0,159 | 0,004 | 0,011 | -21 |
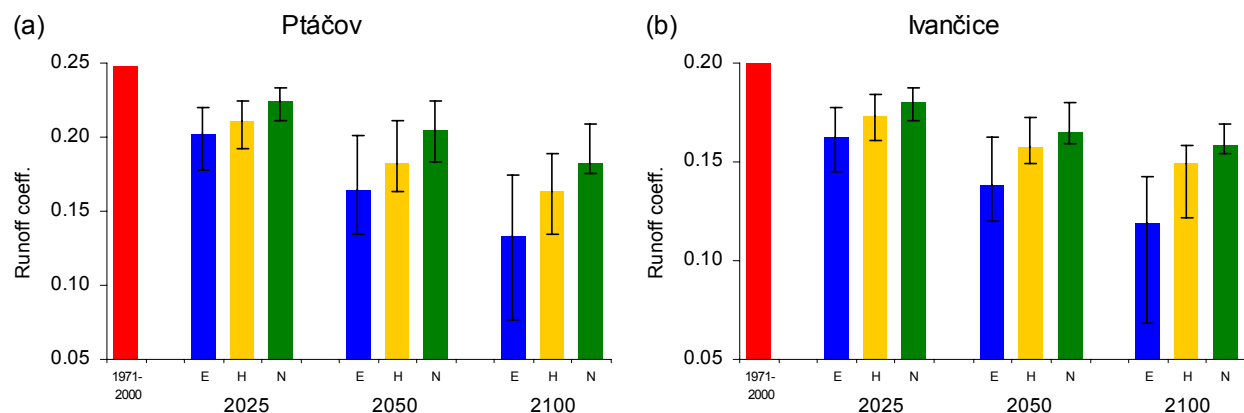


*Figure 4.5. Comparison of runoff coefficients simulated with BILAN for the 1971–2000 period and for the GCM model scenarios (E – ECHAM, H – HadCM, N – NCAP) with middle +/- optimistic/pessimistic (error bars) global temperature change development in the Jihlava basin at stations Ptáčov(left) and Ivančice (right)*

The runoff simulations considering the climate change based on outputs of ALADIN regional climate model computed for 10-km grid were done for two catchments of the Jihlava River (to the gauging station Ptáčov with catchment area 963.8 km$^2$ and Ivančice with catchment area 2682.2 km$^2$) and two time periods (2021–2050 and 2071–2100). The differences in monthly average values of flow between the 1971–2000 simulation and the ALADIN scenarios are shown in Fig. 4.6.
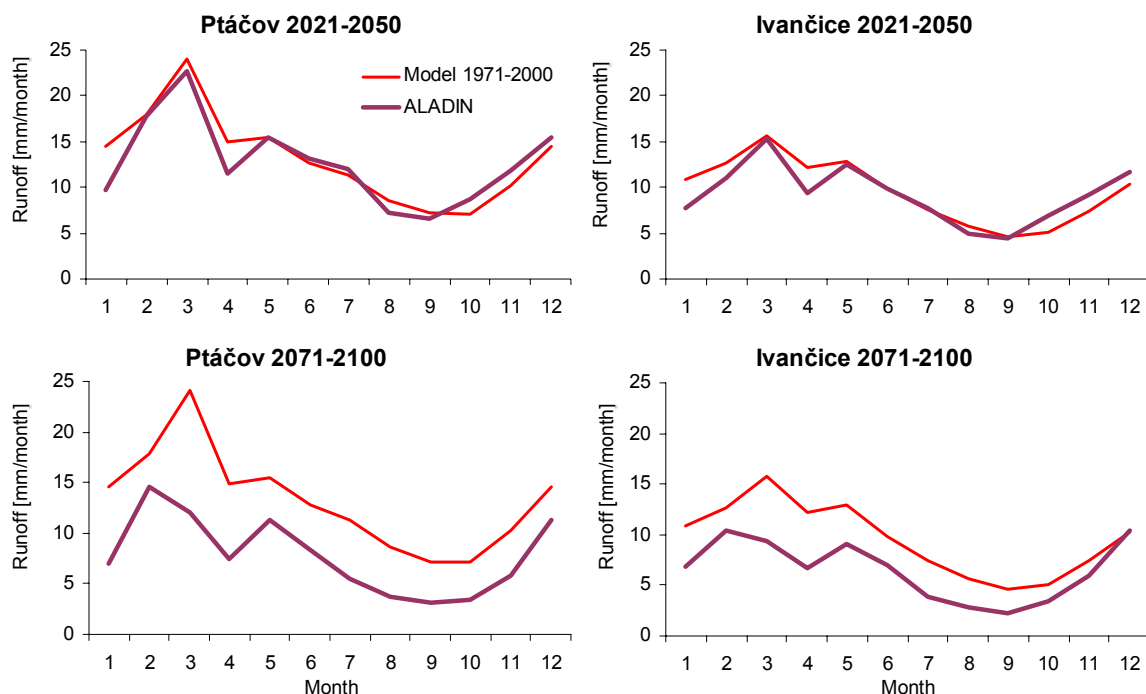
*Fig. 4.6. Comparison of simulated runoff 1971–2000 with ALADIN scenarios for time periods 2021–2050 and 2071–2100 at Ptáčov and Ivančice*

Runoff values for the time period of 2021-2050 are from January to April and from August to September lower than the 1971–2000 simulation; from May to July both values are essentially without any change and from October to December the ALADIN values are higher than the 1971–2000 simulation. For the period of 2071–2100 the ALADIN runoffs are generally lower than the 1971–2000 simulation. All ALADIN runoff profiles are relatively similar in both time periods.

The mean values of runoff coefficient for both catchments decreased in all ALADIN scenarios of the future climate change when compared with the period 1971–2000 (Tab. 4.3). Of course, a higher decrease was obtained for the period of 2071–2100.

*Tab. 4.3. Comparison of runoff coefficients simulated with BILAN for the 1971-2000 period and for the ALADIN scenarios for the periods of 2021-2050 and 2071-2100 in the Jihlava basin at stations Ptáčov and Ivančice. (The deviation between the 1971-2000 period and the ALADIN's scenarios is expressed by equation: dev.=100\*(RA-RM)/RM [%], where RM is runoff coefficient over the simulated period of 1971-2000 and RA is the ALADIN's runoff coefficient.)*

| Period | Ptáčov | | Ivančice | |
| --- | --- | --- | --- | --- |
| | runoff coeff. | dev. [%] | runoff coeff. | dev. [%] |
| 1971-2000 | 0,248 | - | 0,200 | - |
| 2021-2050 | 0,235 | -5 | 0,179 | -11 |
| 2071-2100 | 0,158 | -36 | 0,138 | -31 |

Runoff simulations based on outputs of ALADIN regional climate model were then compared to runoff simulations done for scenarios of 3 global climate models, i.e. ECHAM3, HadCM3, and NCAR-PCM (Fig. 4.7).
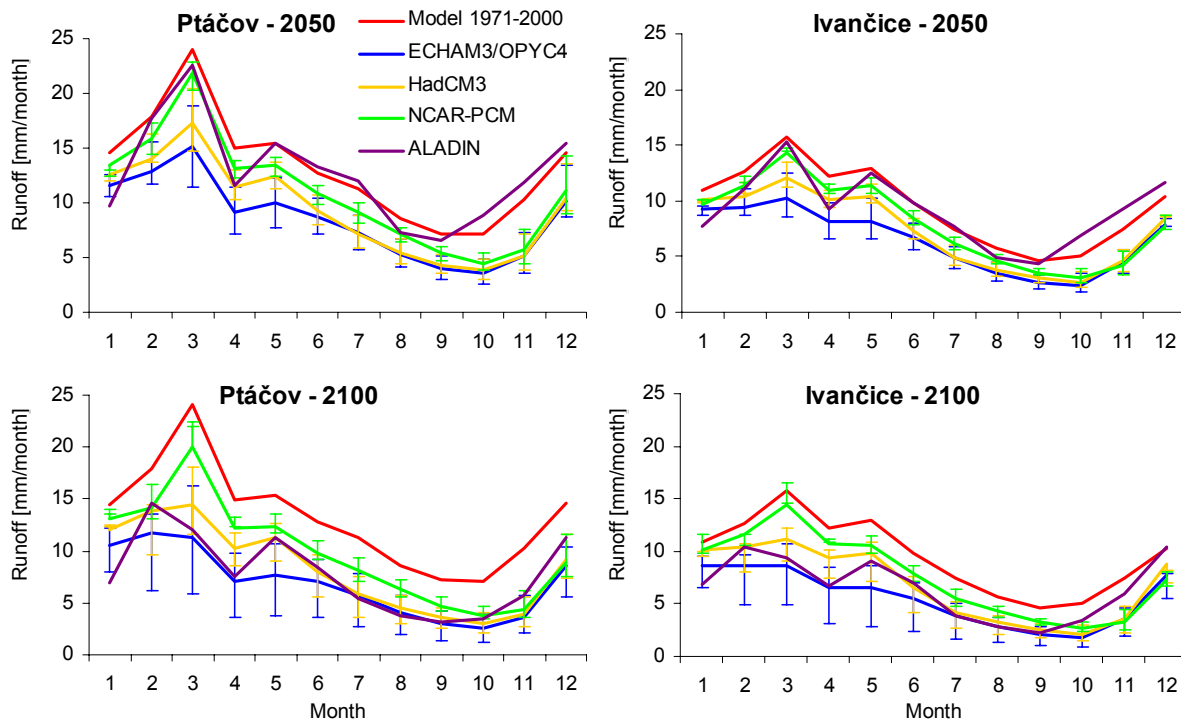


*Fig. 4.7. Comparison of GCM and ALADIN runoff simulations for the time periods of 2050 and 2100*

This comparison shows some differences between runoff simulations based on the GCM and ALADIN scenarios which are caused by different approaches of downscaling – statistical by GCMs and dynamical applied on ALADIN. The differences are signifficant especially for the period of 2050, when the ALADIN runoff simulations are higher than GCM simulations except January and April. For the period of 2100 the GCM and ALADIN runoffs correspond better, except January (ALADIN runoffs are lower) and from November to December (ALADIN runoffs are higher).

## 4.3 References

Gidrometeoizdat (1976): Rekomendatsii po roschotu ispareniia s poverkhnosti sushi. St. Peterburg.

Hladný, J. et al. (1996): Impact of a potential climate change on hydrology and water resources. Country study of climate change for the Czech Republic – Element 2, Publ. No. 20 of the National Climate Program of the Czech Republic. Prague, 137 pp.

Hulme, M., Conway, D., Brown, O., Barrow, E. (1994): Climate change scenarios for Great Britain and Europe. Climate Research Unit, University of East Anglia, Norwich.

Kašpárek, L. et al. (1995): Vliv změn klimatu na vodní zdroje (Impacts of climate change on water resources). Výzkumná zpráva úkolu Metody výpočtu hydrologických dat pro vodní hospodářství a ochranu životního prostředí (Research report of the project on Methods for calculation of hydrological data for water management and protection of the environment). TGM Water Research Institute, Prague.

Kašpárek, L., Blažková, Š. (1995): Vliv klimatické změny na hydrologický režim a vodní zdroje v Evropě (Impact of climate change on water regime and water resources in Europe). Research report, TGM Water Research Institute, Prague.

Krejčová, K. et al. (1994): Vliv změn klimatu na vodní zdroje (Impact of climate change on water resources). Výzkumná zpráva úkolu Metody výpočtu hydrologických dat pro vodní hospodářství a ochranu životního prostředí (Research report of the project on Methods for calculation of hydrological data for water management and protection of the environment). TGM Water Research Institute, Prague.

Krejčová, K., Řičica, J. et al. (1993): Vliv antropogenní činnosti na změny odtokového režimu a vydatnost vodních zdrojů (Impact of man activities on runoff regime and water resources). Research report, TGM Water Research Institute and Czech Hydrometeorological Institute.

## 5. The Hron

*5.1 Introduction and methods*

The potential impact of climate change on river runoff in the Hron river basin with the outlet in Banska Bystrica (area of 1766 km$^2$) was evaluated using a conceptual spatially lumped water balance model. For simulations of climate development according to GCM models, the conceptual water balance model was calibrated with data from the 1971–2000 period. Three climate change scenarios: E = ECHAM4/OPYC3, H = HadCM3, N = NCAR-PCM and 3 types of global temperature change estimation: LO = low (optimistic emission scenario + low estimate of climate sensitivity (1.5 K)), MI = middle (mean emission scenario + mean estimate of climate sensitivity (2.5 K)) and HI = high (high emission scenario + high estimate of climate sensitivity (4.5 K)) have been applied to test the sensitivity of the basins to climate change. Based on these scenarios the possible changes in the mean monthly runoff for the time horizons 2025, 2050 and 2100 were evaluated.

The hydrological scenarios of the changes in the seasonal runoff distribution were constructed using the following methodology:

a) calibration of the conceptual hydrological balance model for a selected pilot basin,

b) simulation of the reference mean monthly runoff series using input climate data from the reference period of 1971−2000,

c) modification of the climate input data from the reference period (precipitation, air temperature and potential evapotranspiration) according to the climate change scenarios for the time horizons of 2025, 2050 and 2100,

d)  simulation of the monthly runoff series using the hydrological balance model based on the changed input data and parameters of the model from the calibration,

e)  comparison of the differences between the seasonal runoff distribution for the individual scenarios and the time horizons considered.

For simulations of climate development according to the high-resolution regional model ALADIN 10×10 km, the conceptual water balance model was calibrated in monthly time step with data from 1971−2000 period and validated with data from 1961−1970 period. Based on outputs of the ALADINE-Climate model the possible changes in the mean monthly runoff for the time horizons of 2021−2050 and 2071−2100 were estimated.

Climate characteristics as precipitation totals, air temperature and relative air humidity were simulated by the ALADIN-Climate model in daily time step with grid resolution of 10 km. These grid climate outputs were spatially averaged over the Hron river basin and recalculated to monthly time step.

Changes in monthly precipitation totals, mean monthly air temperature and relative air humidity were considered for each month as differences between the long-term mean monthly outputs from the ALADIN-Climate model run (uncorrected outputs) in the reference period of 1961−1990 and future time horizons of 2021−2050 and 2071−2100.

Grid points of the ALADIN-Climate model outputs with resolution of 10 km in Slovakia and in the Hron river basin are shown in Fig. 5.1.

*5.2 Scenario modelling*

The results of the changes in the seasonal runoff distribution according to the GCMs predictions are shown in Tables 5.1 and 5.2 and in Fig. 5.2 indicate future changes in the long-term mean monthly runoff in the Hron river basin. The most extreme changes in runoff have been indicated according to pessimistic versions of all the three considered scenarios for the time horizon of 2100.

According to the pessimistic version of the ECHAM runs, the highest relative increase in runoff in comparison with the reference period can be expected in February, i.e. +24 % in 2025, +34 in 2050; and in December/January, i.e. +63 % in 2100. This increase can be caused by the increase in air temperature during winter and shift of the snow melting period from spring months to the winter period. The most extreme relative decrease in runoff can occur in April, i.e. -18 % in 2025, −39 % in 2050, −63 % in 2100; and in September, i.e. −17 % in 2025, −31 % in 2050 and −55 % in 2100. The decrease in April is caused by an increase in air temperature (+1.5 ℃ in 2025, +2.9 ℃ in 2050 and +6.2 ℃ in 2100) and by a decrease in precipitation (about −7 % in 2025, -13 % in 2050 and -29 % in 2100). The decrease in September is caused by the increase in air temperature (+1.8 ℃ in 2025, +3.4 ℃ in 2050 and +7.2 ℃ in 2100) and by the decrease in precipitation (−10 % in 2025, −18 % in 2050 and −39 % in 2100) if compared to the reference period.
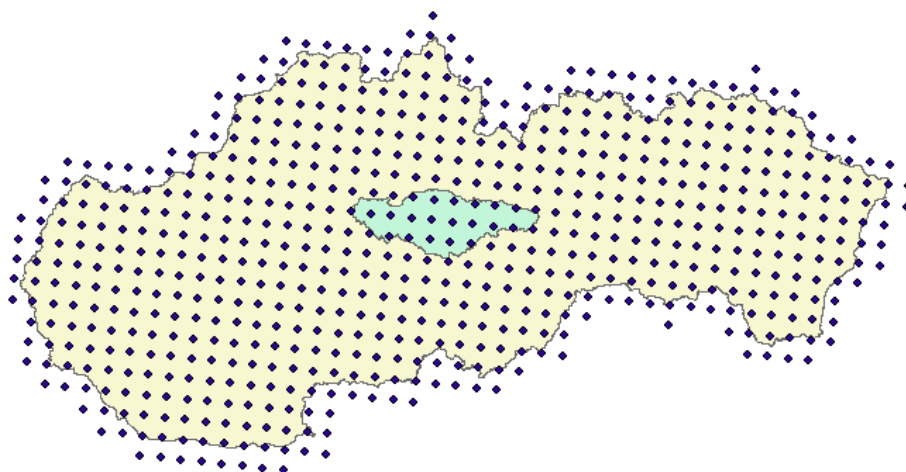
*Fig. 5.1. ALADIN-Climate grid spacing of 10 km resolution in Slovakia and in the upper Hron river basin*

According to the pessimistic version of the HadCM runs, the highest relative increase in runoff in comparison with the reference period can be expected in February, i.e. +30 % in 2025, +53 % in 2050; and in December, i.e. +77 % in 2100. The most extreme relative decrease in runoff can occur from July to September, i.e. -28 % in 2025, -49 % in 2050 and -75 % in 2100. The lower runoff, except of the increase in air temperature (in August: +2.3 ºC in 2025, +4.3 ºC in 2050 and +9 ºC in 2075), is caused by the decrease in precipitation (in August: −15 % in 2025, −29 % in 2050 and -62 % in 2100).

For the pessimistic version of NCAR scenario, the highest relative increase in runoff can be again expected in February, i.e. +25 % in 2025, +45 % in 2050 and in December, i.e. +85 % in 2100. The most extreme relative decrease in runoff can occur from September to October/November, i.e. −22 % in 2025, −42 % in 2050 and −73 % in 2100.  This decrease in caused mainly by the considerable decrease in precipitation (in October: −19 % in 2025, −35 % in 2050 and −76 % in 2100).

Generally, for all of the investigated runs it can be concluded that during the winter and early spring period, an increase in the long-term mean monthly runoff can be assumed. The period of the increase in runoff may occur from November/December to March. This increase can be caused by the increase in air temperature and shift of the snow melting period from spring months to the winter period. The period of the decrease in runoff may occur from April to October/November. The most extreme decrease can be expected in April–May and July to September/October. The decrease in summer runoff is expected to be more extreme for later time horizons.

In Table 5.2 and Fig. 5.3 mean runoff coefficients for the reference period of 1971–2000 and those for all of the scenarios in future time horizons are compared.

*Table 5.1. Long-term mean monthly runoff (mm) in the reference period 1971–2000 and in time horizons of 2025, 2050, and 2100 for all considered climate change scenarios*

| Scenario | Month | | | | | | | | | | | |
|---|---|---|---|---|---|---|---|---|---|---|---|---|
| | 1 | 2 | 3 | 4 | 5 | 6 | 7 | 8 | 9 | 10 | 11 | 12 |
| 1971–2000 | 20.2 | 22.5 | 42.9 | 62.6 | 51.7 | 42 | 30.1 | 24.8 | 23.9 | 30.3 | 26.9 | 21.1 |
| | | | | | | | | | | | | |
| E-25HI | 24.4 | 28 | 45.5 | 51.1 | 43.9 | 39.7 | 29 | 22.6 | 19.9 | 29.1 | 28.3 | 25 |
| E-25LO | 21.7 | 24.6 | 43.9 | 57.8 | 47.7 | 40.6 | 29.5 | 23.9 | 22.2 | 29.9 | 27.6 | 22.5 |
| E-25MI | 22.8 | 26 | 44.3 | 54.3 | 45.5 | 39.8 | 29 | 23.3 | 21.2 | 29.5 | 28 | 23.5 |
| H-25HI | 24.3 | 29.3 | 47.1 | 57.5 | 47.4 | 36.2 | 23.4 | 17.9 | 17.6 | 26 | 26.6 | 25.3 |
| H-25LO | 21.7 | 25.2 | 44.8 | 60.7 | 49.3 | 39.1 | 27.1 | 21.7 | 21.1 | 28.6 | 26.8 | 22.6 |
| H-25MI | 22.8 | 26.9 | 45.8 | 59.3 | 48.1 | 37.5 | 25.1 | 19.9 | 19.4 | 27.5 | 26.8 | 23.7 |
| N-25HI | 23.1 | 28 | 46.6 | 59.7 | 47.9 | 40.1 | 26.7 | 21.5 | 19.8 | 23.5 | 24.3 | 22.1 |
| N-25LO | 21.2 | 24.7 | 44.6 | 61.6 | 50.1 | 41.4 | 28.7 | 23.3 | 22.2 | 27.7 | 26 | 21.5 |
| N-25MI | 22 | 26.1 | 45.4 | 60.7 | 49 | 40.7 | 27.9 | 22.7 | 21.4 | 26 | 25.4 | 21.9 |
| | | | | | | | | | | | | |
| E-50HI | 26.5 | 30.1 | 43 | 38.4 | 37 | 37.3 | 27.8 | 20.5 | 16.5 | 27.2 | 29.1 | 27.8 |
| E-50LO | 22.9 | 26.1 | 44.5 | 54.2 | 45.3 | 39.6 | 28.9 | 22.8 | 20.8 | 29.2 | 27.9 | 23.5 |
| E-50MI | 24.7 | 28.2 | 44.4 | 47 | 41.5 | 38.4 | 28.1 | 21.4 | 18.4 | 28.1 | 28.3 | 25.5 |
| H-50HI | 27.5 | 34.4 | 48.6 | 51.9 | 44.1 | 30.7 | 17.7 | 12.7 | 12.7 | 21.9 | 25.9 | 29 |
| H-50LO | 22.8 | 27 | 45.9 | 59.3 | 48.1 | 37.4 | 25 | 19.8 | 19.4 | 27.5 | 26.8 | 23.8 |
| H-50MI | 24.9 | 30.1 | 47.2 | 56 | 46.2 | 34.6 | 21.6 | 16.3 | 16.1 | 25 | 26.3 | 26 |
| N-50HI | 25.3 | 32.6 | 49.1 | 56.5 | 45.3 | 39 | 24.3 | 19.1 | 16.8 | 17.7 | 21.2 | 22.7 |
| N-50LO | 23.7 | 28.6 | 49.2 | 64.1 | 50.6 | 42 | 28.8 | 23.4 | 21.9 | 26.9 | 27 | 23.6 |
| N-50MI | 23.6 | 29.1 | 47.1 | 58.8 | 47.2 | 39.8 | 26.1 | 21 | 19.2 | 22.2 | 23.6 | 22.3 |
| | | | | | | | | | | | | |
| E-00HI | 31 | 31.3 | 35.6 | 23.4 | 27.2 | 32.4 | 25.4 | 16.7 | 10.7 | 21.9 | 29.1 | 34.5 |
| E-00LO | 25.2 | 28 | 45.4 | 43.6 | 40.6 | 42.8 | 32.5 | 21.9 | 14.7 | 27.8 | 28.9 | 26.4 |
| E-00MI | 26.6 | 30.2 | 42.9 | 38.1 | 36.8 | 37 | 27.6 | 20.3 | 16.3 | 27.1 | 29.1 | 27.9 |
| H-00HI | 35 | 43.5 | 46.6 | 44.4 | 40.7 | 22.1 | 9.7 | 6.2 | 6.3 | 14 | 24 | 37.4 |
| H-00LO | 25.8 | 31.3 | 49.5 | 59.2 | 48.4 | 36.3 | 23 | 17.6 | 17.3 | 26.4 | 27.7 | 26.8 |
| H-00MI | 27.6 | 34.7 | 48.6 | 51.6 | 44.2 | 30.8 | 17.5 | 12.5 | 12.5 | 21.8 | 25.8 | 29.2 |
| N-00HI | 30.9 | 41.6 | 53.6 | 51.3 | 42 | 37.5 | 19.6 | 14.5 | 11.4 | 8.1 | 12.8 | 22.4 |
| N-00LO | 23.2 | 28.3 | 46.9 | 59.5 | 47.7 | 40.2 | 26.7 | 21.4 | 19.6 | 23.1 | 24.1 | 22.2 |
| N-00MI | 25.4 | 32.8 | 49.3 | 56.5 | 45.4 | 39.2 | 24.3 | 19 | 16.7 | 17.5 | 21.1 | 22.7 |

*Table 5.2. Percentage changes in the long-term mean monthly runoff for all considered climate change scenarios in comparison with the reference period of 1971–2000*

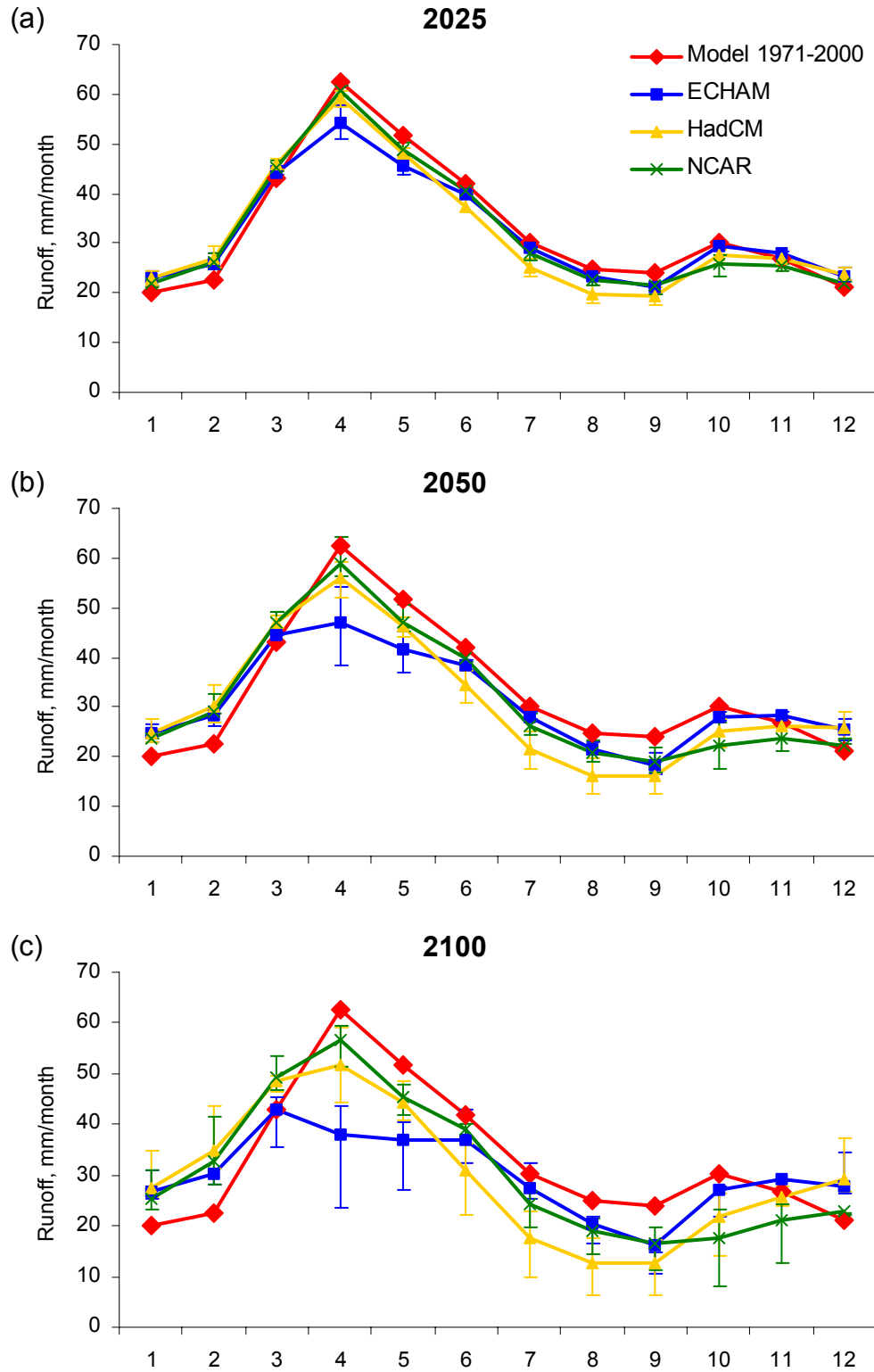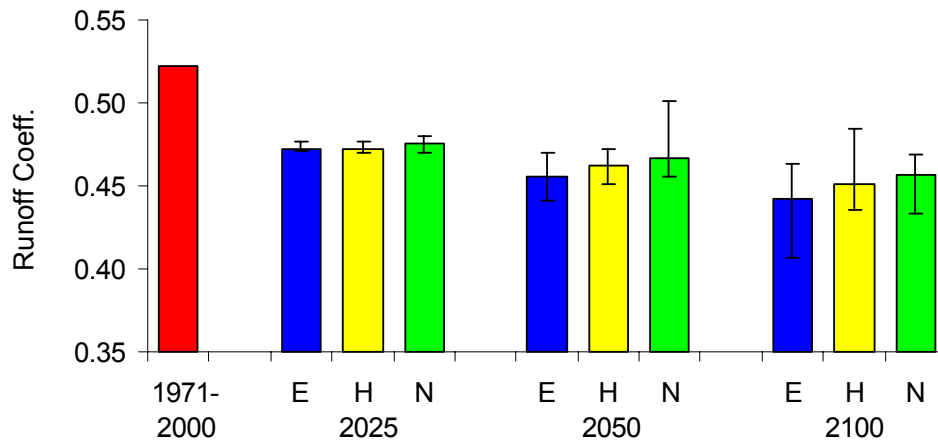| Scenario | Month | | | | | | | | | | | |
|---|---|---|---|---|---|---|---|---|---|---|---|---|
| | 1 | 2 | 3 | 4 | 5 | 6 | 7 | 8 | 9 | 10 | 11 | 12 |
| E-25HI | 21 | 24 | 6 | -18 | -15 | -6 | -4 | -9 | -17 | -4 | 5 | 18 |
| E-25LO | 8 | 9 | 3 | -8 | -8 | -3 | -2 | -4 | -7 | -1 | 3 | 7 |
| E-25MI | 13 | 16 | 3 | -13 | -12 | -5 | | -6 | -11 | -3 | 4 | 11 |
| H-25HI | 21 | 30 | 10 | -8 | -8 | -14 | -22 | -28 | -26 | -14 | -1 | 20 |
| H-25LO | 8 | 12 | 5 | -3 | -5 | -7 | -10 | -13 | -12 | -6 | 0 | 7 |
| H-25MI | 13 | 19 | 7 | -5 | -7 | -11 | -17 | -20 | -19 | -9 | 0 | 12 |
| N-25HI | 14 | 25 | 9 | -5 | -7 | -5 | -12 | -13 | -17 | -22 | -10 | 5 |
| N-25LO | 5 | 10 | 4 | -2 | -3 | -1 | -5 | -6 | -7 | -9 | -3 | 2 |
| N-25MI | 9 | 16 | 6 | -3 | -5 | -3 | -7 | -9 | -10 | -14 | -6 | 3 |
| | | | | | | | | | | | | |
| E-50HI | 32 | 34 | 0 | -39 | -28 | -11 | -8 | -17 | -31 | -10 | 8 | 31 |
| E-50LO | 13 | 16 | 4 | -13 | -12 | -6 | -4 | -8 | -13 | -4 | 4 | 11 |
| E-50MI | 23 | 25 | 4 | -25 | -20 | -9 | -7 | -14 | -23 | -7 | 5 | 21 |
| H//-50HI | 36 | 53 | 13 | -17 | -15 | -27 | -41 | -49 | -47 | -28 | -4 | 37 |
| H-50LO | 13 | 20 | 7 | -5 | -7 | -11 | -17 | -20 | -19 | -9 | 0 | 12 |
| H-50MI | 23 | 34 | 10 | -11 | -11 | -18 | -28 | -34 | -32 | -18 | -2 | 23 |
| N-50HI | 26 | 45 | 14 | -10 | -12 | -7 | -19 | -23 | -30 | -42 | -21 | 7 |
| N-50LO | 18 | 27 | 15 | 2 | -2 | 0 | -5 | -6 | -8 | -11 | 0 | 11 |
| N-50MI | 17 | 29 | 10 | -6 | -9 | -5 | -13 | -15 | -19 | -27 | -12 | 6 |
| | | | | | | | | | | | | |
| E-00HI | 54 | 39 | -17 | -63 | -47 | -23 | -16 | -32 | -55 | -28 | 8 | 63 |
| E-00LO | 25 | 24 | 6 | -30 | -22 | 2 | 8 | -12 | -38 | -8 | 7 | 25 |
| E-00MI | 32 | 34 | 0 | -39 | -29 | -12 | -9 | -18 | -32 | -11 | 8 | 32 |
| H-00HI | 74 | 93 | 9 | -29 | -21 | -47 | -68 | -75 | -74 | -54 | -11 | 77 |
| H-00LO | 28 | 39 | 16 | -5 | -6 | -14 | -24 | -29 | -27 | -13 | 3 | 27 |
| H-00MI | 37 | 54 | 13 | -18 | -14 | -27 | -42 | -50 | -48 | -28 | -4 | 38 |
| N-00HI | 53 | 85 | 25 | -18 | -19 | -11 | -35 | -42 | -52 | -73 | -53 | 6 |
| N-00LO | 15 | 26 | 9 | -5 | -8 | -4 | -11 | -14 | -18 | -24 | -10 | 5 |
| N-00MI | 26 | 46 | 15 | -10 | -12 | -7 | -19 | -23 | -30 | -42 | -22 | 7 |

*Fig. 5.2. Long-term mean monthly runoff in the reference period 1971–2000 and in the time horizons of 2025, 2050, and 2100 for all considered climate change scenarios*

*Table 5.3. Comparison of mean runoff coefficient (runoff depth/ precipitation depth) in the reference period 1971–2000 and in future time horizons for all considered climate change scenarios*

| Model 1971-2000 | Sensi-tivity | Scenario | | | | | | | | |
|---|---|---|---|---|---|---|---|---|---|---|
| | | 2025 | | | 2050 | | | 2100 | | |
| | | E | H | N | E | H | N | E | H | N |
| 0.522 | HI | 0.471 | 0.47 | 0.47 | 0.441 | 0.451 | 0.456 | 0.407 | 0.436 | 0.433 |
| | LO | 0.477 | 0.477 | 0.48 | 0.47 | 0.472 | 0.501 | 0.463 | 0.484 | 0.469 |
| | MI | 0.472 | 0.472 | 0.476 | 0.456 | 0.462 | 0.467 | 0.442 | 0.451 | 0.457 |



*Fig. 5.3. Comparison of mean runoff coefficient (runoff depth/ precipitation depth) in the reference period 1971–2000 and in future time horizons for all considered climate change scenarios*

Changes in the long-term mean monthly precipitation totals for the future time horizons according to the high-resolution ALADIN-Climate model in comparison with the reference period of 1961–1990 are presentend in Table 5.4 and Fig 5.4. The long-term mean monthly precipitation totals in the time horizons of 1961–1990 (measured), 2021–2050 and 2071–2100 are presented in Table 5.5 and Fig. 5.5.

*Table 5.4. Absolute and percentage changes in the long-term mean monthly precipitation totals according to the high-resolution ALADIN-Climate model for the time horizons of 2021–2050 and 2071–2100 in comparison with the reference period of 1961–1990 in the Hron river basin*

| Period | Month | | | | | | | | | | | |
|--------|------|------|------|------|------|------|------|------|------|------|------|------|
| | 1 | 2 | 3 | 4 | 5 | 6 | 7 | 8 | 9 | 10 | 11 | 12 |
| | Changes in mm/month | | | | | | | | | | | |
| 2021-2050 | -7.4 | -1.2 | 4.8 | 4.5 | -4.8 | 15.8 | 0.2 | -6.0 | -0.2 | 4.2 | 6.6 | -5.0 |
| 2071-2100 | 3.0 | 2.2 | -3.6 | 1.3 | 2.1 | -5.5 | -18.5 | -29.6 | -24.4 | 5.4 | 7.0 | -2.2 |
| | Changes in % | | | | | | | | | | | |
| 2021-2050 | -15.0 | -2.3 | 9.8 | 7.7 | -5.2 | 14.5 | 0.2 | -7.1 | -0.3 | 6.8 | 8.6 | -7.7 |
| 2071-2100 | 6.2 | 4.4 | -7.4 | 2.3 | 2.3 | -5.0 | -22.4 | -35.5 | -39.0 | 8.8 | 9.1 | -3.4 |
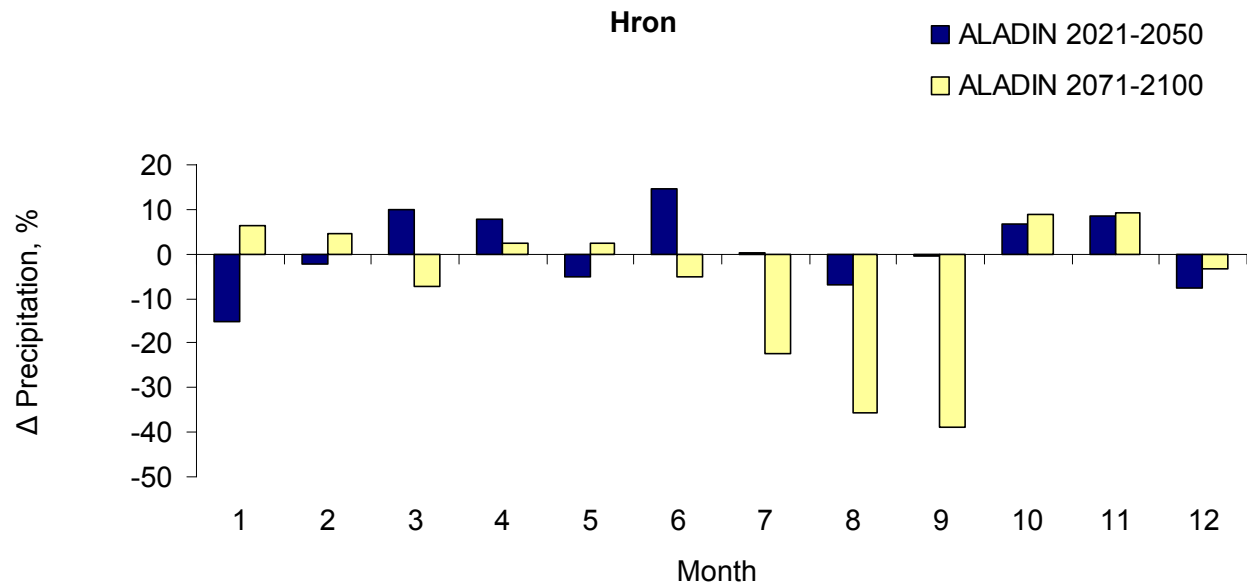


*Fig. 5.4. Percentage changes in the long-term mean monthly precipitation totals in time horizons of 2021–2050 and 2071–2100 in comparison with the reference period of 1961–1990 in the Hron river basin*

*Table 5.5. Long-term mean monthly precipitation totals in mm/month in the reference period 1961–1990 (measured) and in time horizons of 2021–2050 and 2071–2100 in the Hron river basin simulated by the high-resolution ALADIN-Climate model*

| Period | Month | | | | | | | | | | | |
|---|---|---|---|---|---|---|---|---|---|---|---|---|
| | 1 | 2 | 3 | 4 | 5 | 6 | 7 | 8 | 9 | 10 | 11 | 12 |
| 1961-1990 | 49.2 | 49.5 | 48.7 | 57.8 | 91.7 | 109.2 | 82.5 | 83.4 | 62.5 | 60.8 | 77.0 | 64.5 |
| 2021-2050 | 41.8 | 48.4 | 53.4 | 62.2 | 87.0 | 125.0 | 82.6 | 77.5 | 62.4 | 65.0 | 83.6 | 59.6 |
| 2071-2100 | 52.2 | 51.7 | 45.1 | 59.1 | 93.8 | 103.7 | 64.0 | 53.9 | 38.1 | 66.2 | 84.0 | 62.4 |
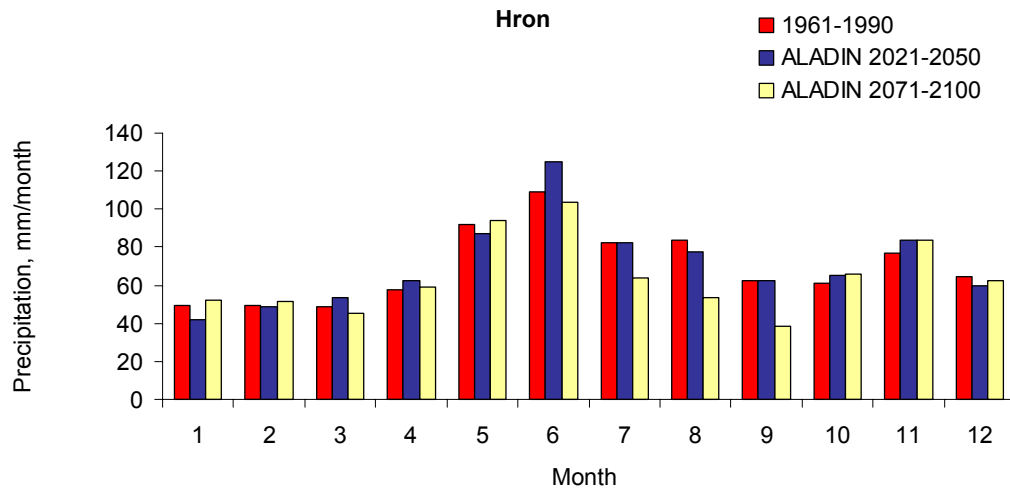


*Fig. 5.5. Long-term mean monthly precipitation totals in mm/month in the reference period of 1961–1990 and in time horizons of 2021–2050 and 2071–2100 in the Hron river basin*

Changes in the long-term mean monthly air temperature for the future time horizons in comparison with the reference period of 1961–1990 are presentend in Table 5.6 and Fig 5.6. Values of the long-term mean monthly air temperature in the time horizons of 1961–1990 (measured), 2021–2050 and 2071–2100 are presented in Table 5.7 and Fig. 5.7.
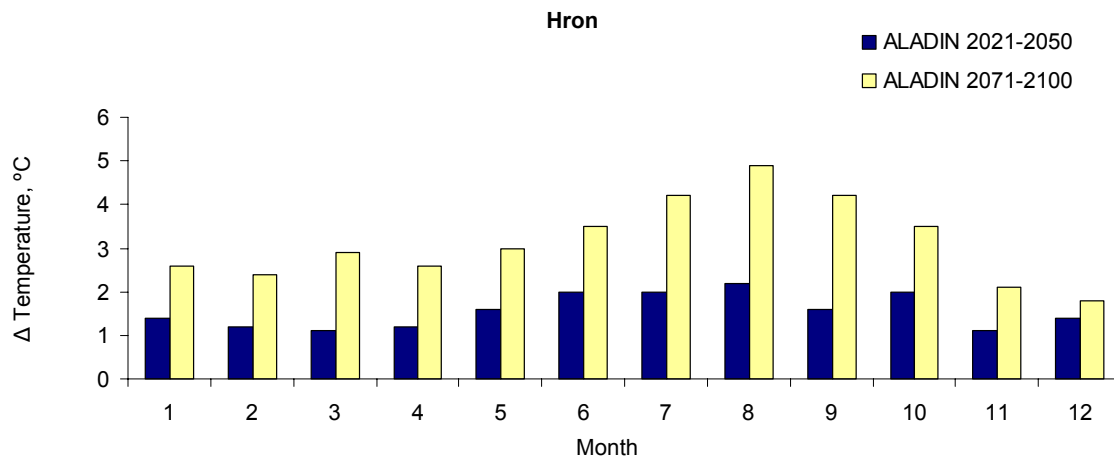
*Table 5.6. Absolute changes in the long-term mean monthly air temperature in time horizons of of 2021–2050 and 2071–2100 in comparison with the reference period of 1961–1990 in the Hron river basin predicted with ALADIN-Climate model*

| Period | Month | | | | | | | | | | | |
|---|---|---|---|---|---|---|---|---|---|---|---|---|
| | 1 | 2 | 3 | 4 | 5 | 6 | 7 | 8 | 9 | 10 | 11 | 12 |
| | Changes in ºC | | | | | | | | | | | |
| 2021-2050 | 1.4 | 1.2 | 1.1 | 1.2 | 1.6 | 2.0 | 2.0 | 2.2 | 1.6 | 2.0 | 1.1 | 1.4 |
| 2071-2100 | 2.6 | 2.4 | 2.9 | 2.6 | 3.0 | 3.5 | 4.2 | 4.9 | 4.2 | 3.5 | 2.1 | 1.8 |

44

*Fig. 5.6. Absolute changes in the long-term mean monthly air temperature in time horizons of 2021–2050 and 2071–2100 in comparison with the reference period of 1961–1990 in the Hron river basin*
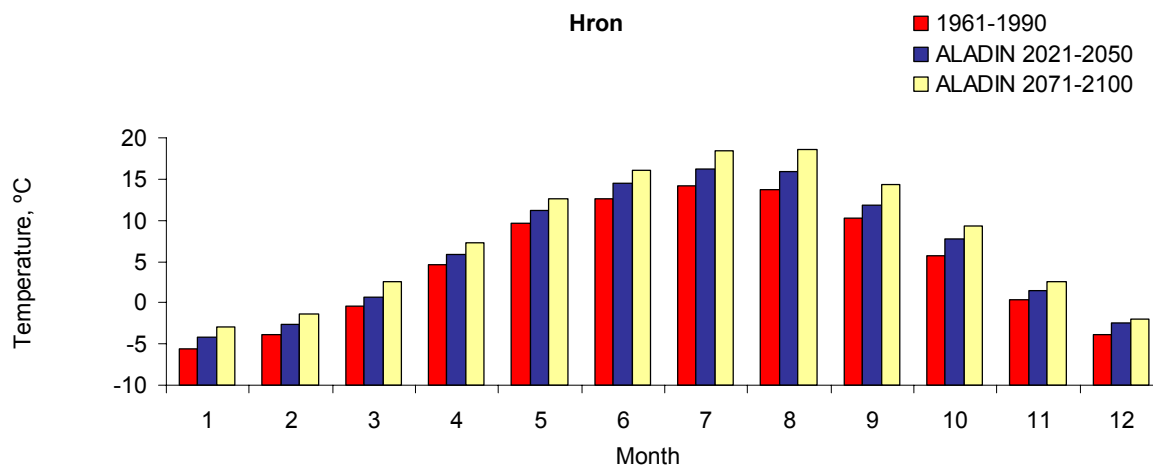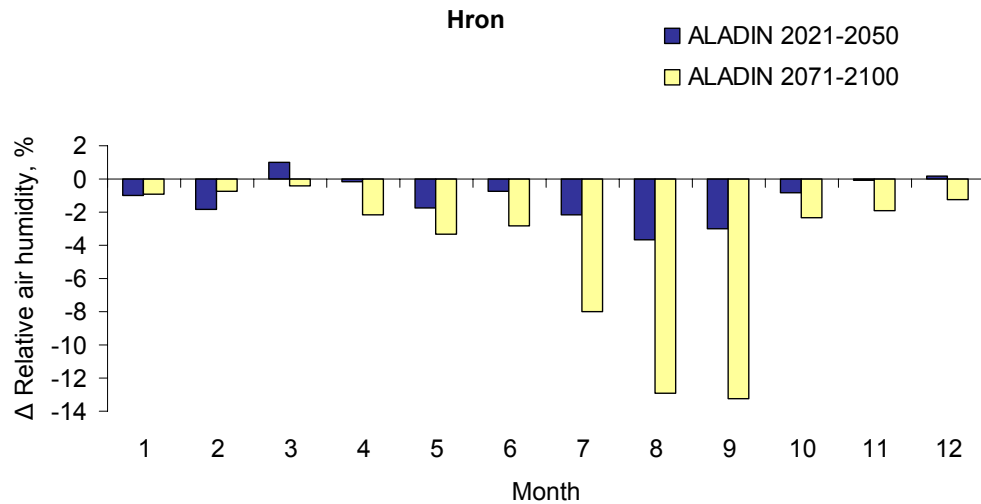
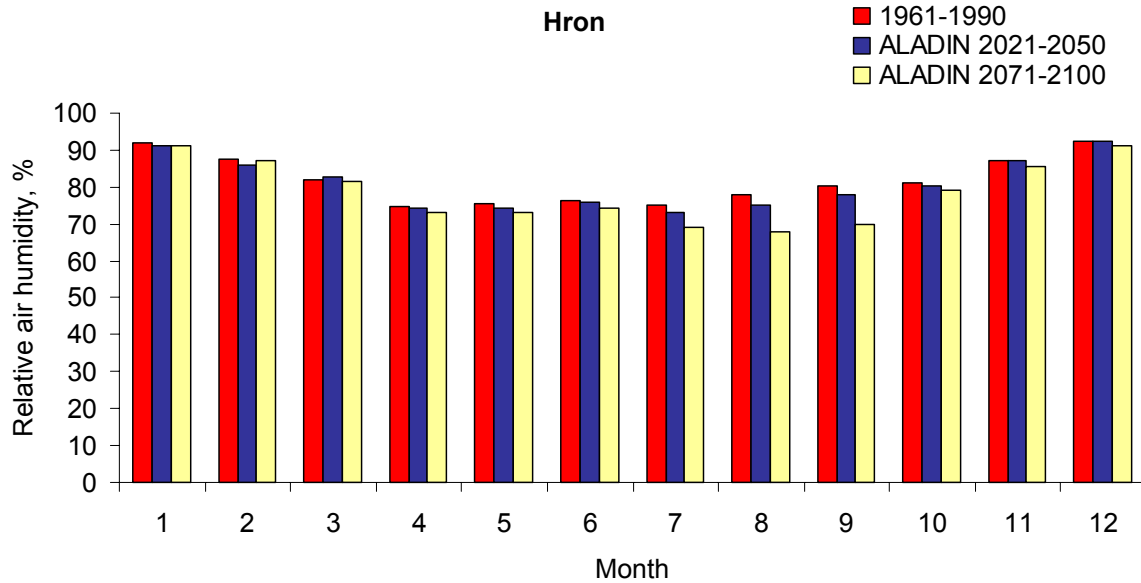*Table 5.7. Long-term mean monthly air temperature in ℃ in the reference period of 1961–1990 and in time horizons of 2021–2050 and 2071–2100 in the Hron river basin*

| Period | Month | | | | | | | | | | | |
|---|---|---|---|---|---|---|---|---|---|---|---|---|
| | 1 | 2 | 3 | 4 | 5 | 6 | 7 | 8 | 9 | 10 | 11 | 12 |
| 1961-1990 | -5.6 | -3.8 | -0.4 | 4.6 | 9.6 | 12.6 | 14.2 | 13.7 | 10.3 | 5.7 | 0.4 | -3.9 |
| 2021-2050 | -4.2 | -2.6 | 0.7 | 5.9 | 11.2 | 14.5 | 16.2 | 15.8 | 11.9 | 7.8 | 1.5 | -2.4 |
| 2071-2100 | -3.0 | -1.4 | 2.5 | 7.3 | 12.7 | 16.0 | 18.4 | 18.6 | 14.4 | 9.3 | 2.5 | -2.0 |



*Fig. 5.7. Long-term mean monthly air temperature in ℃ in the reference period of 1961–1990 and in time horizons of 2021–2050 and 2071–2100 in the Hron river basin*

Percentage changes in the long-term mean monthly relative air humidity accoring to the ALADIN-Climate model for the future time horizons in comparison with the reference period of 1961–1990 are presented in Table 5.8 and Fig 5.8. Values of the long-term mean monthly relative air humidity in the time horizons of 1961–1990 (measured), 2021–2050 and 2071–2100 are presented in Table 5.9 and Fig. 5.9.

*Table 5.8. Percentage changes in the long-term mean monthly relative air humidity in time horizons of 2021–2050 and 2071–2100 according to the ALADIN-Climate model in comparison with the reference period of 1961–1990 in the Hron river basin*

| Period | Month | | | | | | | | | | | |
|--------|------|------|-----|------|------|------|------|-------|-------|------|------|------|
| | 1 | 2 | 3 | 4 | 5 | 6 | 7 | 8 | 9 | 10 | 11 | 12 |
| | Changes in % | | | | | | | | | | | |
| 2021-2050 | -1.0 | -1.8 | 1.0 | -0.1 | -1.8 | -0.8 | -2.2 | -3.7 | -3.0 | -0.9 | -0.1 | 0.2 |
| 2071-2100 | -0.9 | -0.7 | -0.4 | -2.2 | -3.3 | -2.9 | -8.0 | -12.9 | -13.2 | -2.3 | -2.0 | -1.2 |



*Fig. 5.8. Percentage changes in the long-term mean monthly relative air humidity in time horizons of 2021–2050 and 2071–2100 in comparison with the reference period of 1961–1990 in the Hron river basin*

*Table 5.9. Long-term mean monthly air humidity in % in the reference period of 1961–1990 and in time horizons of 2021–2050 and 2071–2100 in the Hron river basin*

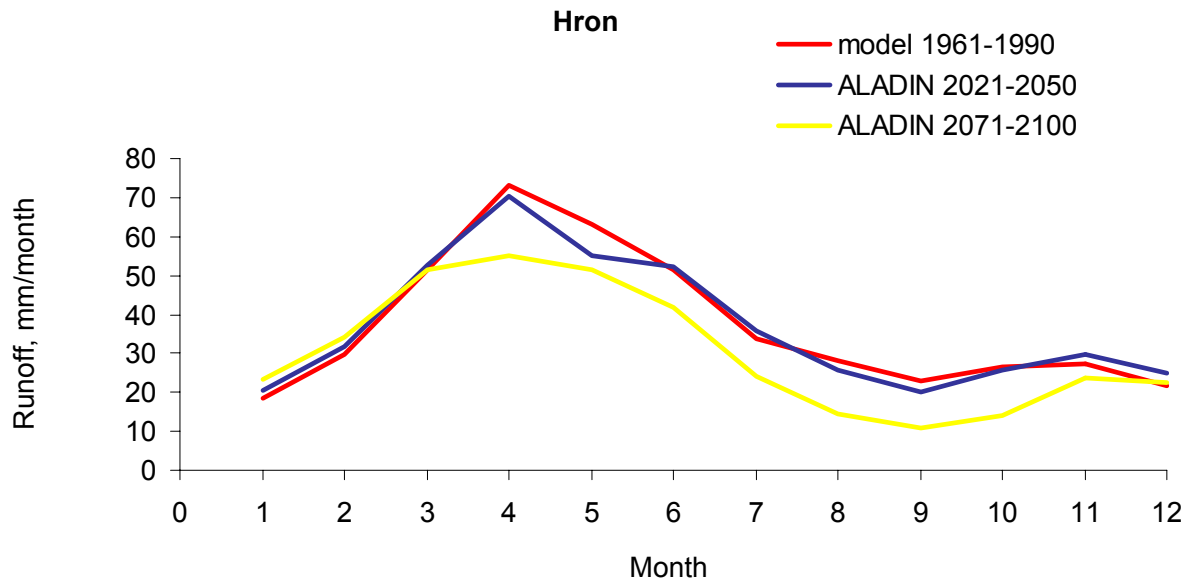| Period | Month | | | | | | | | | | | |
|--------|------|------|------|------|------|------|------|------|------|------|------|------|
| | 1 | 2 | 3 | 4 | 5 | 6 | 7 | 8 | 9 | 10 | 11 | 12 |
| 1961-1990 | 92.1 | 87.7 | 81.8 | 74.5 | 75.5 | 76.5 | 74.9 | 77.9 | 80.4 | 81.1 | 87.2 | 92.3 |
| 2021-2050 | 91.2 | 86.1 | 82.6 | 74.5 | 74.2 | 75.9 | 73.3 | 75.0 | 78.1 | 80.4 | 87.1 | 92.4 |
| 2071-2100 | 91.3 | 87.1 | 81.5 | 72.9 | 73.0 | 74.3 | 68.9 | 67.8 | 69.8 | 79.2 | 85.5 | 91.1 |

*Fig. 5.9. Long-term mean monthly relative air humidity in % in the reference period of 1961–1990 and in time horizons of 2021–2050 and 2071–2100 in the Hron river basin according the ALADIN-Climate model*

The monthly runoff series were simulated using the hydrological balance model with the changed input climate data according to the ALADIN-Climate model, and differences in the seasonal runoff distribution in the reference and future time horizons were estimated and compared. Values of the long-term mean monthly runoff in the time horizons of 1961–1990, 2021–2050 and 2071–2100 are presented in Table 5.10 and Fig. 5.10, the differences in the long-term mean monthly runoff for the future time horizons in comparison with the reference period are presentend in Table 5.11 and Fig 5.11, and the overall differnces in the mean values of funoff coeffients are given in Table 5.12 and Fig. 5.12.
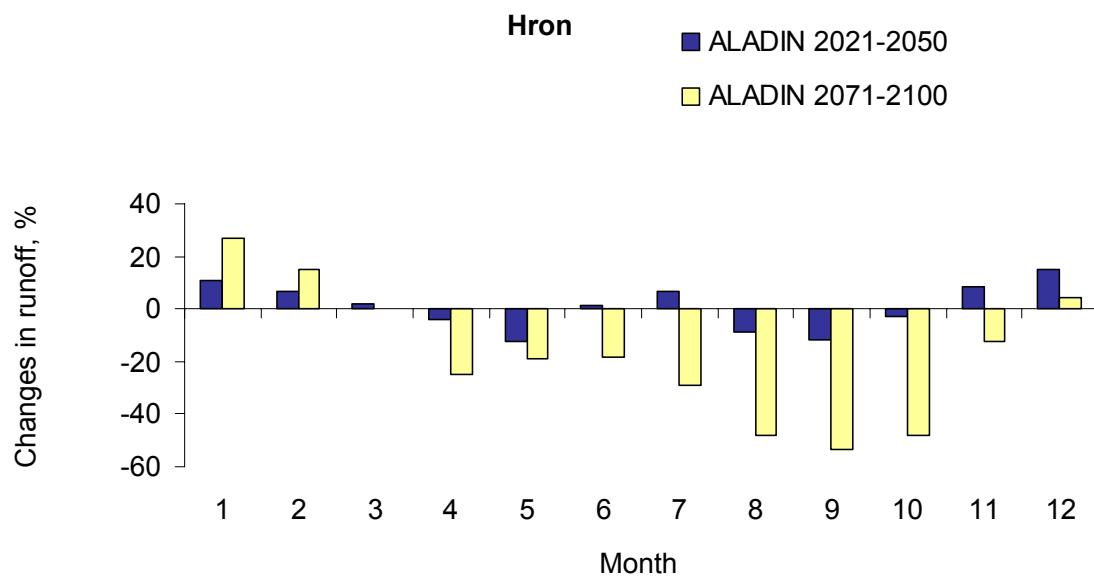
*Table 5.10. Long-term mean monthly runoff in mm/month in the reference period of 1961–1990 and in time horizons of 2021–2050 and 2071–2100 in the Hron river basin*

| Period | Month | | | | | | | | | | | |
|--------|------|------|------|------|------|------|------|------|------|------|------|------|
| | 1 | 2 | 3 | 4 | 5 | 6 | 7 | 8 | 9 | 10 | 11 | 12 |
| 1961-1990 | 18.4 | 29.6 | 51.5 | 73.3 | 63.2 | 51.3 | 33.8 | 28.1 | 22.8 | 26.6 | 27.3 | 21.5 |
| 2021-2050 | 20.4 | 31.6 | 52.5 | 70.2 | 55.3 | 52.1 | 36.0 | 25.6 | 20.1 | 25.9 | 29.6 | 24.7 |
| 2071-2100 | 23.4 | 34.0 | 51.4 | 55.3 | 51.3 | 41.8 | 24.0 | 14.6 | 10.7 | 13.9 | 23.8 | 22.5 |

*Fig. 5.10. Long-term mean monthly runoff in mm/month in the reference period of 1961–1990 and in time horizons of 2021–2050 and 2071–2100 in the Hron river basin simulated according to the ALADIN-Climate model*

*Table 5.11. Absolute and percentage changes in the long-term mean monthly runoff in time horizons of 2021–2050 and 2071–2100 in comparison with the reference period of 1961–1990 in the Hron river basin*

| Period | Month | | | | | | | | | | | |
|---|---|---|---|---|---|---|---|---|---|---|---|---|
| | 1 | 2 | 3 | 4 | 5 | 6 | 7 | 8 | 9 | 10 | 11 | 12 |
| Changes in mm/month | | | | | | | | | | | | |
| 2021-2050 | 2.0 | 2.0 | 1.0 | -3.0 | -7.9 | 0.7 | 2.2 | -2.5 | -2.7 | -0.8 | 2.3 | 3.2 |
| 2071-2100 | 5.0 | 4.5 | 0.0 | -18.0 | -11.9 | -9.5 | -9.8 | -13.5 | -12.1 | -12.7 | -3.4 | 0.9 |
| Changes in % | | | | | | | | | | | | |
| 2021-2050 | 10.9 | 6.9 | 2.0 | -4.1 | -12.5 | 1.5 | 6.4 | -8.9 | -11.9 | -2.8 | 8.4 | 14.8 |
| 2071-2100 | 26.9 | 15.1 | -0.1 | -24.6 | -18.8 | -18.5 | | -47.9 | -53.2 | -47.9 | -12.6 | 4.3 |

*Fig. 5.11. Percentage changes in the long-term mean monthly runoff in time horizons of 2021–2050 and 2071–2100 in comparison with the reference period of 1961–1990 in the Hron river basin*

*Table 5.12. Comparison of mean runoff coefficient (runoff depth/ precipitation depth) in the reference period 1961–1990 and in future time horizons*

| Time horizon | Runoff coefficient |
|---|---|
| 1961-1990 | 0.53 |
| 2021-2050 | 0.52 |
| 2071-2100 | 0.47 |
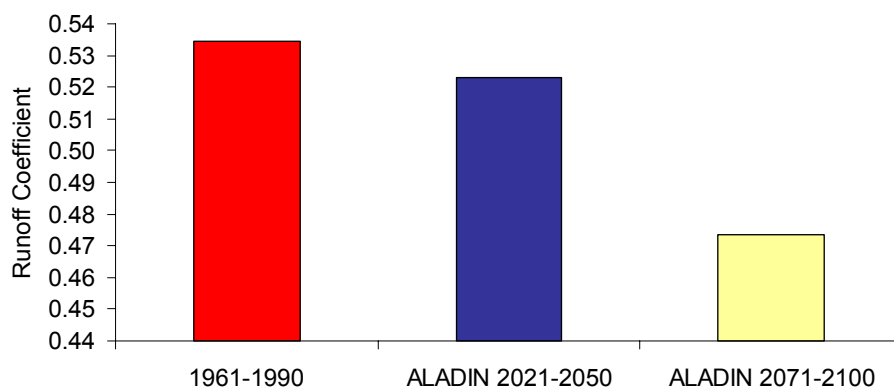


*Fig. 5.12. Comparison of mean runoff coefficient (runoff depth/ precipitation depth) in the reference period 1961–1990 and in future time horizons*

The presented results of modelling the long-term mean monthly runoff indicate future changes in the seasonal runoff distribution in the upper Hron river basin. According to the ALADIN-Climate runs, an increase in the long-term mean monthly runoff can be expected from November/December to February/March. The highest relative increase in mean monthly runoff in comparison with the reference period can be assumed in January, i.e., +11 % (+2 mm/month) in 2021–2050 and +27 % (+5 mm/month) in 2071-2100. This increase could be caused by an increase in air temperature during winter and a shift in the snow melting period from the spring months to the winter period. A decline in the long-term mean monthly runoff may occur from April to October/November. The most extreme relative decrease in monthly runoff could occur in May in 2021-2050, i.e., −12.5 % (−8 mm/month) and in August/September in 2071–2100, i.e., -53 % (−12 mm/month). In 2021–2050 there is a slight increase in runoff in June/July, i.e., +6 % (+2 mm/month). This increase may be caused by the increase in precipitation in 2021–2050 in comparison with the period of 1961–1990 (which generally was considered as a dry period). The decrease in runoff in August/September in 2021–2050 and 2071–2100 is mainly caused by the increase in air temperature (+2.2ºC in 2021–2050 and +4.9ºC in 2071–2100).

It could generally be concluded for both of the investigated time horizons, that during the winter and early spring periods, an increase in the long-term mean monthly runoff could be assumed. The period of an increase in runoff could occur from November/December to February/March. This increase could be caused by the increase in air temperature and a shift of the snow melting period the from spring months to the winter period. The period of the decrease in runoff could occur from May to October/November. The increase in winter runoff and the decrease in summer runoff are expected to be more extreme for the later time horizon.

*5.3 References*

Danihlík, R., Hlavčová, K., Kohnová, S., Parajka, J., Szolgay, J.: Scenarios of the change in the mean annual and monthly runoff in the Hron basin. J. Hydrol. Hydromech., 52, 2004, 4, pp. 291-302.

Hlavčová, K., Kohnová, S.: Proposed Framework Adaptive Measures. In: Pekárová, P., Szolgay, J., eds.: Assessment of Climate Change Impact on Selected Components of the Hydrosphere and Biosphere in the Hron and Váh River Basins. VEDA, Bratislava 2005, 419-492, ISBN 80-224-0884-0 (in Slovak).

Hlavčová, K., Lapin, M., Szolgay, J., Kohnová, S.: A simple model for estimation of climate change induced extreme daily precipitation changes. In: Heinonen, M., ed.: Proceedings of the Third international conference on Climate and Water. Finish Environment Institute SYKE, Helsinki 2007, 188-193.

Hlavčová, K., Parajka, J., Szolgay, J., Kohnová, S: Grid-based and conceptual approaches to modeling impact of climate change on runoff. Slovak Journal of Civil Engineering, XIV, 2006, 1, 19–29.

Hlavčová, K., Szolgay, J., Čunderlík, J., Parajka, J., Lapin, M.: Impact of climate change on the hydrological regime of rivers in Slovakia. Publication of the Slovak Committee for Hydrology No. 3. SUT, SNC IHP UNESCO, Bratislava 1999, 101 pp.

**Hlavčová, K., Szolgay, J., Kohnová, S., Hlásny, T.: Simulation of hydrological response to the future climate in the Hron river basin. Journal of Hydrology and Hydromechanics, 56, 2008, 3, 2008, 163−175.**

Hlavčová, K., Szolgay, J., Kohnová, S., Parajka, J.: Hydrological scenarios of changes in the mean annual and monthly runoff in Slovakia. In: Bruk, S., Petkovic, T., eds.: 23nd Conference of the Danube Countries on the Hydrological Forecasting and Hydrological Bases of Water Management. National Committee of Serbia for the IHP of UNESCO, Belgrade 2006, CD, 11 pp.

Szolgay, J., Hlavčová, K., Dušička, P.: Climate change and hydroenergetical potential in Slovakia. Environment, XXXVIII, 2004, 5, 257−261 (in Slovak).

Szolgay, J., Hlavčová, K., Lapin, M., Danihlík, R.: Impact of climate change on mean monthly of runoff in Slovakia. Meteorological Journal, 6, 2003, 3, 9–21.

Szolgay, J., Hlavčová, K., Parajka, J., Kohnová, S., Bálint, G.: Combined grid-based and conceptual approach to climate change impact estimation for water resources planning. In: Heinonen, M., ed.: Proceedings of the Third international conference on Climate and Water. Finish Environment Institute SYKE, Helsinki 2007, 449–454.

**Szolgay, J., Hlavčová, K., Parajka, J., Lapin, M., Kohnová, S., Hlásny, T.: Climate change impact on runoff in the Hron river basin. KEY Publishing, Ostrava 2009, 116 pp., ISBN 978-80-7418-006-4.**

Note: The bold-marked references present results of the CECILIA project.

## 6. The Buzău/Ialomița

*6.1 Introduction*

The simulated flow by WatBal model in actual and forthcoming climate change conditions allows the assessment of climate change impact in the water resources of Buzau and Ialomita river basins. WatBal model was calibrated by simulation of monthly average flow during 1971–2000 in 4 cross-sections of Buzau catchment and 13 cross-sections of Ialomita river basin. The time series data input in WatBal model, necessary to calibrate the model parameters of this model in Buzau and Ialomita river basins include: rainfall, air temperature and relative humidity, sunshine duration, wind speed and flow in the analyzed sections.

In order to assess the impacts of climate change in water resources in the selected area ware used as input data the results of different global and regional climatic models, with different spatial resolution, and also it is made a comparison of these hydrological simulations.

In a first stage, the assessment of climate change impacts on water resources was based on a total of 27 climate scenarios dermined by 3 global circulation models, ECHAM3/OPYC4, HadCM3 and NCAR-PCM each of these models being applied for three time horizons (2025 , 2050, 2100) and three intensities of climate changes phenomena.

In the second stage, the analysis of the impact of climate change on hydrological regime was performed using the simulations with a regional climate model with 25 km grid spacing developed by the ICTP (Trieste, Italy) and interpolated at a resolution of approx. 11 km. Potential monthly and annual flow modification was assess for two time horizon 2021–2050 and 2071–2100.

In the third part of the study at the assessing of the impact of climate change in hydrology were used as input data the results of regional climatic model with 10 km resolution, also for the two periods 2021–2050 and 2071–2100.

*6.2 Scenarios based on GCMs*

The output monthly series of climatic parameters from Global Climate Models (GCMs) were used to estimate forthcoming changes in global precipitation amount, daily average temperature and wind speed in Buzau and Ialomita river basins region.

The change of climate parameters estimated by the output of the meteorological models ECHAM3/OPYC4, HadCM3, NCAR-PCM  (noted below with E, H and N, respectively), for 3 time moments: 2025, 2050, 2100 (noted below with 25, 50 and 00, respectively) and for 3 estimations of the global temperature changes: LO = low (low estimate of climate sensitivity) - optimistic emission scenario, MI = middle (mean estimate of climate sensitivity) - mean emission scenario, HI = high (high estimate of climate sensitivity) - high emission scenario.

For each analysed sub-basin, the climatic input parameters used in the hydrological model were obtained by correcting of measured values with the modifications prescript for every parameter by the above-mentioned climatic models.

The monthly precipitation and mean wind speed, in the case of the three climate models (E, H and N), were obtained by addition of monthly deviation of monthly parameter, estimated for 2025, 2050 or 2100 (Tables 6.1, 6.2 and 6.3 respectively), to its measured values. Mean monthly temperatures used to hydrological simulation were obtained by addition to the actual temperatures of temperature increase in climate change hypothesis (Tables 6.1–6.3). Air temperature increase will have important effects over the snow depth. The rain will represent the most important part of precipitation and the snow depth will decrease.

The analysis of the variation of the simulated mean monthly discharges based on climate models generally show that they decrease compared to the current regime, except the river basins with a small reception surface and elevated mean altitude where there is a tendency of increase in mean monthly discharges in March–May. This tendency is more accentuated in the case of the simulations that were made using the outputs of the NCAR-PCM climate model, which indicates an increase in extreme phenomena.

To all analyzed stations it is observed a tendency of increase in mean monthly discharges during winter and spring periods and decrease during summer and autumn periods (Figures 6.3 and 6.4).

*Table 6.1. Monthly variations of air temperature (T), precipitation (P) and wind speed (V), obtained using ECHAM4/OPYC3 model, for the time moments 2025, 2050, 2100 and for 3 types of global temperature changes (LO, MI and HI)*

| Time period | Type | Parameter | Month | | | | | | | | | | | | Mean annual |
| --- | --- | --- | --- | --- | --- | --- | --- | --- | --- | --- | --- | --- | --- | --- | --- |
| | | | I | II | III | IV | V | VI | VII | VIII | IX | X | XI | XII | |
| 2025 | LO | T (°C) | 0.595 | 0.482 | 0.479 | 0.545 | 0.383 | 0.638 | 0.794 | 0.883 | 0.745 | 0.609 | 0.615 | 0.627 | 0.616 |
| | | P (%) | 1.616 | -3.696 | -1.366 | -2.294 | -0.566 | -2.804 | -1.751 | -3.752 | -2.893 | -0.858 | -0.664 | 0.286 | -1.604 |
| | | V (%) | -0.024 | -0.26 | 0.315 | -0.167 | 0.616 | -1.213 | -0.575 | -1.595 | -1.342 | -0.063 | -0.113 | -0.279 | -0.392 |
| | MI | T (°C) | 0.982 | 0.795 | 0.79 | 0.9 | 0.631 | 1.052 | 1.31 | 1.458 | 1.229 | 1.004 | 1.014 | 1.034 | 1.017 |
| | | P (%) | 2.666 | -6.098 | -2.255 | -3.784 | -0.934 | -4.627 | -2.889 | -6.19 | -4.774 | -1.416 | -1.095 | 0.473 | -2.647 |
| | | V (%) | -0.04 | -0.43 | 0.52 | -0.275 | 1.016 | -2.001 | -0.949 | -2.631 | -2.215 | -0.104 | -0.186 | -0.461 | -0.646 |
| | HI | T (°C) | 1.517 | 1.228 | 1.222 | 1.39 | 0.976 | 1.627 | 2.025 | 2.253 | 1.899 | 1.552 | 1.567 | 1.598 | 1.571 |
| | | P (%) | 4.121 | -9.424 | -3.484 | -5.849 | -1.443 | -7.15 | -4.465 | -9.567 | -7.378 | -2.189 | -1.692 | 0.73 | -4.091 |
| | | V (%) | -0.061 | -0.664 | 0.804 | -0.425 | 1.571 | -3.093 | -1.467 | -4.067 | -3.423 | -0.16 | -0.288 | -0.712 | -0.999 |
| 2050 | LO | T (°C) | 0.996 | 0.807 | 0.802 | 0.913 | 0.641 | 1.068 | 1.33 | 1.48 | 1.247 | 1.019 | 1.03 | 1.05 | 1.032 |
| | | P (%) | 2.707 | -6.19 | -2.289 | -3.842 | -0.948 | -4.697 | -2.933 | -6.284 | -4.846 | -1.438 | -1.112 | 0.48 | -2.687 |
| | | V (%) | -0.04 | -0.436 | 0.528 | -0.279 | 1.032 | -2.031 | -0.963 | -2.671 | -2.249 | -0.105 | -0.189 | -0.468 | -0.656 |
| | MI | T (°C) | 1.829 | 1.481 | 1.473 | 1.676 | 1.177 | 1.961 | 2.442 | 2.716 | 2.29 | 1.871 | 1.89 | 1.927 | 1.895 |
| | | P (%) | 4.969 | -11.364 | -4.202 | -7.053 | -1.74 | -8.622 | -5.384 | -11.536 | -8.897 | -2.64 | -2.041 | 0.881 | -4.934 |
| | | V (%) | -0.074 | -0.801 | 0.969 | -0.513 | 1.894 | -3.729 | -1.769 | -4.904 | -4.128 | -0.193 | -0.347 | -0.859 | -1.204 |
| | HI | T (°C) | 2.87 | 2.324 | 2.311 | 2.631 | 1.846 | 3.078 | 3.831 | 4.262 | 3.593 | 2.936 | 2.966 | 3.024 | 2.973 |
| | | P (%) | 7.797 | -17.831 | -6.593 | -11.067 | -2.731 | -13.529 | -8.448 | -18.101 | -13.96 | -4.142 | -3.202 | 1.382 | -7.741 |
| | | V (%) | -0.116 | -1.256 | 1.521 | -0.805 | 2.972 | -5.852 | -2.775 | -7.695 | -6.477 | -0.303 | -0.544 | -1.347 | -1.889 |
| 2100 | LO | T (°C) | 1.606 | 1.301 | 1.293 | 1.472 | 1.033 | 1.722 | 2.144 | 2.385 | 2.011 | 1.643 | 1.66 | 1.692 | 1.664 |
| | | P (%) | 4.363 | -9.978 | -3.689 | -6.193 | -1.528 | -7.571 | -4.727 | -10.129 | -7.812 | -2.318 | -1.792 | 0.773 | -4.332 |
| | | V (%) | -0.065 | -0.703 | 0.851 | -0.45 | 1.663 | -3.275 | -1.553 | -4.306 | -3.624 | -0.17 | -0.305 | -0.754 | -1.057 |
| | MI | T (°C) | 2.93 | 2.372 | 2.359 | 2.685 | 1.885 | 3.141 | 3.911 | 4.351 | 3.668 | 2.997 | 3.027 | 3.086 | 3.034 |
| | | P (%) | 7.959 | -18.201 | -6.73 | -11.296 | -2.788 | -13.81 | -8.623 | -18.477 | -14.249 | -4.228 | -3.268 | 1.411 | -7.902 |
| | | V (%) | -0.118 | -1.282 | 1.552 | -0.821 | 3.034 | -5.973 | -2.833 | -7.854 | -6.611 | -0.309 | -0.556 | -1.375 | -1.928 |
| | HI | T (°C) | 6.157 | 4.986 | 4.958 | 5.643 | 3.96 | 6.602 | 8.218 | 9.143 | 7.708 | 6.298 | 6.362 | 6.486 | 6.377 |
| | | P (%) | 16.726 | -38.249 | -14.142 | -23.739 | -5.858 | -29.021 | -18.121 | -38.829 | -29.945 | -8.884 | -6.868 | 2.964 | -16.606 |
| | | V (%) | -0.248 | -2.695 | 3.262 | -1.726 | 6.376 | -12.552 | -5.953 | -16.506 | -13.894 | -0.65 | -1.167 | -2.89 | -4.053 |

*Table 6.2. Monthly variations of air temperature (T), precipitation (P) and wind speed (V), output of HadCM3 model, estimations at the time period 2025, 2050, 2100 and for 3 types of global temperature change (LO, MI and HI)*

| Time period | Type | Parameter | Month | | | | | | | | | | | | Mean annual |
| | | | I | II | III | IV | V | VI | VII | VIII | IX | X | XI | XII | |
|---|---|---|---|---|---|---|---|---|---|---|---|---|---|---|---|
| 2025 | LO | T (°C) | 0.55 | 0.645 | 0.523 | 0.582 | 0.562 | 0.664 | 0.948 | 1.011 | 0.765 | 0.579 | 0.531 | 0.697 | 0.671 |
| | | P (%) | 1.796 | 1.717 | 2.931 | 1.464 | -2.03 | -4.946 | -7.014 | -4.257 | -3.124 | -1.196 | 1.443 | 2.883 | -0.861 |
| | | V (%) | 0.556 | 0.389 | 0.296 | 0.631 | 0.379 | 1.444 | 0.843 | -1.092 | 0.273 | 0.458 | 0.15 | 0.435 | 0.396 |
| | MI | T (°C) | 0.907 | 1.064 | 0.864 | 0.96 | 0.928 | 1.095 | 1.564 | 1.669 | 1.262 | 0.956 | 0.877 | 1.15 | 1.108 |
| | | P (%) | 2.963 | 2.833 | 4.836 | 2.416 | -3.35 | -8.16 | -11.57 | -7.024 | -5.155 | -1.974 | 2.381 | 4.757 | -1.42 |
| | | V (%) | 0.917 | 0.642 | 0.488 | 1.041 | 0.625 | 2.383 | 1.391 | -1.802 | 0.45 | 0.756 | 0.247 | 0.718 | 0.654 |
| | HI | T (°C) | 1.402 | 1.645 | 1.335 | 1.484 | 1.434 | 1.692 | 2.417 | 2.579 | 1.95 | 1.477 | 1.355 | 1.777 | 1.712 |
| | | P (%) | 4.58 | 4.378 | 7.475 | 3.733 | -5.176 | -12.61 | -17.89 | -10.86 | -7.966 | -3.051 | 3.679 | 7.351 | -2.195 |
| | | V (%) | 1.417 | 0.992 | 0.755 | 1.609 | 0.966 | 3.683 | 2.149 | -2.786 | 0.696 | 1.168 | 0.381 | 1.11 | 1.011 |
| 2050 | LO | T (°C) | 0.921 | 1.08 | 0.877 | 0.974 | 0.942 | 1.112 | 1.588 | 1.694 | 1.281 | 0.97 | 0.89 | 1.167 | 1.124 |
| | | P (%) | 3.008 | 2.876 | 4.91 | 2.452 | -3.4 | -8.284 | -11.75 | -7.13 | -5.233 | -2.004 | 2.417 | 4.829 | -1.442 |
| | | V (%) | 0.931 | 0.652 | 0.496 | 1.057 | 0.634 | 2.419 | 1.412 | -1.83 | 0.457 | 0.767 | 0.251 | 0.729 | 0.664 |
| | MI | T (°C) | 1.691 | 1.983 | 1.61 | 1.789 | 1.729 | 2.041 | 2.915 | 3.11 | 2.352 | 1.781 | 1.634 | 2.143 | 2.064 |
| | | P (%) | 5.523 | 5.279 | 9.013 | 4.502 | -6.242 | -15.21 | -21.57 | -13.09 | -9.606 | -3.679 | 4.437 | 8.865 | -2.647 |
| | | V (%) | 1.708 | 1.197 | 0.91 | 1.94 | 1.165 | 4.442 | 2.592 | -3.359 | 0.839 | 1.408 | 0.46 | 1.338 | 1.22 |
| | HI | T (°C) | 2.654 | 3.112 | 2.526 | 2.807 | 2.713 | 3.202 | 4.573 | 4.879 | 3.69 | 2.794 | 2.563 | 3.362 | 3.239 |
| | | P (%) | 8.666 | 8.284 | 14.14 | 7.064 | -9.795 | -23.86 | -33.84 | -20.54 | -15.07 | -5.773 | 6.962 | 13.91 | -4.154 |
| | | V (%) | 2.681 | 1.878 | 1.428 | 3.044 | 1.828 | 6.969 | 4.067 | -5.271 | 1.316 | 2.21 | 0.722 | 2.1 | 1.914 |
| 2100 | LO | T (°C) | 1.485 | 1.741 | 1.413 | 1.571 | 1.518 | 1.792 | 2.559 | 2.73 | 2.065 | 1.564 | 1.434 | 1.882 | 1.812 |
| | | P (%) | 4.849 | 4.635 | 7.914 | 3.953 | -5.481 | -13.35 | -18.94 | -11.49 | -8.435 | -3.23 | 3.896 | 7.784 | -2.324 |
| | | V (%) | 1.5 | 1.051 | 0.799 | 1.703 | 1.023 | 3.9 | 2.276 | -2.949 | 0.737 | 1.237 | 0.404 | 1.175 | 1.071 |
| | MI | T (°C) | 2.709 | 3.176 | 2.578 | 2.865 | 2.77 | 3.268 | 4.668 | 4.98 | 3.767 | 2.852 | 2.616 | 3.432 | 3.306 |
| | | P (%) | 8.845 | 8.455 | 14.44 | 7.21 | -9.998 | -24.36 | -34.54 | -20.97 | -15.39 | -5.892 | 7.106 | 14.2 | -4.241 |
| | | V (%) | 2.736 | 1.917 | 1.458 | 3.107 | 1.866 | 7.114 | 4.151 | -5.38 | 1.344 | 2.256 | 0.737 | 2.143 | 1.954 |
| | HI | T (°C) | 5.692 | 6.675 | 5.418 | 6.021 | 5.82 | 6.869 | 9.81 | 10.467 | 7.916 | 5.994 | 5.498 | 7.212 | 6.949 |
| | | P (%) | 18.59 | 17.77 | 30.34 | 15.15 | -21.01 | -51.19 | -72.6 | -44.06 | -32.33 | -12.38 | 14.93 | 29.84 | -8.912 |
| | | V (%) | 5.75 | 4.028 | 3.064 | 6.529 | 3.921 | 14.95 | 8.723 | -11.31 | 2.823 | 4.74 | 1.548 | 4.504 | 4.106 |

*Table 6.3. Monthly variations of air temperature (T), precipitation (P) and wind speed (V), output of NCAR-PCM model, estimations at the time periods 2025, 2050, 2100 and for 3 types of global temperature change (LO, MI and HI)*

| Time period | Type | Parameter | Month | | | | | | | | | | | | Mean annual |
| --- | --- | --- | --- | --- | --- | --- | --- | --- | --- | --- | --- | --- | --- | --- | --- |
| | | | I | II | III | IV | V | VI | VII | VIII | IX | X | XI | XII | |
| 2025 | LO | T (°C) | 0.468 | 0.439 | 0.351 | 0.23 | 0.257 | 0.383 | 0.732 | 0.776 | 0.665 | 0.586 | 0.455 | 0.495 | 0.486 |
| | | P (%) | 3.62 | 1.066 | 6.614 | 2.509 | 1.32 | -3.689 | -8.476 | -7.534 | -5.358 | -9.163 | -0.493 | 4.846 | -1.228 |
| | | V (%) | -1.062 | 0.705 | 1.713 | 4.219 | 4.097 | 4.572 | -3.416 | -1.337 | -0.997 | 0.385 | -1.498 | -0.075 | 0.609 |
| | MI | T (°C) | 0.772 | 0.725 | 0.579 | 0.38 | 0.425 | 0.631 | 1.208 | 1.28 | 1.097 | 0.967 | 0.751 | 0.817 | 0.803 |
| | | P (%) | 5.974 | 1.758 | 10.91 | 4.14 | 2.177 | -6.087 | -13.99 | -12.43 | -8.84 | -15.12 | -0.814 | 7.995 | -2.027 |
| | | V (%) | -1.752 | 1.163 | 2.827 | 6.962 | 6.76 | 7.543 | -5.636 | -2.206 | -1.645 | 0.635 | -2.472 | -0.124 | 1.005 |
| | HI | T (°C) | 1.193 | 1.12 | 0.894 | 0.587 | 0.656 | 0.976 | 1.867 | 1.978 | 1.696 | 1.494 | 1.16 | 1.263 | 1.24 |
| | | P (%) | 9.232 | 2.717 | 16.87 | 6.397 | 3.365 | -9.407 | -21.62 | -19.21 | -13.66 | -23.37 | -1.258 | 12.36 | -3.132 |
| | | V (%) | -2.708 | 1.797 | 4.369 | 10.76 | 10.45 | 11.658 | -8.71 | -3.41 | -2.543 | 0.981 | -3.821 | -0.192 | 1.552 |
| 2050 | LO | T (°C) | 0.784 | 0.736 | 0.587 | 0.385 | 0.431 | 0.641 | 1.226 | 1.3 | 1.114 | 0.981 | 0.762 | 0.83 | 0.815 |
| | | P (%) | 6.064 | 1.785 | 11.08 | 4.202 | 2.21 | -6.179 | -14.2 | -12.62 | -8.974 | -15.35 | -0.826 | 8.116 | -2.058 |
| | | V (%) | -1.779 | 1.181 | 2.87 | 7.067 | 6.863 | 7.657 | -5.721 | -2.24 | -1.67 | 0.645 | -2.51 | -0.126 | 1.02 |
| | MI | T (°C) | 1.439 | 1.351 | 1.078 | 0.708 | 0.791 | 1.176 | 2.251 | 2.386 | 2.045 | 1.801 | 1.399 | 1.523 | 1.496 |
| | | P (%) | 11.133 | 3.277 | 20.34 | 7.715 | 4.058 | -11.34 | -26.07 | -23.17 | -16.48 | -28.18 | -1.517 | 14.9 | -3.777 |
| | | V (%) | -3.266 | 2.167 | 5.268 | 12.97 | 12.6 | 14.058 | -10.5 | -4.112 | -3.066 | 1.183 | -4.608 | -0.231 | 1.872 |
| | HI | T (°C) | 2.257 | 2.119 | 1.692 | 1.11 | 1.242 | 1.846 | 3.532 | 3.743 | 3.209 | 2.827 | 2.195 | 2.39 | 2.347 |
| | | P (%) | 17.468 | 5.142 | 31.91 | 12.11 | 6.367 | -17.8 | -40.9 | -36.35 | -25.85 | -44.21 | -2.38 | 23.38 | -5.927 |
| | | V (%) | -5.124 | 3.401 | 8.266 | 20.36 | 19.77 | 22.058 | -16.48 | -6.452 | -4.811 | 1.857 | -7.23 | -0.363 | 2.937 |
| 2100 | LO | T (°C) | 1.263 | 1.186 | 0.947 | 0.621 | 0.695 | 1.033 | 1.976 | 2.095 | 1.796 | 1.582 | 1.228 | 1.337 | 1.313 |
| | | P (%) | 9.775 | 2.877 | 17.86 | 6.774 | 3.563 | -9.961 | -22.89 | -20.34 | -14.47 | -24.74 | -1.332 | 13.08 | -3.317 |
| | | V (%) | -2.867 | 1.903 | 4.626 | 11.39 | 11.06 | 12.343 | -9.222 | -3.61 | -2.692 | 1.039 | -4.046 | -0.203 | 1.644 |
| | MI | T (°C) | 2.304 | 2.163 | 1.727 | 1.133 | 1.268 | 1.884 | 3.605 | 3.821 | 3.275 | 2.885 | 2.241 | 2.439 | 2.395 |
| | | P (%) | 17.83 | 5.248 | 32.57 | 12.36 | 6.499 | -18.17 | -41.75 | -37.11 | -26.39 | -45.13 | -2.429 | 23.87 | -6.049 |
| | | V (%) | -5.23 | 3.471 | 8.438 | 20.78 | 20.18 | 22.515 | -16.82 | -6.586 | -4.911 | 1.895 | -7.38 | -0.37 | 2.998 |
| | HI | T (°C) | 4.842 | 4.546 | 3.629 | 2.381 | 2.664 | 3.96 | 7.576 | 8.03 | 6.883 | 6.063 | 4.709 | 5.127 | 5.034 |
| | | P (%) | 37.471 | 11.03 | 68.46 | 25.97 | 13.66 | -38.18 | -87.73 | -77.98 | -55.45 | -94.84 | -5.105 | 50.15 | -12.713 |
| | | V (%) | -10.99 | 7.295 | 17.73 | 43.67 | 42.41 | 47.316 | -35.35 | -13.84 | -10.32 | 3.983 | -15.51 | -0.778 | 6.301 |

Potential evapotranspiration was computed by the Penman equation. Real evapotranspiration is a function of soil moisture and transpiration of vegetation.

Annual real evapotranspiration, in hypothesis of scenarios 1, increases as a result of mean annual temperature increasing. During the season with intense vegetation growth (May - July) one produces the most intense real monthly evapotranspiration.

Taking into account the variation in air temperature, the precipitation and wind speed on the Buzau and Ialomita river basins in the hypothesis of climate changes, estimated at the level of 2025, 2050 and 2100, there were simulated the hydrographs of the mean monthly discharges at the 17 analyzed hydrometric stations. For each analyzed hydrometric station there were also calculated the deviations relative to the mean monthly discharges simulated in the hypothesis of the climate changes compared to the current flow regime (Tables 6.4–6.6).

As it can be observed both in Figures 6.1 and 6.2, and Tables 6.4–6.6, the mean annual discharge decreases in the conditions of climate changes, the relative errors to the current regime being larger for all climate models especially for the waiting horizon 2100, for which they reach 50 % (in case of high estimation scenario).

The analysis of the variation of the simulated mean monthly discharges based on climate models generally show that they decrease compared to the current regime, except the river basins with a small reception surface and elevated mean altitude where there is a tendency of increase in mean monthly discharges in March-May. This tendency is more accentuated in the case of the simulations that were made using the outputs of the NCAR-PCM climate model, which indicates an increase in extreme phenomena.

At all analyzed stations there is a tendency of increase in mean monthly discharges during winter and spring periods and decrease during summer and autumn periods (Figures 6.5 to 6.8).

For the comparison of the current multi-annual monthly hydrological regime with the modified one as a result of climate changes, in Tables 6.7 and 6.8 there are presented the mean monthly discharges as well as the maximum and minimum monthly discharges in the current regime and modified according to the scenario resulted from the NCAR-PCM (N) model (in the hypothesis of certain medium changes in climate parameters, MI) for two river basins, Buzau at the Racovita Hydrometric station and respectively Ialomita at the Tandarei hydrometric station. Also, in these tables there are also presented the relative deviations $\varepsilon$ (%), between the current regime and the modified one, correspondent to the three elements of monthly flow (minimum, maximum and average) for the three simulated waiting horizons 2025 (N25MI), 2050 (N50MI) and 2100 (N00MI).

From the analysis of the presented data it is noticed that the minimum flow can suffer major decreases in the June–September period, with relative deviations of up to 20–23%. Also, the regime of the maximum flow is strongly influenced by the decrease in the maximum discharges during summer period and possible increases of the maximum discharge in spring months (March–May).

*Table 6.4. Simulated mean annual discharges (Q_1) based on the ECHAM4/OPYC3 climate model and the relative errors (ε) to the current regime (Q_0)*

| Model E – ECHAM4/OPYC3 (German) | | 2025 | | | 2050 | | | 2100 | | |
|---|---|---|---|---|---|---|---|---|---|---|
| *Sub-basin/* *Surface (km$^2$)* | *Q_0* *(m$^3$/s)* | *Q_1* *(m$^3$/s)* | | | | | | | | |
| | | *LO* | *MI* | *HI* | *LO* | *MI* | *HI* | *LO* | *MI* | *HI* |
| NEHOIU | 18.91 | 18.24 | 17.8 | 17.21 | 17.78 | 16.86 | 15.76 | 17.11 | 15.7 | 12.63 |
| 1572 | ε (%) | -3.53 | -5.83 | -8.95 | -5.95 | -10.8 | -16.62 | -9.49 | -16.98 | -33.2 |
| MĂGURA | 24.4 | 25.07 | 24.42 | 23.54 | 24.4 | 23.03 | 21.38 | 23.39 | 21.28 | 16.83 |
| 2290 | ε (%) | 2.75 | 0.1 | -3.52 | 0 | -5.59 | -12.38 | -4.13 | -12.76 | -31.02 |
| BANIȚA | 27.68 | 26.79 | 26.09 | 25.16 | 26.07 | 24.63 | 22.94 | 25.01 | 22.85 | 18.45 |
| 3997 | ε (%). | -3.22 | -5.73 | -9.11 | -5.82 | -11.04 | -17.11 | -9.66 | -17.45 | -33.36 |
| RACOVITA | 27.27 | 25.55 | 24.46 | 23.02 | 24.42 | 22.22 | 19.78 | 22.79 | 19.65 | 13.97 |
| 5066 | ε (%). | -6.31 | -10.29 | -15.57 | -10.44 | -18.5 | -27.46 | -16.42 | -27.94 | -48.78 |
| MOROIENI | 4.69 | 4.6 | 4.54 | 4.45 | 4.54 | 4.4 | 4.22 | 4.44 | 4.2 | 3.65 |
| 263 | ε (%). | -1.76 | -3.05 | -4.94 | -3.11 | -6.12 | -10.04 | -5.28 | -10.26 | -22.03 |
| TÂRGOVIȘTE | 7.7 | 8.13 | 7.83 | 7.45 | 7.82 | 7.23 | 6.51 | 7.38 | 6.47 | 4.54 |
| 686 | ε (%). | 5.55 | 1.66 | -3.33 | 1.51 | -6.18 | -15.47 | -4.15 | -15.97 | -41.05 |
| BALENI ROMANI | 8.14 | 8.83 | 8.43 | 7.88 | 8.41 | 7.57 | 6.59 | 7.79 | 6.53 | 4.03 |
| 924 | ε (%). | 8.55 | 3.54 | -3.17 | 3.35 | -6.97 | -19.07 | -4.26 | -19.73 | -50.47 |
| SILIȘTEA SNAGOVULUI | 10.46 | 10 | 9.55 | 8.89 | 9.53 | 8.53 | 7.44 | 8.81 | 7.38 | 4.77 |
| 1885 | ε (%) | -4.36 | -8.66 | -14.95 | -8.84 | -18.39 | -28.84 | -15.77 | -29.41 | -54.37 |
| CÂMPINA | 7.83 | 8 | 7.81 | 7.56 | 7.81 | 7.41 | 6.93 | 7.52 | 6.9 | 5.61 |
| 476 | ε (%) | 2.2 | -0.2 | -3.46 | -0.29 | -5.34 | -11.51 | -4 | -11.86 | -28.39 |
| HALTA PRAHOVA | 11.44 | 11.12 | 10.91 | 10.62 | 10.9 | 10.46 | 9.93 | 10.58 | 9.9 | 8.49 |
| 978 | ε (%) | -2.82 | -4.63 | -7.14 | -4.7 | -8.6 | -13.24 | -7.55 | -13.49 | -25.8 |
| ADÂNCATA | 26.56 | 28.03 | 26.95 | 25.51 | 26.91 | 24.72 | 22.33 | 25.28 | 22.2 | 16.69 |
| 3682 | ε (%) | 5.53 | 1.47 | -3.94 | 1.32 | -6.93 | -15.92 | -4.82 | -16.4 | -37.15 |
| GURA VITIOAREI | 4.61 | 4.51 | 4.42 | 4.28 | 4.41 | 4.2 | 3.95 | 4.26 | 3.94 | 3.25 |
| 491 | ε (%) | -2.14 | -4.28 | -7.22 | -4.36 | -8.91 | -14.31 | -7.7 | -14.61 | -29.62 |
| MOARA DOMNEASCĂ | 9.97 | 9.45 | 9.12 | 8.69 | 9.11 | 8.45 | 7.74 | 8.62 | 7.7 | 6.16 |
| 1398 | ε (%) | -5.21 | -8.51 | -12.82 | -8.63 | -15.19 | -22.38 | -13.51 | -22.75 | -38.24 |
| CIORANI | 1.55 | 1.73 | 1.61 | 1.46 | 1.61 | 1.38 | 1.15 | 1.44 | 1.13 | 0.7 |
| 601 | ε (%) | 11.61 | 3.92 | -5.8 | 3.63 | -10.99 | -26 | -7.32 | -26.75 | -54.9 |
| COȘERENI | 39.37 | 41.07 | 39.35 | 37.03 | 39.28 | 35.76 | 31.84 | 36.66 | 31.63 | 22.69 |
| 6265 | ε (%) | 4.31 | -0.06 | -5.95 | -0.23 | -9.19 | -19.14 | -6.89 | -19.67 | -42.38 |
| SLOBOZIA | 40.04 | 43.92 | 41.57 | 38.47 | 41.48 | 36.8 | 31.83 | 37.99 | 31.58 | 21.39 |
| 9154 | ε (%) | 9.7 | 3.82 | -3.9 | 3.6 | -8.09 | -20.49 | -5.12 | -21.13 | -46.56 |
| ȚĂNDĂREI | 40.83 | 37.69 | 35.8 | 33.39 | 35.73 | 32.09 | 28.25 | 33.01 | 28.05 | 20.26 |
| 10309 | ε (%) | -7.69 | -12.32 | -18.24 | -12.49 | -21.43 | -30.82 | -19.17 | -31.3 | -50.38 |

*Table 6.5. Simulated mean annual discharges (Q_1) based on the HadCM3 climate model and the relative errors (ε) to the current regime (Q_0)*

| Model H - HadCM3 (British) | | 2025 | | | 2050 | | | 2100 | | |
|---|---|---|---|---|---|---|---|---|---|---|
| *Sub-basin/* *Surface (km$^2$)* | $Q\_0$ $(m^3/s)$ | $Q\_1$ $(m^3/s)$ | | | | | | | | |
| | | LO | MI | HI | LO | MI | HI | LO | MI | HI |
| NEHOIU | 18.91 | 18.19 | 17.73 | 17.11 | 17.7 | 16.75 | 15.62 | 17 | 15.56 | 12.8 |
| 1572 | ε (%) | -3.79 | -6.23 | -9.52 | -6.36 | -11.41 | -17.37 | -10.09 | -17.7 | -32.3 |
| MĂGURA | 24.4 | 25.02 | 24.35 | 23.44 | 24.32 | 22.93 | 21.28 | 23.3 | 21.19 | 17.3 |
| 2290 | ε (%) | 2.56 | -0.2 | -3.9 | -0.3 | -6.03 | -12.78 | -4.51 | -13.15 | -29.09 |
| BANIȚA | 27.68 | 26.97 | 26.4 | 25.63 | 26.38 | 25.19 | 23.81 | 25.51 | 23.74 | 20.31 |
| 3997 | ε (%). | -2.57 | -4.64 | -7.41 | -4.71 | -8.98 | -13.97 | -7.85 | -14.24 | -26.64 |
| RACOVITA | 27.27 | 25.52 | 24.45 | 23.06 | 24.41 | 22.3 | 20.05 | 22.84 | 19.94 | 15.55 |
| 5066 | ε (%). | -6.41 | -10.33 | -15.44 | -10.47 | -18.22 | -26.46 | -16.25 | -26.88 | -42.96 |
| MOROIENI | 4.69 | 4.62 | 4.57 | 4.49 | 4.56 | 4.44 | 4.29 | 4.48 | 4.28 | 3.78 |
| 263 | ε (%). | -1.45 | -2.55 | -4.19 | -2.59 | -5.15 | -8.55 | -4.47 | -8.74 | -19.37 |
| TÂRGOVIŞTE | 7.7 | 8.13 | 7.84 | 7.45 | 7.83 | 7.23 | 6.53 | 7.39 | 6.49 | 4.77 |
| 686 | ε (%). | 5.54 | 1.84 | -3.27 | 1.7 | -6.17 | -15.21 | -4.08 | -15.7 | -38.09 |
| BALENI ROMANI | 8.14 | 8.81 | 8.4 | 7.84 | 8.38 | 7.53 | 6.55 | 7.75 | 6.5 | 4.16 |
| 924 | ε (%). | 8.28 | 3.2 | -3.64 | 3.01 | -7.49 | -19.52 | -4.76 | -20.18 | -48.91 |
| SILIŞTEA SNAGOVULUI | 10.46 | 10.08 | 9.64 | 9.06 | 9.63 | 8.7 | 7.68 | 8.96 | 7.62 | 5.09 |
| 1885 | ε (%) | -3.61 | -7.76 | -13.38 | -7.92 | -16.77 | -26.57 | -14.32 | -27.11 | -51.31 |
| CÂMPINA | 7.83 | 7.99 | 7.8 | 7.54 | 7.79 | 7.39 | 6.9 | 7.49 | 6.87 | 5.71 |
| 476 | ε (%) | 2.08 | -0.38 | -3.74 | -0.47 | -5.66 | -11.86 | -4.29 | -12.2 | -27.05 |
| HALTA PRAHOVA | 11.44 | 11.17 | 10.99 | 10.75 | 10.99 | 10.61 | 10.16 | 10.71 | 10.14 | 9 |
| 978 | ε (%) | -2.35 | -3.89 | -6.02 | -3.95 | -7.26 | -11.14 | -6.38 | -11.35 | -21.34 |
| ADÂNCATA | 26.56 | 28.06 | 26.94 | 25.5 | 26.9 | 24.72 | 22.36 | 25.27 | 22.25 | 17.75 |
| 3682 | ε (%) | 5.65 | 1.45 | -4 | 1.29 | -6.9 | -15.8 | -4.84 | -16.23 | -33.17 |
| GURA VITIOAREI | 4.61 | 4.54 | 4.46 | 4.35 | 4.46 | 4.28 | 4.08 | 4.33 | 4.07 | 3.53 |
| 491 | ε (%) | -1.58 | -3.33 | -5.79 | -3.4 | -7.19 | -11.56 | -6.2 | -11.81 | -23.5 |
| MOARA DOMNEASCĂ | 9.97 | 9.46 | 9.14 | 8.73 | 9.13 | 8.52 | 7.88 | 8.67 | 7.85 | 6.72 |
| 1398 | ε (%) | -5.08 | -8.29 | -12.39 | -8.4 | -14.54 | -20.92 | -13.02 | -21.23 | -32.6 |
| CIORANI | 1.55 | 1.73 | 1.61 | 1.46 | 1.6 | 1.39 | 1.17 | 1.44 | 1.16 | 0.82 |
| 601 | ε (%) | 11.46 | 3.83 | -5.66 | 3.55 | -10.6 | -24.31 | -7.1 | -24.98 | -47.39 |
| COŞERENI | 39.37 | 41.03 | 39.3 | 37.02 | 39.24 | 35.78 | 32.09 | 36.66 | 31.9 | 24.63 |
| 6265 | ε (%) | 4.22 | -0.18 | -5.98 | -0.34 | -9.12 | -18.49 | -6.89 | -18.97 | -37.45 |
| SLOBOZIA | 40.04 | 43.84 | 41.44 | 38.36 | 41.35 | 36.71 | 31.94 | 37.87 | 31.7 | 22.87 |
| 9154 | ε (%) | 9.51 | 3.51 | -4.18 | 3.29 | -8.31 | -20.22 | -5.4 | -20.82 | -42.87 |
| ȚĂNDĂREI | 40.83 | 37.7 | 35.84 | 33.51 | 35.77 | 32.29 | 28.75 | 33.15 | 28.57 | 22.16 |
| 10309 | ε (%) | -7.68 | -12.23 | -17.94 | -12.4 | -20.93 | -29.6 | -18.81 | -30.03 | -45.72 |

*Table 6.6. Simulated mean annual discharges (Q_1) based on the NCAR-PCM climate model and the relative errors (ε) to the current regime (Q_0)*

| Model N - NCAR-PCM (USA) | | 2025 | | | 2050 | | | 2100 | | |
|---|---|---|---|---|---|---|---|---|---|---|
| *Sub-basin/* Surface (km²) | $Q\_0$ $(m^3/s)$ | $Q\_1$ $(m^3/s)$ | | | | | | | | |
| | | *LO* | *MI* | *HI* | *LO* | *MI* | *HI* | *LO* | *MI* | *HI* |
| NEHOIU | 18.91 | 18.16 | 17.66 | 17.04 | 17.64 | 16.68 | 15.58 | 16.93 | 15.52 | 13.07 |
| 1572 | ε (%) | -3.93 | -6.57 | -9.87 | -6.68 | -11.78 | -17.59 | -10.44 | -17.91 | -30.88 |
| MĂGURA | 24.4 | 25.02 | 24.37 | 23.49 | 24.34 | 23 | 21.51 | 23.35 | 21.42 | 18.26 |
| 2290 | ε (%) | 2.56 | -0.12 | -3.72 | -0.23 | -5.72 | -11.85 | -4.3 | -12.18 | -25.14 |
| BANIȚA | 27.68 | 27.11 | 26.64 | 26.01 | 26.62 | 25.66 | 24.55 | 25.91 | 24.66 | 21.86 |
| 3997 | ε (%). | -2.05 | -3.76 | -6.03 | -3.82 | -7.29 | -11.31 | -6.4 | -10.9 | -21.01 |
| RACOVITA | 27.27 | 25.62 | 24.63 | 23.33 | 24.59 | 22.62 | 20.57 | 23.12 | 20.47 | 16.72 |
| 5066 | ε (%). | -6.03 | -9.68 | -14.44 | -9.82 | -17.03 | -24.56 | -15.19 | -24.94 | -38.68 |
| MOROIENI | 4.69 | 4.63 | 4.59 | 4.53 | 4.59 | 4.49 | 4.38 | 4.52 | 4.37 | 4.01 |
| 263 | ε (%) | -1.16 | -2.11 | -3.37 | -2.14 | -4.08 | -6.52 | -3.57 | -6.65 | -14.35 |
| TÂRGOVIŞTE | 7.7 | 8.15 | 7.88 | 7.53 | 7.87 | 6.08 | 6.7 | 7.48 | 6.08 | 5.19 |
| 686 | ε (%). | 5.83 | 2.29 | -2.23 | 2.17 | -21.02 | -13.02 | -2.95 | -21.02 | -32.61 |
| BALENI ROMANI | 8.14 | 8.86 | 8.49 | 7.98 | 8.47 | 7.7 | 6.81 | 7.9 | 5.85 | 4.69 |
| 924 | ε (%). | 8.87 | 4.28 | -1.93 | 4.11 | -5.4 | -16.28 | -2.93 | -28.14 | -42.35 |
| SILIŞTEA SNAGOVULUI | 10.46 | 10.23 | 9.9 | 9.45 | 9.89 | 9.16 | 8.33 | 9.38 | 8.29 | 6.15 |
| 1885 | ε (%) | -2.12 | -5.28 | -9.6 | -5.39 | -12.39 | -20.3 | -10.34 | -20.71 | -41.19 |
| CÂMPINA | 7.83 | 7.99 | 7.8 | 7.55 | 7.79 | 7.4 | 6.95 | 7.5 | 6.62 | 5.89 |
| 476 | ε (%) | 2.08 | -0.36 | -3.61 | -0.45 | -5.44 | -11.25 | -4.13 | -15.42 | -24.76 |
| HALTA PRAHOVA | 11.44 | 11.22 | 11.08 | 10.89 | 11.07 | 10.78 | 10.43 | 10.85 | 10.41 | 9.56 |
| 978 | ε (%) | -1.95 | -3.16 | -4.84 | -3.2 | -5.79 | -8.85 | -5.11 | -9.02 | -16.47 |
| ADÂNCATA | 26.56 | 28.19 | 27.17 | 25.82 | 27.13 | 25.12 | 23.01 | 25.62 | 31.04 | 19.01 |
| 3682 | ε (%) | 6.15 | 2.3 | -2.76 | 2.16 | -5.41 | -13.35 | -3.54 | 16.88 | -28.44 |
| GURA VITIOAREI | 4.61 | 4.56 | 4.49 | 4.4 | 4.49 | 4.35 | 4.18 | 4.38 | 4.17 | 3.77 |
| 491 | ε (%) | -1.16 | -2.64 | -4.66 | -2.7 | -5.81 | -9.35 | -4.99 | -9.54 | -18.33 |
| MOARA DOMNEASCĂ | 9.97 | 9.51 | 9.21 | 8.85 | 9.2 | 8.66 | 8.1 | 8.79 | 8.07 | 7.21 |
| 1398 | ε (%) | -4.65 | -7.58 | -11.23 | -7.68 | -13.18 | -18.73 | -11.79 | -19 | -27.63 |
| CIORANI | 1.55 | 1.75 | 1.65 | 1.52 | 1.65 | 1.45 | 1.27 | 1.5 | 1.09 | 1 |
| 601 | ε (%) | 13.08 | 6.47 | -1.79 | 6.23 | -6.12 | -17.83 | -3.04 | -29.55 | -35.75 |
| COŞERENI | 39.37 | 41.25 | 39.68 | 37.64 | 39.62 | 36.51 | 33.22 | 37.31 | 33.64 | 26.92 |
| 6265 | ε (%) | 4.76 | 0.77 | -4.41 | 0.63 | -7.28 | -15.63 | -5.24 | -14.57 | -31.62 |
| SLOBOZIA | 40.04 | 44.18 | 42.02 | 39.22 | 41.93 | 37.71 | 33.35 | 38.78 | 33.13 | 25.27 |
| 9154 | ε (%) | 10.34 | 4.95 | -2.04 | 4.74 | -5.82 | -16.71 | -3.14 | -17.26 | -36.89 |
| ȚĂNDĂREI | 40.83 | 37.96 | 36.27 | 34.13 | 36.2 | 33.01 | 29.77 | 33.8 | 29.61 | 23.99 |
| 10309 | ε (%) | -7.04 | -11.19 | -16.42 | -11.34 | -19.15 | -27.1 | -17.23 | -27.5 | -41.24 |

*Figure 6.1. The mean annual discharges simulated for the Buzau River Basin at NEHOIU and RACOVIȚA gauging stations, for mean emission scenario (MI)*
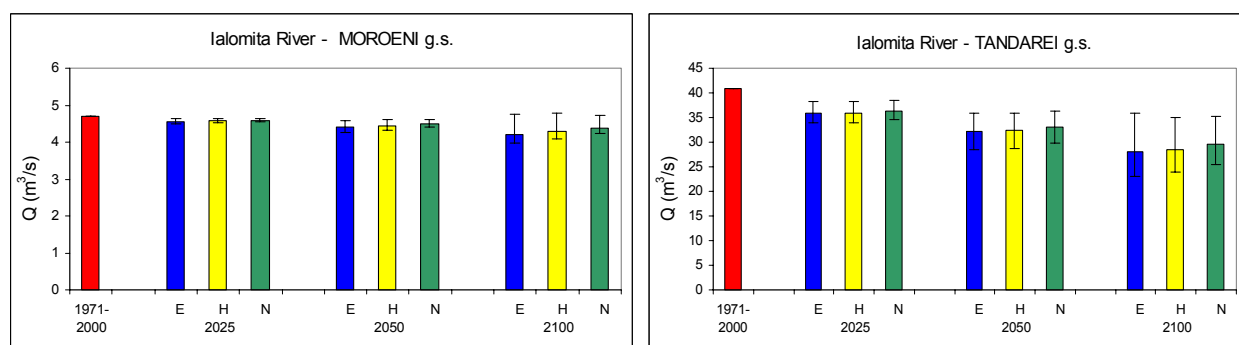


*Figure 6.2. The mean annual discharges simulated for the Ialomita River Basin at MOROENI and ȚĂNDĂREI gauging stations, for mean emission scenario (MI)*
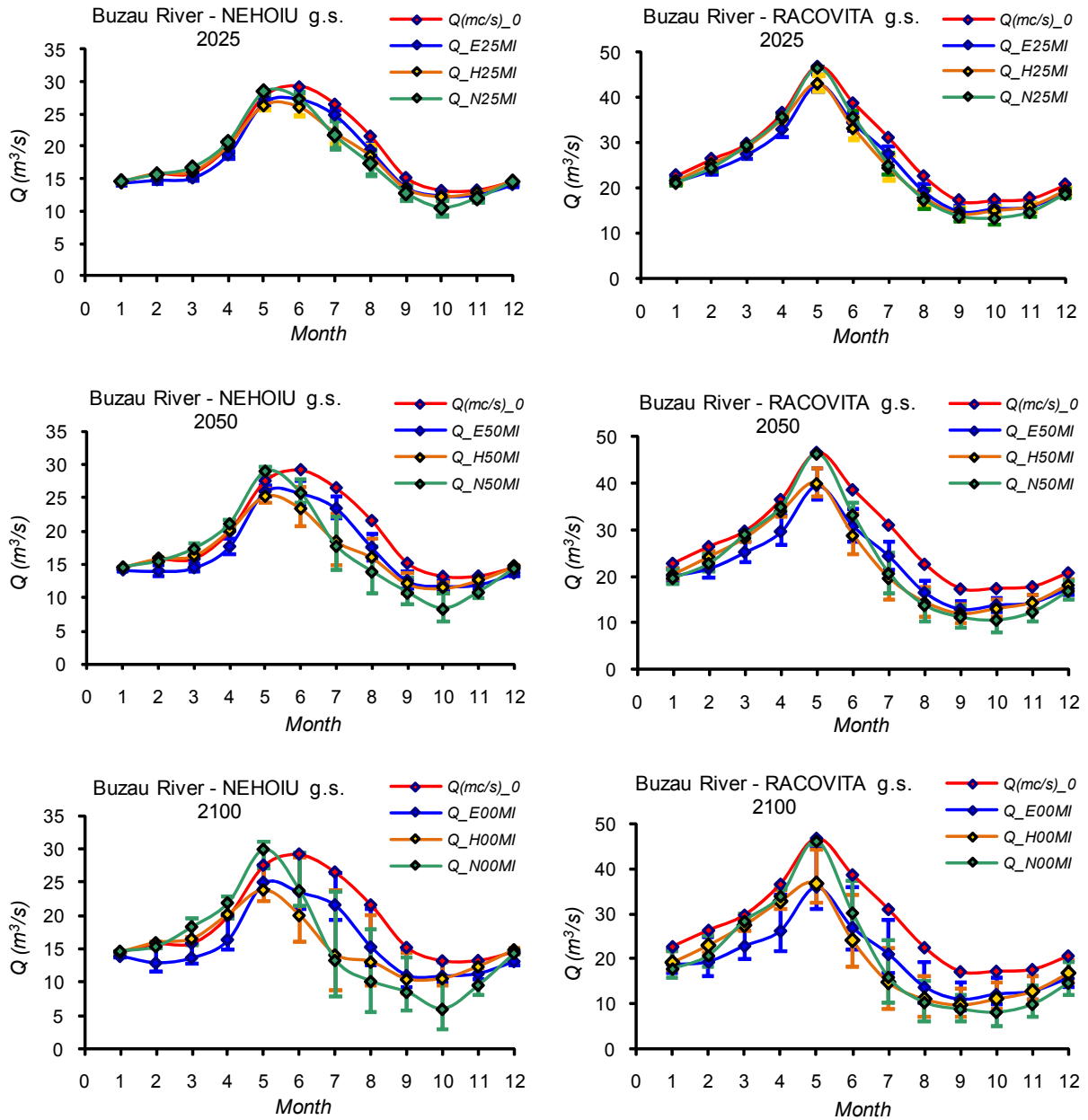
*Figure 6.3. Variation of current and simulated mean monthly discharges, Buzău River at NEHOIU and RACOVIȚA gauging stations, for mean emission scenario (MI)*
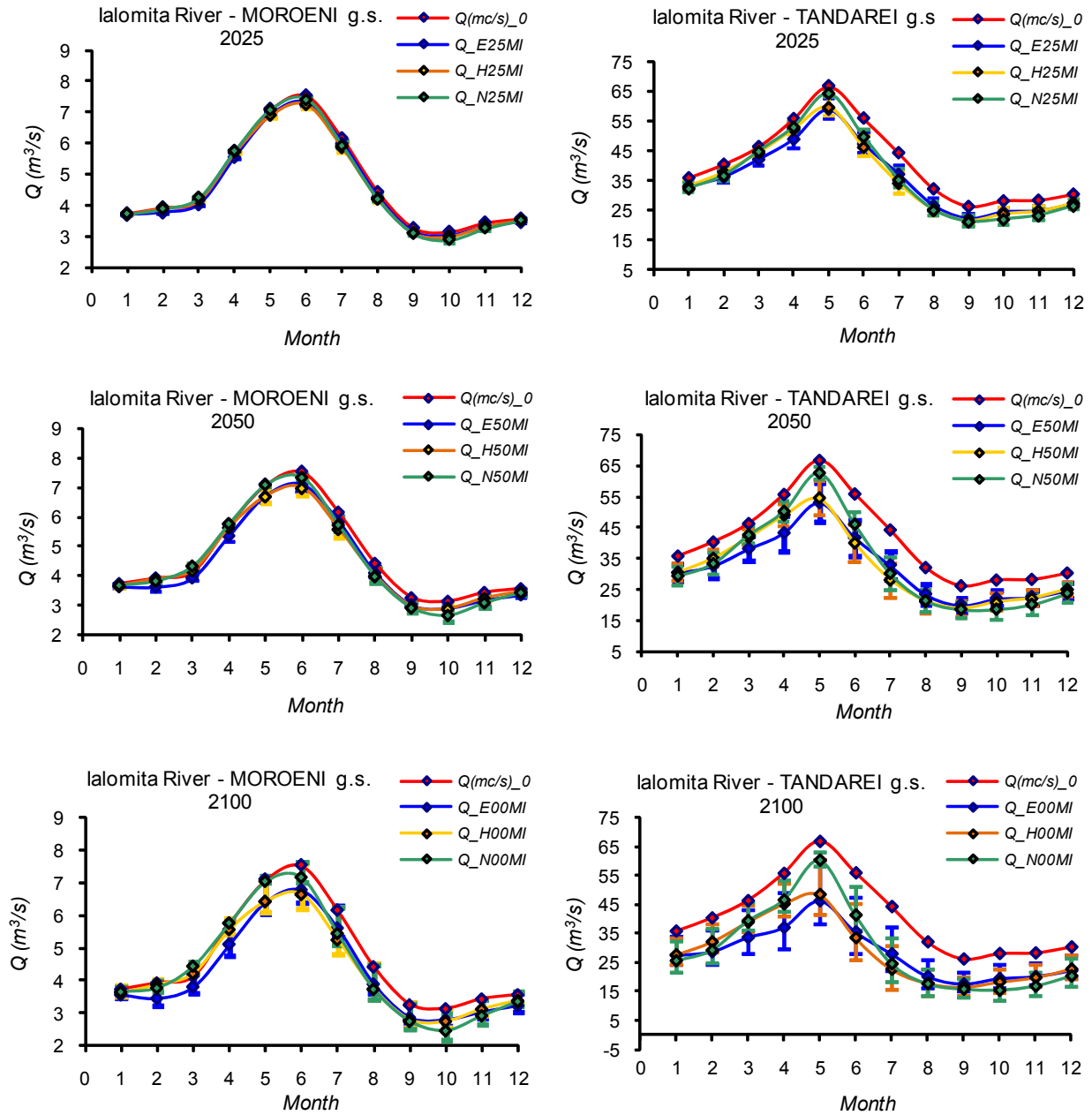
*Figure 6.4. Variation of current and simulated mean monthly discharges, Ialomita River at MOROEN and TANDAREI gauging station, for mean emission scenario (MI)*

## 6.3 Scenarios based on regional climate model with 25×25 km spatial resolution

In the second stage, the analysis of the impact of climate change on hydrological regime was performed using the simulations with a regional climate model with 25 km grid spacing developed by the ICTP (Trieste, Italy) and interpolated at a resolution of about 11 km. Potential changes of the main climatic parameters were calculated as differences between climatic parameters values corresponding to the two periods 2021–2050 and 2071–2100 over the reference period 1971–2000, for each calendar month.

The modification of climatic parameters used in hydrological scenarios, i.e. the difference

between reference period (1971–2000) and near future (1921–2050) or the end of century (2050–2100), are provided by Romanian National Administration of Meteorology (NAM) as grid with the values of each needed parameters.

The obtained grid points of the RegCM outputs for Buzau – Ialomita area (Romania) and the limits of each sub-basins are presented in Figure 6.5.
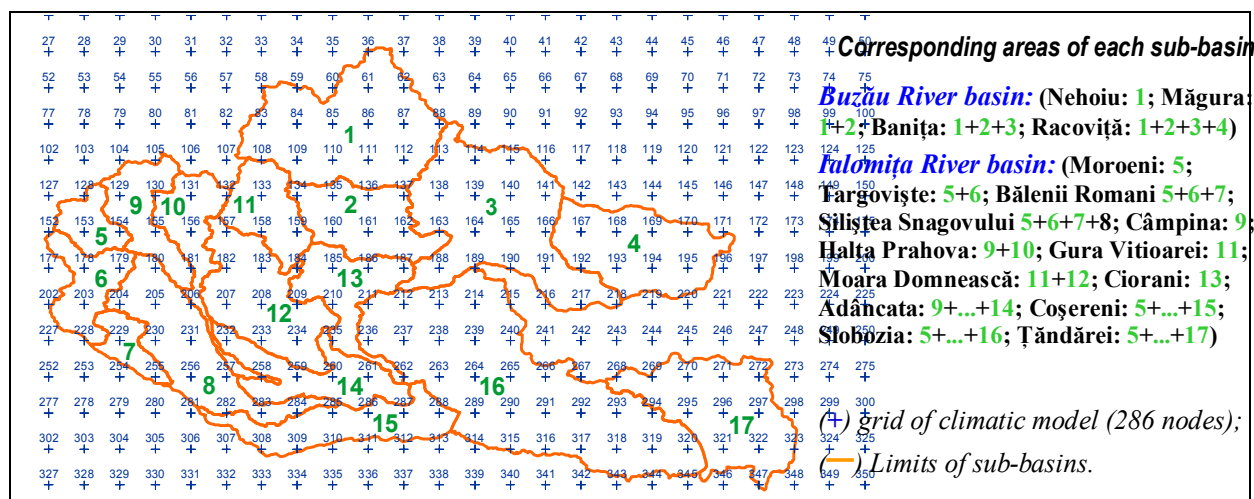


*Figure 6.5. Grid points of the RegCM (25 km resolution) outputs and the limits of sub-basins for Buzau – Ialomita area*

As an example, in the Figures 6.6 and 6.7, for the near future (2021–2050) the variation of these differences within the Romanian pilot area for the main climatic parameters precipitation and temperature respectively, are presented. Figures show a bigger variation of precipitation along the analysed area and a smaller temperature variation.

The mean monthly differences of the climatic parameters for each sub-basins ware computed as an average of corresponding grid point's values. In Figures 6.8 and 6.9 are presented the monthly values of the differences between the precipitation and temperature simulated for the two times horizon and for reference period, computed for 4 of the analyzed river basins, situated at different mean altitude and having different surfaces.

The Figure 6.8 show that generally, for the near time period the variation of precipitation within of each studied sub-basins increase in spring and summer and decrease in autumn and winter

As for the end of century the average precipitation on the sub-basins decrease in the months of spring and summer and increase in the autumn and winter.

Except August, for the near-future time period, the simulated temperature for the analyzed area increase, this increase can reach 2–3 °C for the period 2071–2100. (Figure 6.9).
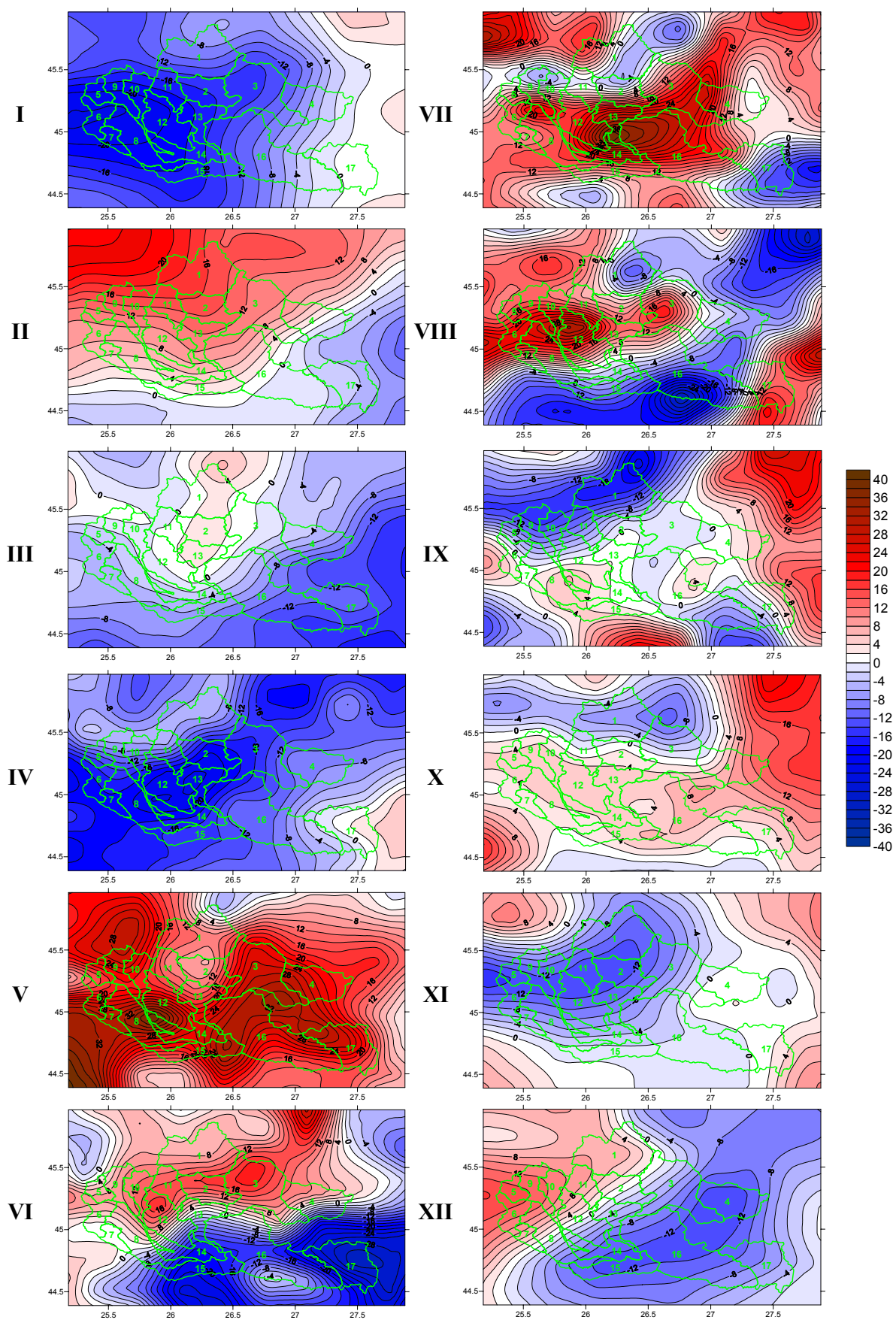
*Figure6.6. Ialomita – Buzau area -monthly difference in precipitation variation (%)*
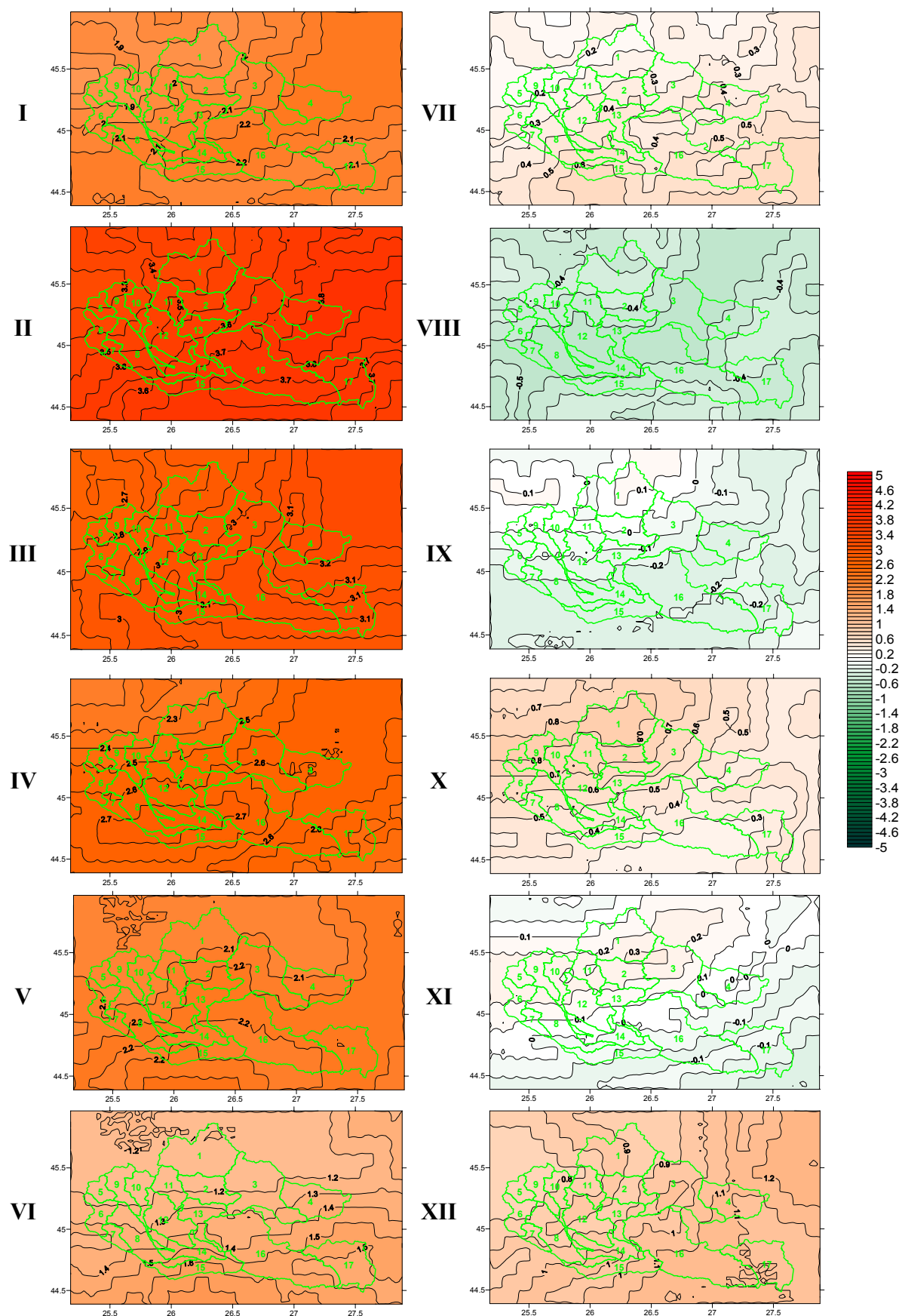
*Figure 6.7. Ialomita – Buzau area -monthly difference in temperature variation (ºC)*

66
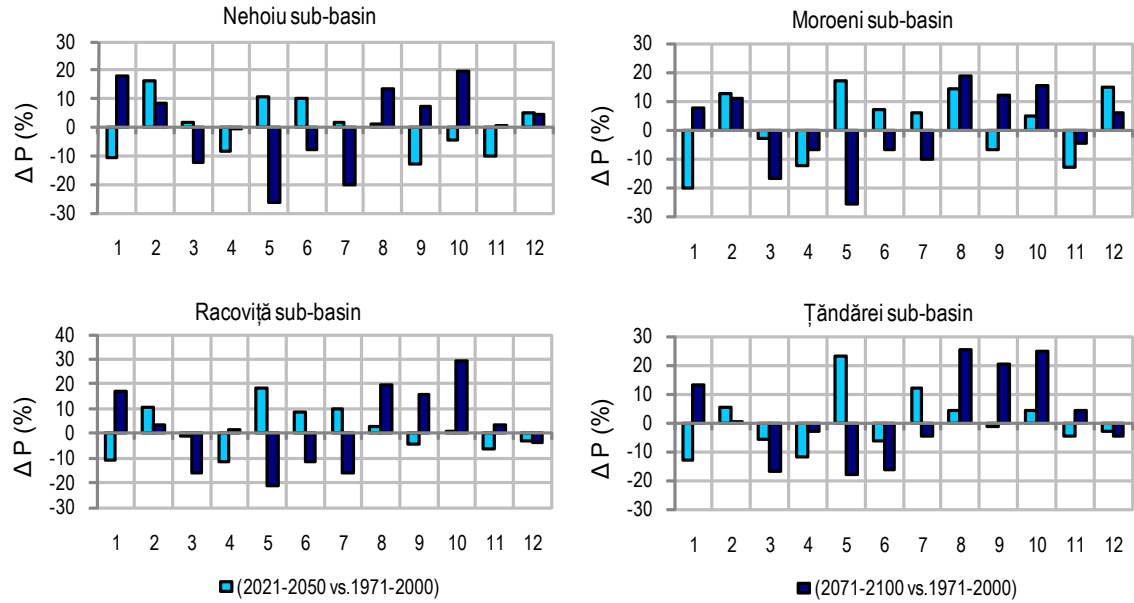
*Figure 6.8. Monthly values of the differences between the precipitations simulated for future periods and for reference period*
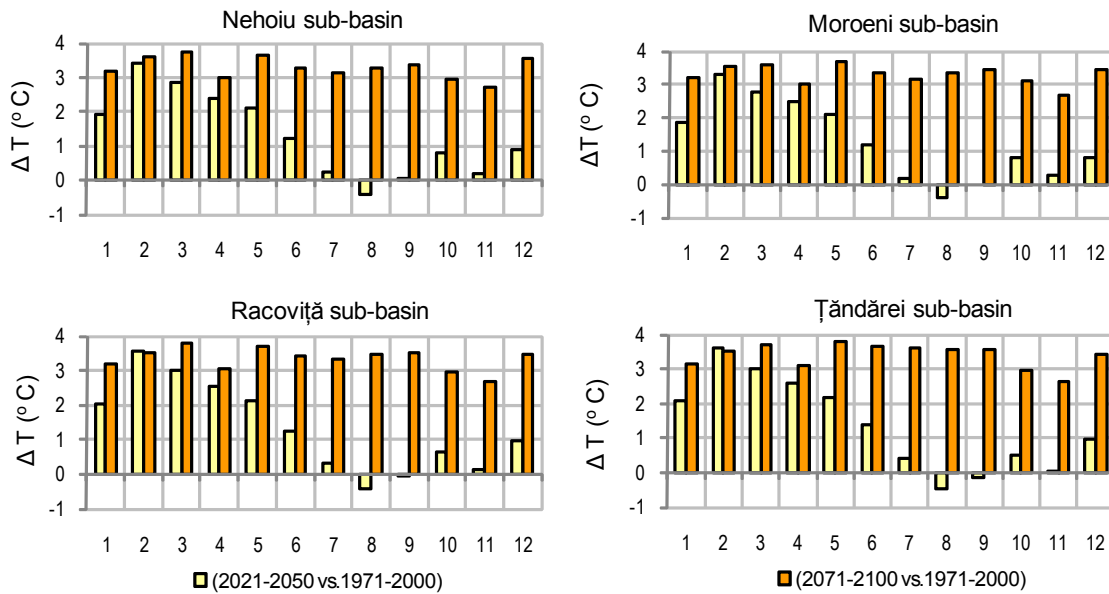


*Figure 6.9. Monthly values of the differences between the temperatures simulated for future periods and for reference period*

Finally, with the changed input climate data, the monthly discharge series were simulated using the hydrological balance model WatBal at all 17 gauging stations from the Buzau and Ialomita river basins, estimated for the above mentioned time horizons.

Analyses of the results showed that the variation of mean monthly flow presented a reduction from the lowland to the highland, having an uniform trend in parallel with its global decrease.

The Figure 6.10 shows the simulated monthly average discharges at four of the analysed sub-basins for the future time horizons in comparison with the reference period. We can observe

for both time horizons an increasing of mean monthly discharges in December - February, and a decreasing from Mars to May-June.

Also, for each sub-basin, the mean annual discharge was computed in climate change condition and compared with the mean annual discharge of the reference period (Figure 6.11). The mean annual discharge will decrease, especially at the end of century. The decreasing is more accentuate to the sub-basins having a smaller mean altitude.
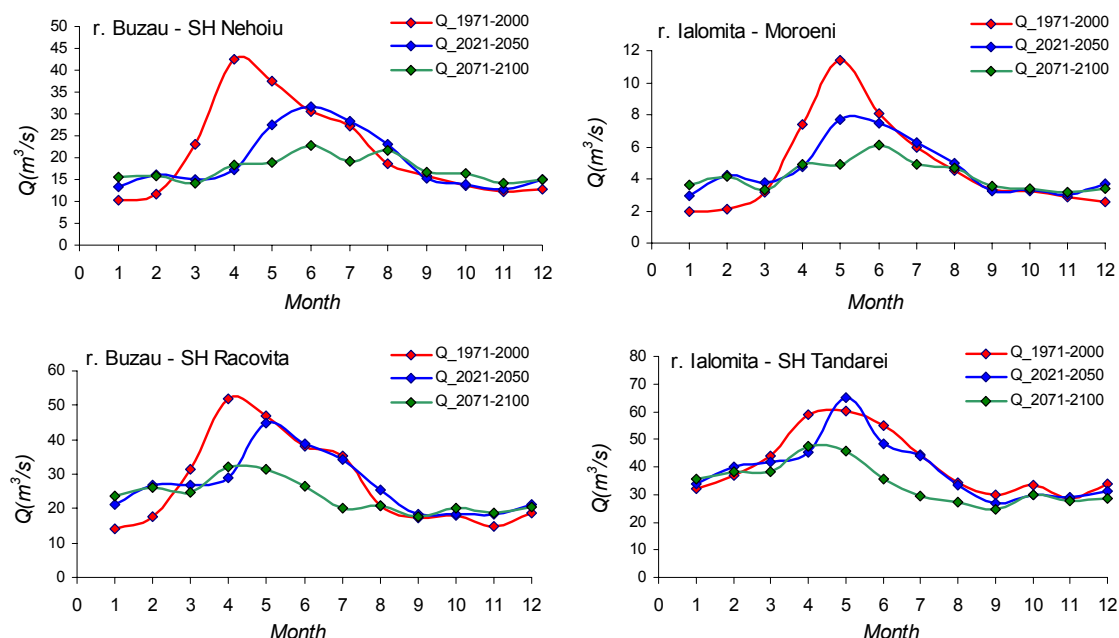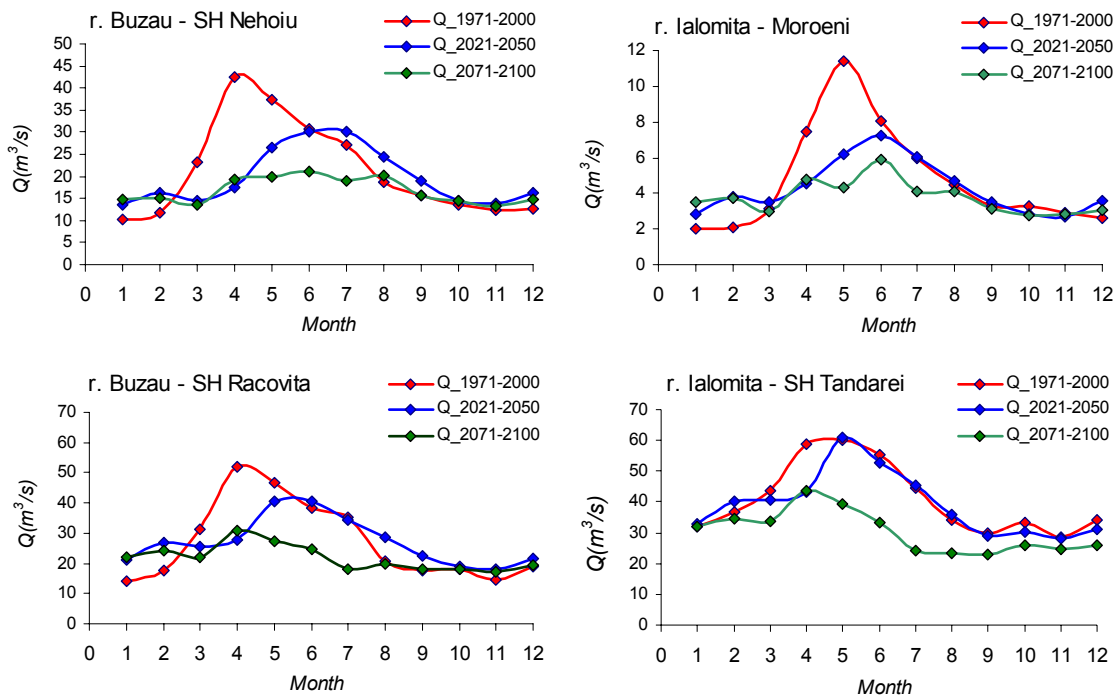


*Figure 6.10. Mean monthly discharge modification in climate change conditions due by RegCM with 25 km resolution*
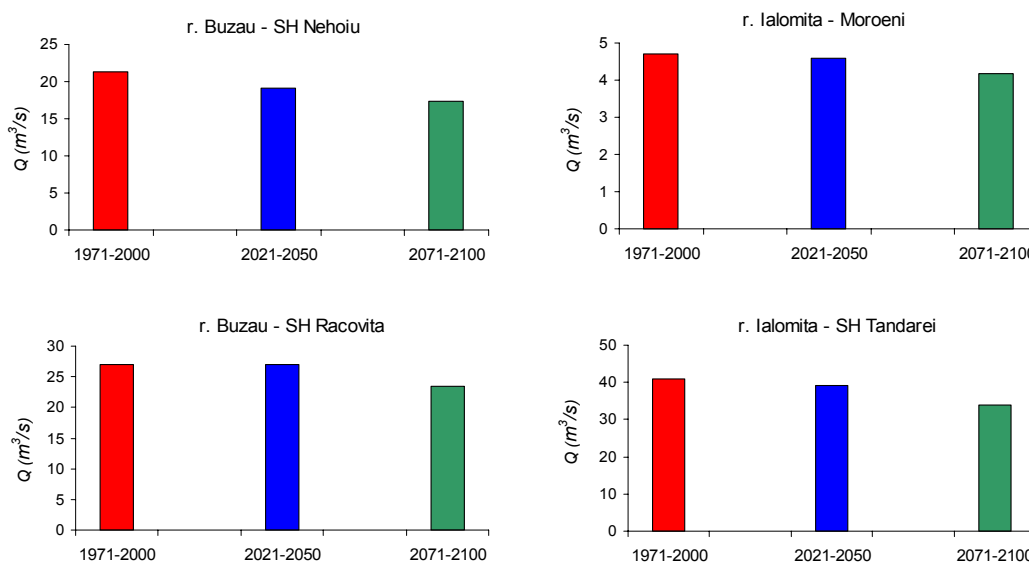


*Figure 6.11. Mean annual flow modification in climate change conditions due by RegCM with 25 km resolution.*

*6.4 Scenarios based on regional climate model with 10×10 km spatial resolution*

The third part of the study assess the impact of climate change in water resources, also for the two periods 2021-2050 and 2071-2100, using as input data the results of regional climatic model with 10 km resolution. The modifications of climatic parameters were provided by NAM as grid with the values of each needed parameters. This new grid of RegCM outputs, with 10 km spatial resolution, and the limits of each sub-basins of Buzau – Ialomita area are presented in Figure 6.12.
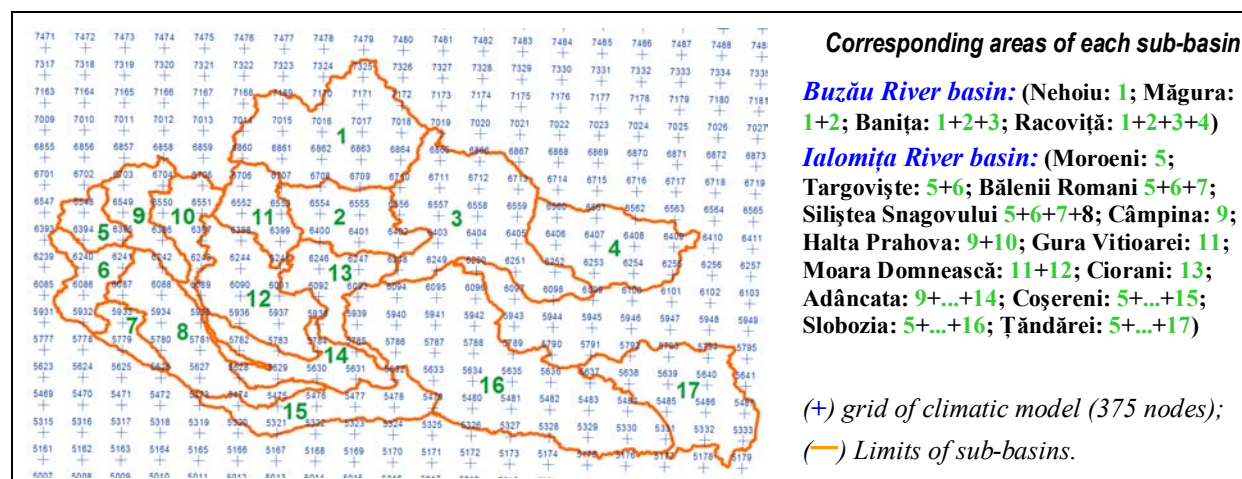


*Figure 6.12. Grid points of the RegCM (10 km resolution) outputs for Buzau – Ialomita area*

Figures 6.13–6.16 present the modification of precipitation and temperature for the tow future time periods and the comparison with the differences which resulted from RegCM with 25 km resolution.
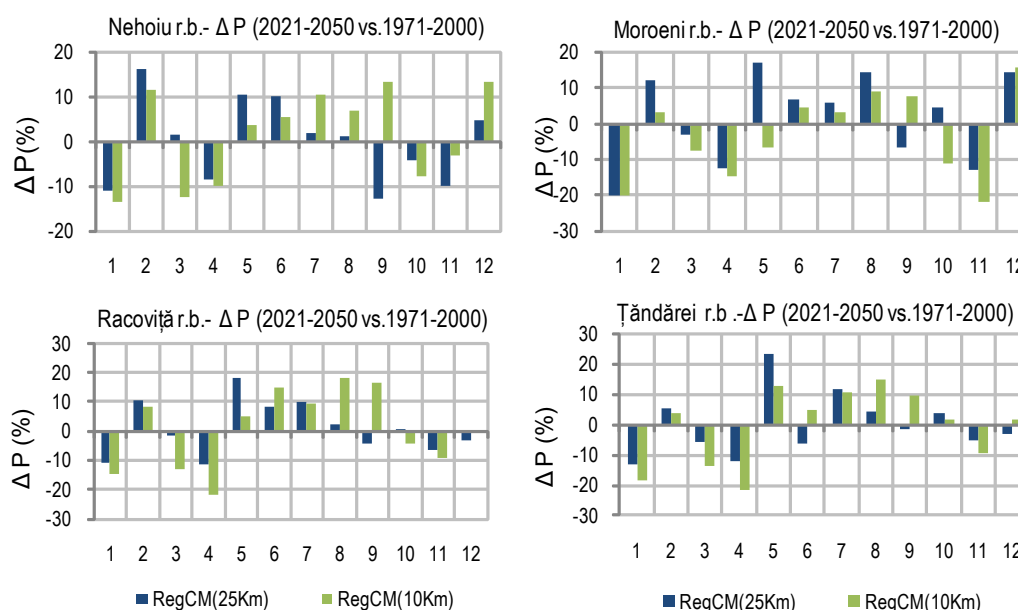


*Figure 6.13. Monthly differences between the values of precipitation simulated for the period 2021-2050 in comparison with the reference period 1971-2000*
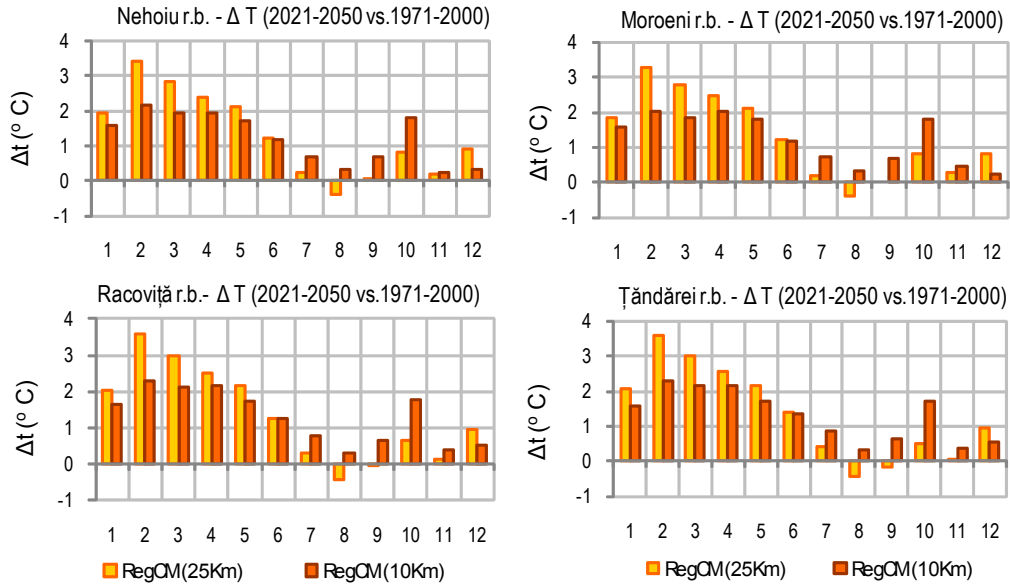
*Figure 6.14. Monthly differences between the values of temperature simulated for the period 2021−2050 in comparison with the reference period 1971−2000*
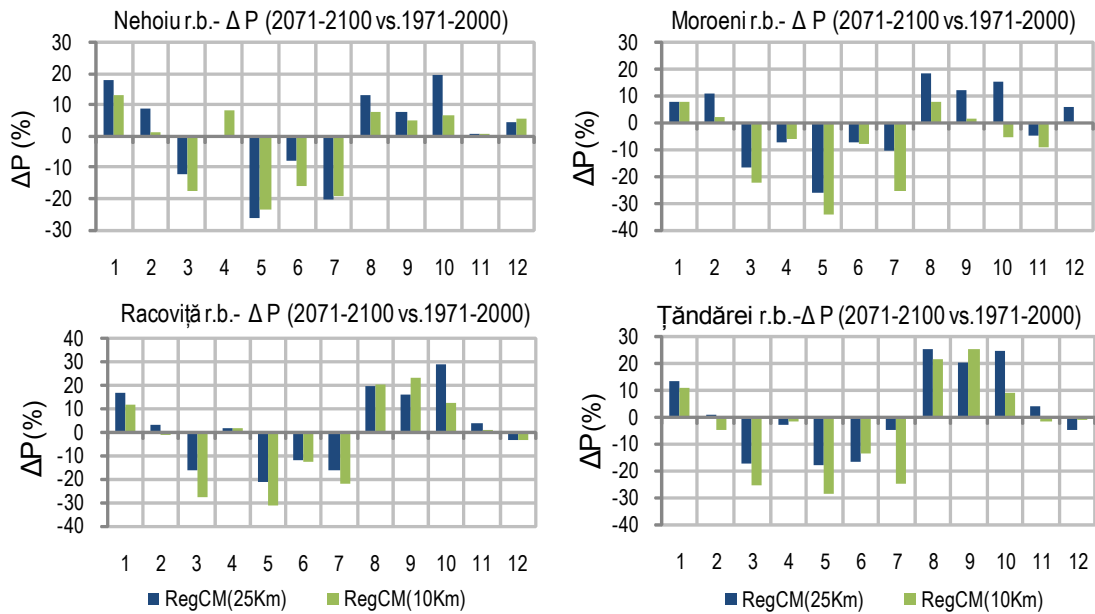


*Figure 6.15. Monthly differences between the values of precipitation simulated for the period 2071−2100 in comparison with the reference period 1971−2000*
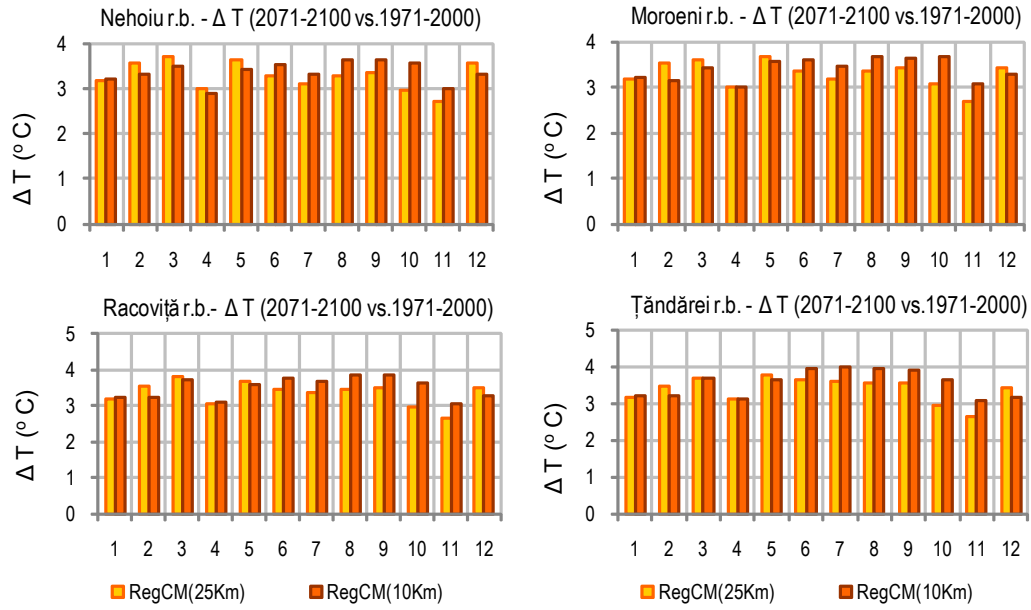
*Figure 6.16. Monthly differences between the values of temperature simulated for the period 2071–2100 in comparison with the reference period 19712000*



*Figure 6.17. Mean monthly discharge modifications in climate change conditions due by RegCM with 10 km resolution*

71
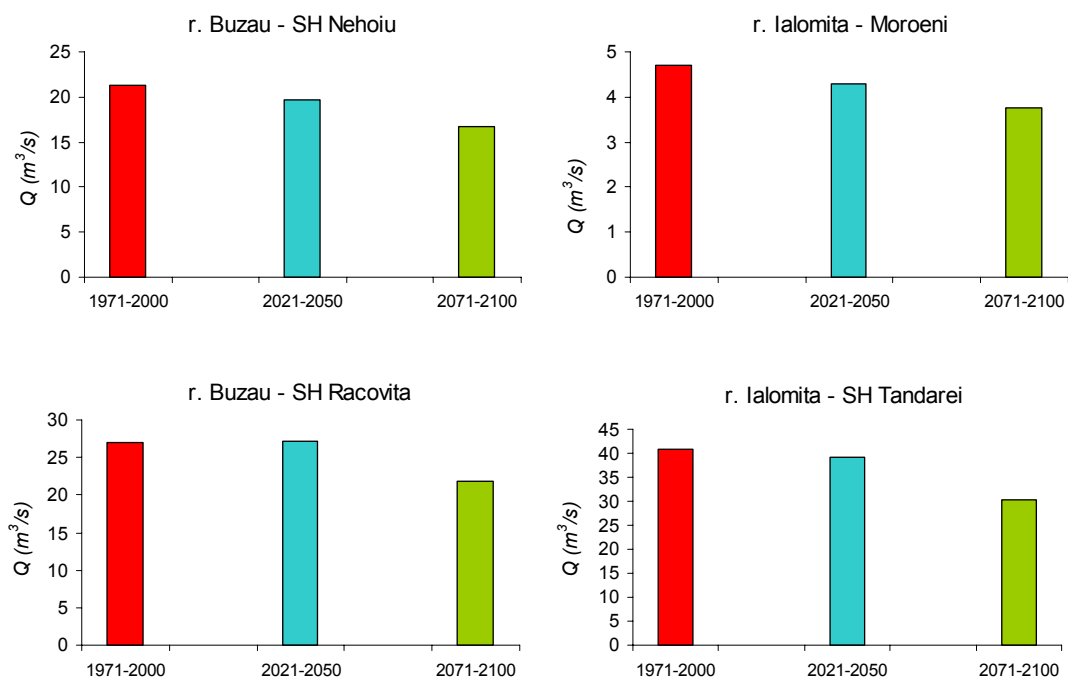
*Figure 4.18. Mean annual flow modification in climate change conditions due by RegCM with 25 km resolution.*
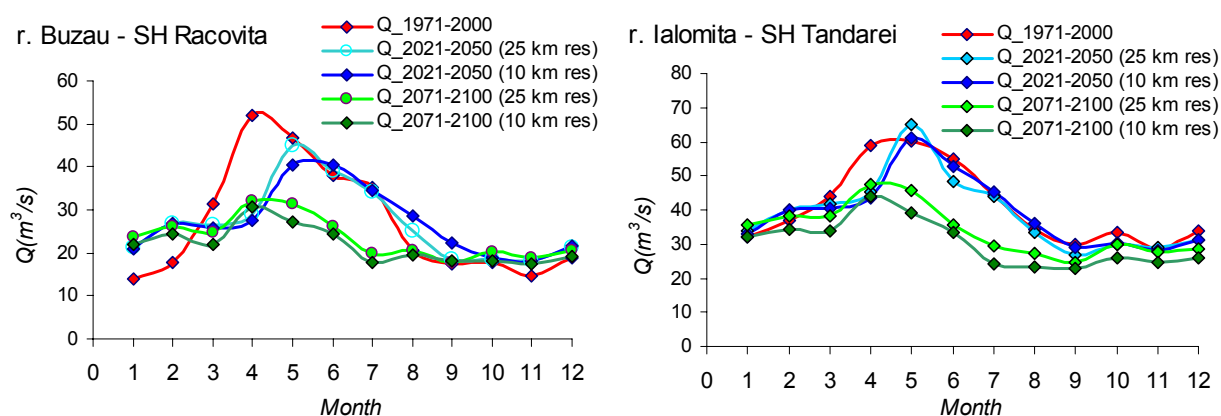


*Figure 4.19. Comparison of mean monthly discharge modifications in climate change conditions due by RegCM with 10 and 25 km resolution*
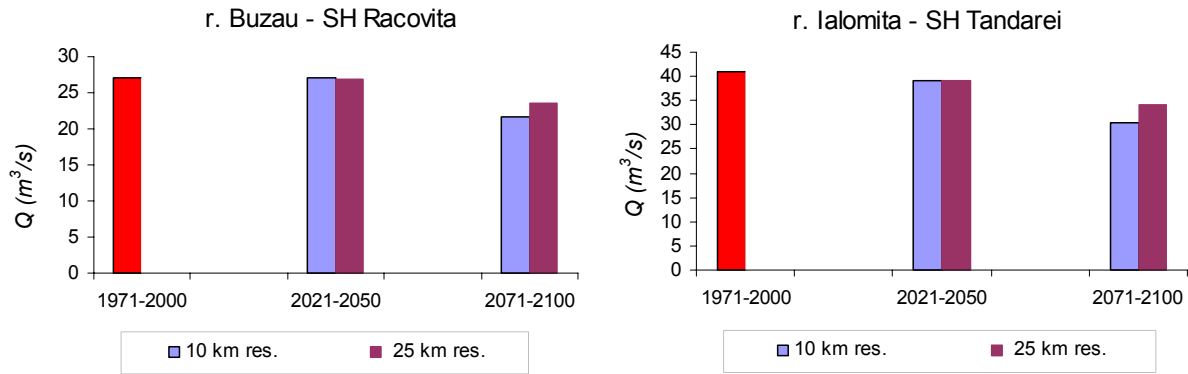
*Figure 4.20. Comparison of mean annual flow modification in climate change conditions due by RegCM with 10 and 25 km resolution*

## 6.5 Conclusions

The study emphasizes the following changes in the mean monthly flow due to climate changes:

(i) - Mean annual flow decreases as the time horizon is larger, 15-20 % (2021-2050) or 30-40 % (2070-2100), especially do to the increasing of evapotranspiration.

(ii) Increase of evapotranspiration, mainly during the months of summer-autumn, when air temperature increase.

(iii) Decreasing of the snow depth and duration of snow coverage as a result to the increasing of the air temperature in winter time.

(iv) Variation of mean monthly flow presents a reduction from the lowland to the highland, having an uniformly trend in parallel with it global decreasing.

(v) Earlier occurrence of floods produced by snow-melt and reduction of spring combined floods (snow-melt and rain) through the desynchronisation between the snow-melt and rain occurrence.

(vi) The amplification of extreme phenomena through the increase of maximum mean monthly discharges in the spring period and the decrease in the values of mean monthly flow in summer-autumn period.

(vii) Mean annual flow decreases as the time horizon is larger.

## 6.6 References

Biswas A. K. (1991): Water for sustainable development in the 21 century: a global perspective. Water International 16(4): 219-224.

Carnale K. P., Chapra S. C. (1988): Numerical Methods for Engineers. Second edition. McGraw-Hill, New York.

Dooge J. C. I. (1992): Hydrologic Models and Climate Change. Journal of Geophysical Research, 97(D3): 2677-2686.

Gray D. M., Prowse T. D. (1993): Snow and Floating Ice. În: Maidment D. R., Journal of Hydrology, McGraw-Hill Book Company, New York City, New York, 7.1-7.53.

Kaczmarek Z. (1993): Water Balance Model for Climate Impact Analysis. ACTA Geophysica Polonica, v. 41, no. 4, 1-16.

Kaczmarek Z., Krasuski D. (1991): Sensitivity of Water Balance to Climate Change and Variability. IIASA Working Paper, WP-91-047, Laxenburg, Austria.

Leemans R., Cramer W. P. (1991): The IIASA Database for Mean Monthly Values of Temperature, Precipitation, and Cloudiness on a Global Terrestrial Grid. IIASA Research Report, RR-91-18.

Ozga-Zielinska M., Brzenzinski J., Feluch W. (1994): Meso-Scale Hydrologic Modeling for Climate Impact Assessment: A Conceptual and a Regression Approach. IIASA, CP-94-10, Laxenburg, Austria.

Penman H. L. (1948): Natural Evaporation from Open Water, Bare Soil and Grass. Proc. R. Soc. London, vol. A193, pp. 120-145.

Priestly C., Taylor R. (1972): On the Assessment of Surface Heat Flux and Evaporation Using Large Scale Parameters. Mon. Weather Rev., vol. 100, pp. 81-92.

Shuttelworth W. J. (1993): Evaporation. In: Maidment D. R. (Ed.) Handbook of Hydrology. McGraw-Hill Book Company, New York City, New York, 4.1-4.53.

Yates D. N. (1994): WATBAL - An Integrated Water Balance Model for Climate Impact Assessment of River Basin Runoff. IIASA Working Paper, WP-94-64, Laxenburg, Austria.

## 7. Summary

The aim of this study was to evaluate impacts of the current climate change projections on hydrology of 4 selected river basins in the Czech Republic (Vltava, Dyje), Slovakia (Hron), and Romania (Buzău/Ialomiţa). Considering the mean precipitation and runoff characteristics, all the evaluated basins belonged to the same climatic type, as it is evidenced by rather close dependencies of precipitation, runoff, and runoff coefficient on altitude (Fig. 7.1).
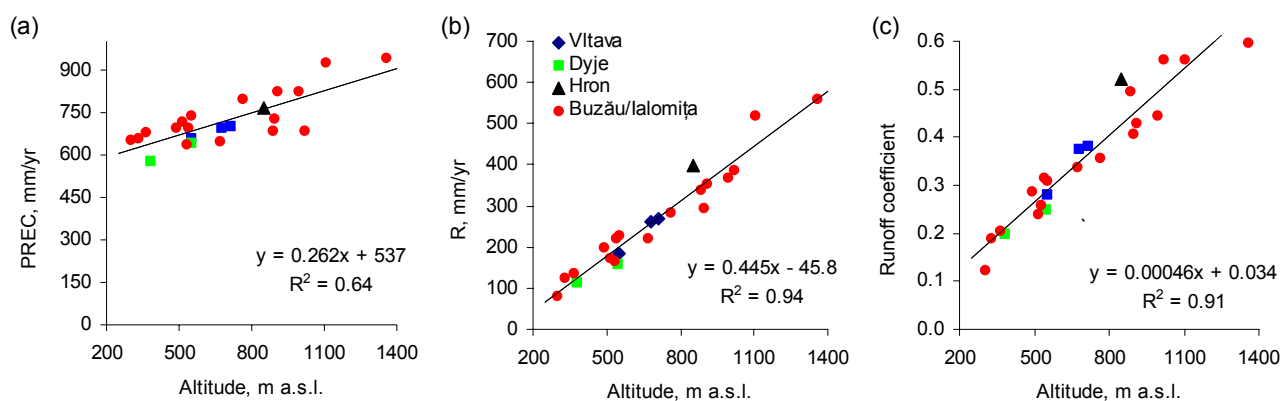


*Figure 7.1. Relationships of altitude vs. mean precipitation (a), mean runoff (b), and runoff coefficient (c) for the mean data 1971-2000 in the subbasins of the Vltava, Dyje, Hron, and Buzău/Ialomiţa basins*

The evaluation was based on mathematical modelling of the precipitation-runoff process with conceptual, spatially lumped water balance models (HSPF, BILAN, KVKH, and WATBAL at the Vltava, Dyje, Hron, and Buzău/Ialomiţa basins, respectively). The models were calibrated with the observed climatic data from the period 1971–2000 and then run with boundary conditions changed according to a series of scenarios of climate change. The scenarios were developed using the pattern scaling techniques from the outputs of 3 GCMs (ECHAM, HadCM, NCAR), representative scenarios for the development of emissions of greenhouse gases and aerosols (SRES A1, A2, B1, and B2 from the IPCC Third Assessment Report), and for varied climatic sensitivity to the emissions. The scenarios were constructed specifically for each basin in three future time horizons, i.e. 2025, 2050, and 2100.

A temperature increase with mean increments of 0.7–1.0 °C, 1.3–2.1 °C, and 2–3 °C in 2025, 2050, and 2100, respectively, was predicted according to the scenarios of climate change. There was a consistent increase in the temperature change along the geographic transect from the Vltava to Buzău/Ialomiţa basins in all three GCMs. Seasonal pattern of temperature changes featured higher temperature increases in the summer and autumn months than in the winter and spring months. The precipitation amounts decreased in most model predictions except for the NCAR outputs at the Czech river basins, where a slight increase occurred. There was a decreasing trend in precipitation depths between the Vltava and Buzău/Ialomiţa basins. Notable differences existed among the GCMs in the seasonal distribution of precipitation. The ECHAM outputs predicted minimum seasonal changes by contrast to the HadCM and NCAR outputs that had an increased precipitation activity in winter and spring

months but deficits in the summer and autumn. The solar radiation change showed almost a mirrored pattern to the pattern of precipitation both in the long-term averages and the seasonality.

The above-described predictions of changes in climatic variables induced significant changes in the modelled runoff. A monotonous, approximately linear decrease in runoff during the period from the reference period of 1971–2000 and the end of 21$^{st}$ century was predicted in all basins for all GCMs and by all hydrologic models (see Figs. 3.3, 4.5, 5.2, and 6.1–6.4). The highest decrease rates occurred in catchments situated at lower altitudes, i.e. in the basins of Vltava, Dyje, and partly also Ialomiţa, whereas the lowest decrease rates showed river profiles where significant fractions of catchment were located in alpine mountainous areas (the Hron and upper parts of the Buzău/Ialomiţa basins). This trend is illustrated in Fig. 7.2, where the modelled decrease in runoff for the time horizon of 2100 is plotted against the value of observed runoff coefficient. In the Czech basins, slightly higher runoff decrease rates and significantly wider uncertainty ranges were predicted in comparison with the Slovak and Romanian basins. It is not clear whether this was caused purely by geographic and climatic differences among the basins or whether differences in modelling methods were also important. A cross-modelling study with the application of each model at each basin might be necessary for answering this question.
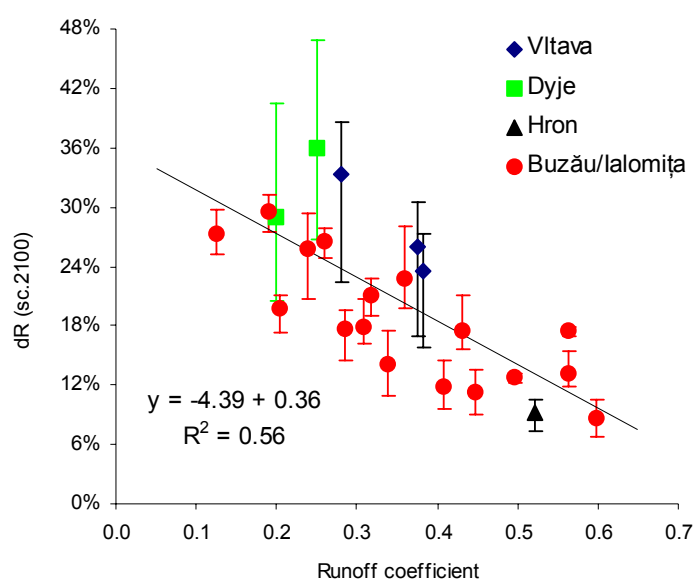


*Figure 7.2. The dependence of the decrease in modelled mean runoff in the middle scenarios of climate change for time horizon 2100, dR (sc.2100) (mean±min-max range from predictions of ECHAM, HadCM, and NCAR) on the runoff coefficient calculated with the mean data 1971-2000 in the subbasins of the Vltava, Dyje, Hron, and Buzău/Ialomiţa basins*

All models predicted notable seasonal changes in the runoff in all basins. However, these changes were locally specific, apparently in connection with the geographical position and altitude of the catchment. In the winter and spring months, an increased and temporally

modified runoff patterns were modelled at those river profiles where significant parts of catchments were situated in alpine mountainous areas (Hron, Fig, 5.1; Buzău/Ialomița, Fig. 6.5). A moderately increased runoff in spring was simulated also in the uppermost catchments of the Vltava basin with for part of the GCMs (Fig. 3.4). At lowland river profiles, runoff decreases occurred in the winter and spring in all basins. In the summer and autumn months, a significant reduction in river flow was modelled for all GCMs in all basins, apparently due to the increase in evapotranspiration. In addition to the general drop in runoff, the predicted climate change induced also amplification in the seasonal inequality of flow, which might have important implication for the management of water resources.

**Part B**
**The „atmosphere-river network-reservoir" modelling system for hydrology and water quality simulations:**
**description, sensitivity analysis and uncertainty analysis**

## 8. Introduction

The second part of this deliverable describes the „atmosphere-river network-reservoir" modelling system that has been developed to provide a tool for evaluations of climate change impacts on hydrology and water quality of water supply reservoirs. This study was elaborated entirely by the IAP partner.

The aim of study was to quantify reliability and precision of hydrological predictions and simulations of selected water quality constituents, mainly those that are used for descriptions of eutrophication problems in standing water bodies. Methods of sensitivity and uncertainty analysis were used to obtain ranges of uncertainty of simulated variables and elucidate sources of bias. The study was accomplished with the „catchment-reservoir" system of Římov Reservoir in South Bohemia, the Czech Republic. This system was selected because of existing long-term and detailed data sets on stream water quality and reservoir limnology that have been collected during the cca 30-year history of this reservoir by the Hydrobiological Institute AS CR.

## 9. Decription of model system and methods

*9.1 Locality, sampling, and data*

Římov Reservoir is situated in the upper part of the Vltava River basin on one of its right side tributaries, the Malše River. It was built in 1978 with the main purpose of raw water supply for the water treatment plant at Plav (WTP Plav) that produces drinking water for approximately 200 thousand inhabitants in the region of South Bohemia. The other purposes include flow maintenance downstream from the dam and hydropower production. The reservoir morphology is canyon-type with very narrow inflow reaches. The reservoir lies in a deep valley that largely protect the water column against mixing by wind action (Fig. 9.1).

Main operational and hydrological characteristics of Římov Reservoir are in Tables 9.1 and 9.2, respectively. The reservoir is operated with a one-year cycle. In most years, the storage pool is full in the spring a then, during the summer and usually precipitation-poor autumnal months, the water level gradually decreases as the outflow and withdrawals exceed inflow. The reservoir is replenished during the next winter or early spring months. The reservoir design guarantee (i) withdrawal of raw water (average 1.48 $m^3$/s) and (ii) minimum flow downstream from the dam (0.65 $m^3$/s).
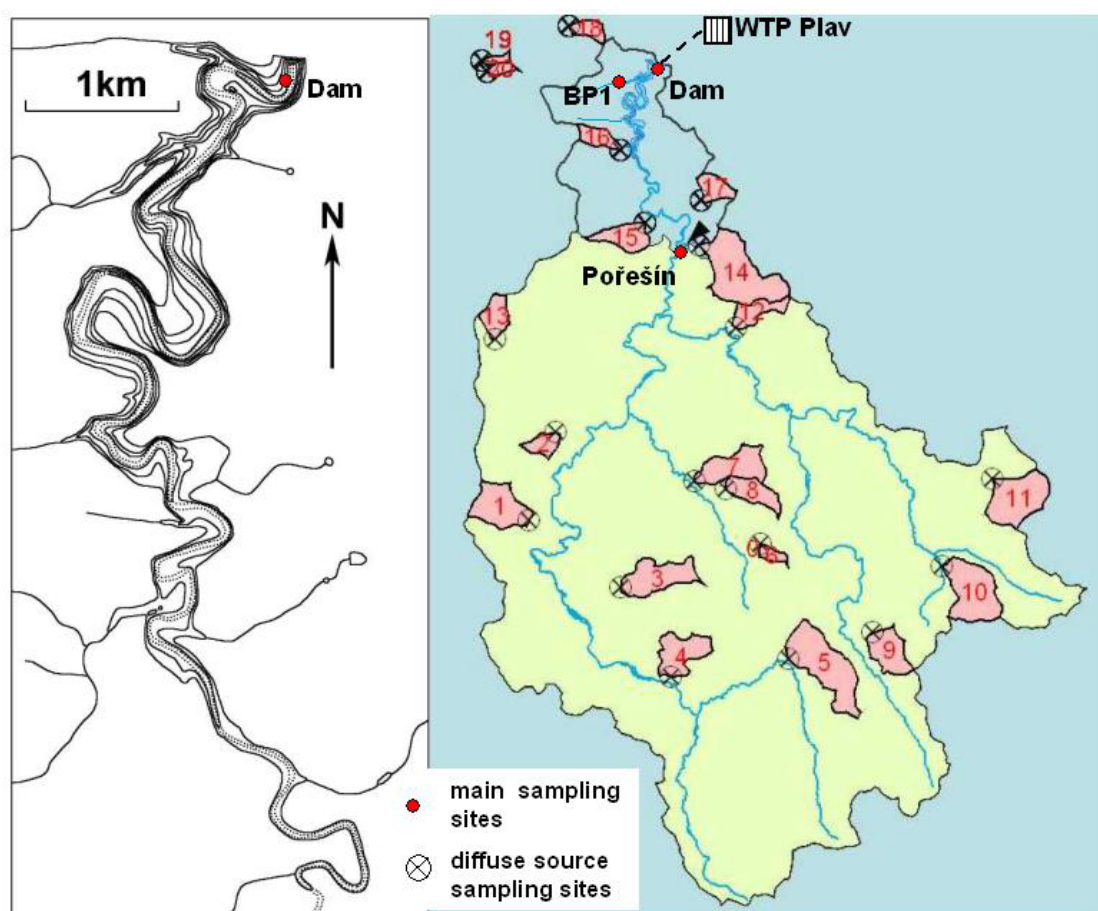


*Figure 9.1. Římov Reservoir and its catchment with main sampling sites and subcatchments for the diffuse-source evaluation study*

The dam structures are equipped with an array of outflow and withdrawal options. The raw water for the treatment plant can be abstracted via five outlets that are at depths between 7 and 32 m (at the water surface level of the full storage pool). The discharges to the river can be accomplished via: (i) three segments of gated spillways from the depth of 5.6 m below the surface at the full storage pool, (ii) two base outlets cca 3 m above the bottom, and (iii) a shaft outlet with adjustable outflow level in the range of depths from 0 to 31 m that brings water to the turbines of hydropower station. Outlet capacities are given in Table 9.1.

The outflow from the reservoir is managed during the year depending on the amount of water in the storage pool according to so called "dispatching graphs" that divide the storage pool into the spaces of free and controlled manipulation. When the surface level is below the level of controlled manipulation for a given period of the year, only the minimum flow plus the raw water withdrawal are allowed. In the space of free manipulation it is possible to increase both the withdrawal and the discharge to the river. During periods of flood (inflow >30 $m^3$/s), both spillways and base outlets can be used for the discharging of water from the reservoir.

*Table 9.1. Main characteristics of Římov Reservoir*

| | |
|---|---|
| Location of dam | 21.85 km Malše |
| Length of impoundment at the Malše River | 13 km |
| *Allocation space:* | |
| elevation of bottom at the dam profile | 427.50 m a.s.l. |
| elevation of permanent pool | 442.50 m a.s.l. |
| elevation of full storage space | 470.65 m a.s.l. |
| elevation of maximum surface level of controllable flood protection space | 471.40 m a.s.l. |
| maximum level at $Q_{100yr}$ | 471.48 m a.s.l. |
| volume of permanent pool | $2.1\times10^6\,m^3$ |
| volume of storage pool | $30.0\times10^6\,m^3$ |
| total controllable space | $33.6\times10^6\,m^3$ |
| total volume | $33.8\times10^6\,m^3$ |
| Surface area* | $2.03\times10^6\,m^2$ |
| Maximum / mean depth* | 43.9 m / 15.8 m |
| Mean flow (1931-1960) | 4.10 $m^3\,s^{-1}$ |
| Mean theoretical water retention time * | 92 d |
| *Options for outflow discharging and raw water withdrawal:* | |
| i. Two base outlets ø2.46 m, capacity 2×41,5 $m^3$/s at the surface level of 471.4 m a.s.l. | 430.50 m a.s.l. |
| ii. Shaft outlet with closing plates 2×1 m, capacity 4,0 $m^3$/s (restricted by the hydropower station to 3.6 $m^3$/s) at the surface level of 471.4 m a.s.l. | 440.5-473.4 m a.s.l. |
| iii. Gated spillways with 3 segments 6.9×5.4 m, capacity 3×135 $m^3$/s at the surface level of 471.4 m a.s.l. or 3×105 $m^3$/s the surface level of 470.65 m a.s.l. | 466.1 m a.s.l. |
| iv. Raw water withdrawal outlets 1.3×1.3 m at elevations:  I | 463.5 m a.s.l. |
| II | 457.0 m a.s.l. |
| III | 450.5 m a.s.l. |
| IV | 444.5 m a.s.l. |
| V | 438.8 m a.s.l. |

*at the maximum level of storage pool (479.65 m a.s.l.)

*Table 9.2. Hydrologic conditions at the profile of Římov Reservoir dam\**

| Catchment area | | | | | | | 489 km$^2$ | | | | | |
|---|---|---|---|---|---|---|---|---|---|---|---|---|
| Mean annual precipitation in the catchment | | | | | | | 749 mm | | | | | |
| Mean flow | | | | | | | 4.10 m3/s | | | | | |
| Flows exceeded on average once per | | | | | | | | | | | | |
| 1 | 2 | 5 | 10 | 20 | 50 | 100 years | | | | | | |
| 50 | 73 | 117 | 156 | 196 | 245 | 282 m$^3$/s | | | | | | |
| Flows exceeded on average in a year for | | | | | | | | | | | | |
| 30 | 60 | 90 | 120 | 150 | 180 | 210 | 240 | 270 | 300 | 330 | 355 | 364 days |
| 9.40 | 6.18 | 4.74 | 3.88 | 3.26 | 2.78 | 2.35 | 1.99 | 1.64 | 1.32 | 0.97 | 0.65 | 0.43 m$^3$/s |
| Estimated volume of theoretical 100-year-recurence non-influenced flood wave | | | | | | | 49×10$^6$ m$^3$ | | | | | |

\*data refer to the hydrological period 1931-1960

The catchment above the dam profile of Římov Reservoir has an area of 489 km$^2$ and extends at mean/maximum/minimum altitudes of 705/1072/428 m above sea level. The bedrock is formed by weathered paragneiss, diorite and granite. Most soils are dystric cambisols and mountainous podsols of acidic character (pH<4.5). About 23 % of the catchment is used as arable land, 21 % as meadows, 53 % for forestry, and 2 % are urban areas. Approximately 18 thousand inhabitants live in the catchment (i.e., population density is 35 inhabitants per square kilometre).

The data for the evaluation of hydrologic conditions of the reservoir and for the modelling were arranged into average daily series for the period 1961–2005. The inflow into the reservoir was reconstructed from the data of the Czech Hydrometeorological Institute at the gauging stations of Římov (21 km Malše River) for the period 1961–1978 and Pořešín (40.1 km Malše River) for the period 1979–2000 and from the operational evidence of the Vltava River Authorities at the Římov Reservoir dam. The inflow into to the Římov Reservoir was calculated from the operational evidence data according to the equation (9.1):

$$Q_{i,1\text{-}2} = \Sigma Q_o + (V_2 - V_1) \tag{9.1}$$

where: $Q_{i,1\text{-}2}$ is the mean inflow into the reservoir during the time interval $t = 1$ to $t = 2$, $\Sigma Q_o$ is total discharge from all outlets and withdrawals, $V_1$ and $V_2$ are reservoir volumes at times $t = 1$ and $t = 2$ that were calculated according to the regression equation (9.2) that was fitted through the volumetric curve of Římov Reservoir in the range of elevations between 428 and 471,5 m a.s.l.:

$$V = 3.168 \times 10^2 E^3 - 4.028 \times 10^5 E^2 + 1.707 \times 10^8 E - 2.410 \times 10^{10} \quad (R^2 = 0.99998) \tag{9.2}$$

where: $V$ is the reservoir volume [m$^3$] and $E$ is water surface elevation [m a.s.l.]

Water quality in the reservoir and its main inflows was characterised employing information sources as follows: (i) The database of Hydrobiological Institute BC ASCR, namely data from the long-term monitoring in three-week intervals at sampling sites Dam, BP1 and Pořešín that has been carried out since 1979. (ii) A dataset of water composition in twenty streams (1$^{st}$–2$^{nd}$ order according to Strahler) in the catchment of Římov Reservoir or its close vicinity that were sampled to assess the export from diffuse sources, i.e., natural background concentrations and agricultural land (Fig. 9.1, Tab. 9.3).

Inputs of phosphorus from municipal sources (point sources) into the river network were determined from available data covering concentrations and amounts of sewage effluents of the largest wastewater treatment plants (WWTPs) (operation evidence of sewage works facility Voodovody a kanalizace Jižní Čechy a.s. for WWTPs in Kaplice, Dolní Dvořiště, Rychnov nad Malší, Malonty, and Benešov nad Černou). The P export from inhabitants not connected to the monitored WWTPs ($P_{noev}$) was calculated according to the equation (9.3):

$$P_{noev} = P_{spec} \times E \times I \tag{9.3}$$

where: $P_{spec}$ is specific human P production (in the Czech Republic 2.3 g per day per inhabitant; in Austria 1,6 g/d/inh., due to the use of phosphate-free washing powders); $E$ is coefficient of P transfer efficiency into surface waters (a value 0.5 is assigned to scattered dwellings, 0.6 to small WWTPs with biological ponds, and 0.8 to septic tanks); $I$ – the population number. Numbers of inhabitants and their connectivity to sewers in the region were based on the census from 1991 of the Czech Statistical Office.

Table 9.3. Catchment characteristics: A, catchment area; $J_m$, mean slope; $E_m$, mean altitude; TP and DP, mean total and dissolved phosphorus concentrations, respectively

| No. | Name of stream–profile | $A$, km² | $J_m$, ° | $E_m$, m a.s.l. | Land use, % | | | | TP, µg/l | DP, µg/l |
|-----|------------------------|----------|----------|-----------------|-------------|--------|--------|--------|----------|----------|
| | | | | | forest | meadow | arable | other* | | |
| | Malše-Pořešín | 436.9 | 6.3 | 708 | 55 | 24 | 18 | 2.1 | 91 | 53 |
| 1 | Trojanský p. | 3.48 | 3.4 | 691 | 75 | 8 | 16 | 0.9 | 83 | 26 |
| 2 | Zdíkovský p. | 1.08 | 2.2 | 639 | 81 | 2 | 17 | - | 45 | 20 |
| 3 | Obecní p. | 3.46 | 5.8 | 685 | 57 | 34 | 9 | - | 85 | 21 |
| 4 | Cetvinský p. | 2.88 | 4.7 | 689 | 52 | 48 | - | - | 97 | 55 |
| 5 | Kabelský p. | 6.00 | 6.8 | 848 | 93 | 7 | - | - | 112 | 14 |
| 6 | Bělský p. | 0.58 | 5.9 | 742 | 100 | - | - | - | 33 | 17 |
| 7 | Jaroměřský p. | 3.17 | 2.5 | 643 | 56 | 8 | 36 | 0.7 | 71 | 21 |
| 8 | Malontský p. | 1.96 | 3.7 | 672 | 8 | 6 | 85 | 1.4 | 72 | 23 |
| 9 | Uhlišťský p. | 2.56 | 7.5 | 869 | 100 | - | - | - | 117 | 13 |
| 10 | Tisový p. | 4.74 | 6.9 | 809 | 99 | 1 | - | 0.2 | 186 | 20 |
| 11 | Mlýnský p. | 4.44 | 6.2 | 878 | 97 | 3 | - | 0.1 | 23 | 13 |
| 12 | Kohoutský p. | 1.64 | 7.7 | 646 | 80 | 17 | 3 | - | 184 | 21 |
| 13 | Krakovický p. | 1.58 | 8.3 | 836 | 99 | 1 | - | 0.0 | 46 | 18 |
| 14 | Budský p. | 6.47 | 5.7 | 616 | 45 | 9 | 45 | 1.3 | 155 | 37 |
| 15 | p. u Výhně-J | 2.01 | 4.7 | 595 | 49 | 7 | 43 | 0.2 | 34 | 7 |
| 16 | Chodečský p. | 1.11 | 3.4 | 553 | 13 | 26 | 59 | 2.1 | 147 | 33 |
| 17 | Chlumský p. | 1.33 | 4.5 | 545 | 36 | 1 | 63 | 0.1 | 134 | 50 |
| 18 | Dolnosvinenský | 0.92 | 2.4 | 534 | 8 | 21 | 71 | 0.1 | 237 | 106 |
| 19 | Černický p. | 0.38 | 1.2 | 549 | - | 7 | 93 | - | 102 | 73 |
| 20 | p. u Mojného | 0.46 | 0.8 | 549 | - | - | 100 | - | 227 | 84 |

*urban, water courses and reservoirs

## 9.2 Model system

The model system that has been developed for the description of effects of climate variability on hydrology and water quality in Římov Reservoir consists of two major model compartments, i.e., HSPF and CE-QUAL-W2 for simulations of the precipitation–runoff

process in the catchment and the reservoir hydrodynamics and water quality, respectively, and several auxiliary submodels that couple these two model together and provide data on inflow water quality (PHOSP, DOM, STEMP) and on reservoir hydrological operation (RESMNG) (Fig. 9.2).
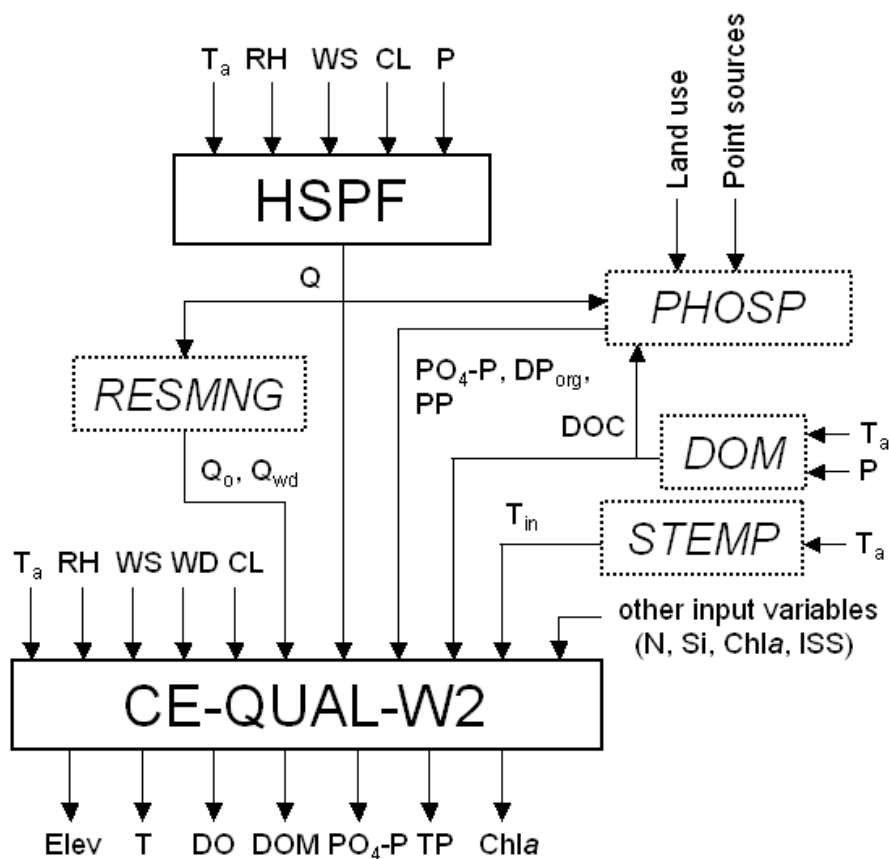


*Figure 9.2. The diagram of the HSPF–CE-QUAL-W2 modelling system showing major(full-line rectangles) and auxiliary (dash-line rectangles) model compartments and their input and output variables. Abbrev.: $T_a$, air temperature; RH, relative humidity; WS, wind speed; WD, wind direction; $PO_4$-P, orthophosphate phosphorus; $DP_{org}$, dissolved organic phosphorus; PP, particulate phosphorus; $T_{in}$, water temperature in reservoir inflow; CL, cloudiness; P, precipitation; Q, flow; $Q_o$, outflow; $Q_{wd}$, withdrawal; Elev, surface level elevation; T, water temperature; DO, dissolved oxygen; DOM, dissolved organic matter; TP, total phosphorus; Chla, chlorophyll-a; N, nitrate and ammonia nitrogen; Si, silicon; ISS, inorganic suspended solids*

*9.2.1. HSPF*

The HSPF model (Bicknell et al. 2001) is a conceptual precipitation-runoff model with a modular structure that enables simulations of transport of multiple substances from the catchment and their transformations in the river network. Simulations are accomplished in user-defined separate parts of the catchment and of the river network that have similar soil, water ecosystem, and climate conditions. The separation of the Římov Reservoir catchment was done into five subcatchments. Each subcatchment was composed of 5 segments that represented farmland, low-slope (<8°) areas, high-slope (>8°) areas, flood areas (maximum distance of 100 m from the channel and with slope <1°), and impervious areas. The modules comprise water balance of pervious and impervious (PWATER and IWATER), snow cover (SNOW), and soil moisture (MSTL), soil erosion and transport (SEDMNT, SOLIDS), and phosphorus transport from the catchment (PHOS). The river network of each subcatchment was divided into two segments. The first, upper one represented $1^{st}$ to $3^{rd}$-order (Strahler) streams and the second one streams of higher orders. Within the stream and river segments the HSPF model used modules of flow transformation (HYDR), advective transport of substances (ADCALC), transport, sedimentation, and resuspension of erosion particles (SEDTRN), nutrient transformations (NUTRX) a phytoplankton growth (PLANK). The model outputs in a format of text files are used as input files for the subsequent simulations with the reservoir model CE-QUAL-W2.

The hydrology of the Římov Reservoir catchment was calibrated within whole Vltava River basin and is described in detail in Deliverable D 5.2. The results of calibration and validation runs are given in Table 9.4 and Fig. 9.3. The model realistically described the seasonal pattern of base flow changes both in periods of higher flow during spring snow melt and during periods of decreasing flow in late summer and autumn. Runoff events following heavy rains were simulated usually also well, including the flood in August 2002. A lower precision of the validation run was probably caused mainly by inhomogeneities in the input data, especially precipitation and discharge measurements and/or evapotranspiration.

*Table 9.4. Comparison of simulated and observed daily flow ($m^3/s$) in the main inflow of Římov Reservoir during the calibration and validation periods*

| Parameter | cal. 99-03 | val. 91-98 |
|---|---|---|
| AME | 1.48 | 1.35 |
| RMSE | 4.23 | 2.59 |
| RE | 0.09 | -0.07 |
| NS | 0.85 | 0.71 |
| AVG-model | 4.26 | 3.47 |
| AVG-observed | 4.30 | 4.00 |
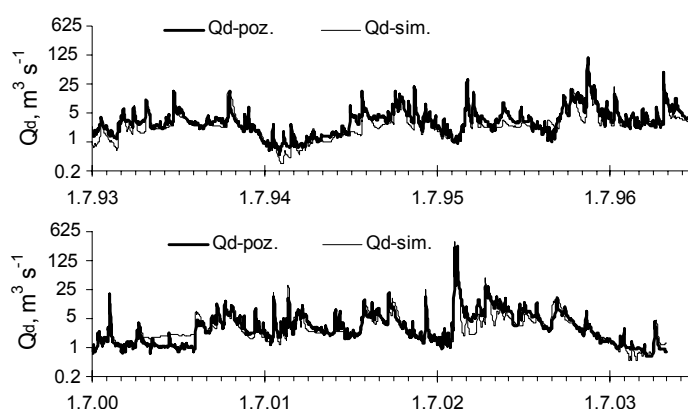


*Fig. 9.3. Observed ($Q_{d-poz.}$) and simulated ($Q_{d-sim.}$) daily discharge in the profile Malše–Pořešín during calibration (bottom) and validation period (top)*

## 9.2.2. CE-QUAL-W2

The two-dimensional, laterally averaged numerical reservoir model CE-QUAL-W2 v. 3.5 (Cole and Wells, 2006) was used. The Římov Reservoirs was approximated with a finite-difference grid that consisted of 24 segments 300 m to 1 km in long and 1 m thick. Water quality simulations included the following quantities: temperature, ice cover thickness, dissolved oxygen, biomass of 3 phytoplankton groups, labile and refractory dissolved and particulate organic matter (LDOM, RDOM, LPOM, RPOM), orthophosphate P ($PO_4$-P), $NO_3$-N, and $NH_4$-N. The model was calibrated and validated in the same periods as the HSPF model. The reservoir hydrodynamics were calibrated against vertical profiles of water temperature that were measured at the Rimov Reservoir dam in the deepest point above the original river channel. The dynamics of chemical and biological changes in the reservoir were set for measured concentrations of dissolved oxygen, dissolved reactive phosphorus ($PO_4$-P), total phosphorus (TP), and chlorophyll-a (Chl*a*) in the surface layer at the dam. An independent validation with inputs from the HSPF model (discharge, concentration of $PO_4$-P) was done for the period from January 1, 1991 to December 31, 2000 and this period was used also for the sensitivity and uncertainty analysis. The model efficiency and reliability of simulations were evaluated by selected statistical parameters: (i) mean values of observed (AVG-observed) and simulated (AVG-model) values, (ii) mean of absolute error (AME), (iii) root mean square error (RMSE), (iv) mean relative error (RE), and (v) Nash-Sutcliffe coefficient of model efficiency (NS; Nash and Sutcliffe 1970) that gives values close to 1 for good agreement between observed and simulated values and values <0 for simulations that have lower prediction force than the mean of observed values. The agreement between observed and modelled values of main output variables of the CE-QUAL-W2 model are shown in Tables 9.5 and 9.6 and Figs 9.4 to 9.6.

*Table 9.4. Statistical parameters of bias between observed and modelled water temperature and dissolved oxygen concentration in Rimov Reservoir with the CE-QUAL-W2 model for the period 1991-2000*

| Parameter | Temperature, °C | | | | | Dissolved oxygen, mg/l | | | | |
|---|---|---|---|---|---|---|---|---|---|---|
| | *Depth, m* | | | | | *Depth, m* | | | | |
| | *0* | *5* | *10* | *20* | *30* | *0* | *5* | *10* | *20* | *30* |
| N | 167 | 234 | 214 | 195 | 192 | 166 | 202 | 188 | 172 | 172 |
| AVG-observed | 11.3 | 10.4 | 8.5 | 5.6 | 4.6 | 10.1 | 8.0 | 6.5 | 7.1 | 6.2 |
| AVG-model | 10.5 | 9.0 | 7.6 | 5.5 | 4.6 | 10.1 | 8.5 | 8.1 | 8.5 | 7.8 |
| ME | -0.6 | -0.5 | 0.3 | 0.2 | 0.0 | 0.1 | -0.4 | 0.5 | 0.8 | 1.1 |
| MAE | 1.0 | 1.0 | 1.1 | 1.0 | 0.7 | 1.6 | 2.2 | 1.4 | 1.7 | 1.7 |
| RMSE | 1.3 | 1.3 | 1.3 | 1.4 | 1.0 | 2.0 | 3.1 | 1.9 | 2.3 | 2.4 |
| NS | 0.97 | 0.94 | 0.89 | 0.59 | 0.58 | 0.20 | -0.04 | 0.75 | 0.49 | 0.53 |

*Table 9.5. Statistical parameters of bias between observed and modelled surface elevation (E), ice thickness, and water quality constituents in Rimov Reservoir in the surface layer at the dam with the CE-QUAL-W2 model for the calibration period 1991-2000*

| Parameter | E, m a.s.l. | Ice, m | NH$_4$-N, mg/l | NO$_3$-N, mg/l | PO$_4$-P, mg/l | TP, mg/l | DOM, mg/l | Chl$a$, µg/l |
|---|---|---|---|---|---|---|---|---|
| N | 3571 | 3571 | 167 | 167 | 167 | 167 | 167 | 167 |
| AVG-observed | 468.67 | 0.016 | 0.041 | 2.18 | 0.013 | 0.031 | 14.55 | 11.03 |
| AVG-model | 468.63 | 0.019 | 0.036 | 2.47 | 0.023 | 0.041 | 14.42 | 11.03 |
| ME | -0.04 | 0.003 | -0.005 | 0.29 | 0.009 | 0.009 | -0.13 | 0.36 |
| MAE | 0.08 | 0.015 | 0.032 | 0.41 | 0.011 | 0.013 | 2.06 | 8.30 |
| RMSE | 0.12 | 0.052 | 0.047 | 0.57 | 0.016 | 0.018 | 2.86 | 13.09 |
| Pearson R | 1.00 | 0.67 | 0.29 | 0.92 | 0.69 | 0.45 | 0.55 | 0.54 |
| R$^2$ | 1.00 | 0.45 | 0.08 | 0.84 | 0.48 | 0.21 | 0.31 | 0.29 |
| NS | 1.00 | 0.25 | 0.01 | 0.59 | -0.95 | -0.62 | 0.26 | 0.29 |

*9.3.3. Auxiliary submodels*

The PHOSP submodel consisted of a series of regression equations (Table 9.6) that described export of phosphorus from the catchment sources and phosphorus retention in the river network. The catchment sources were conceptually divided into diffuse and point sources. The equations for diffuse sources were set up and calibrated with the data from the monitoring of twenty small subcatchments with a range of different proportion of agricultural and forest areas and without any point sources of municipal, industrial, or agricultural pollution as described above (Fig. 9.1, Table 9.3). Equations for the contribution of point sources were based (i) on a principle of simple dilution of the amount of phosphorus discharged from WWTPs and from not evidenced inhabitants with the daily runoff from the catchment and (ii) on separation of total P into 90 % of dissolved P and 10 % of particulate P. Phosphorus export from the catchment was calculated for its three basic fraction, i.e. dissolved orthophospate (PO$_4$-P), dissolved non-orthophosphate (mainly organic) phosphorus (DP$_{org}$), and particulate P (PP).

The DOM (=dissolved organic matter) submodel included an empirical regression equation that was developed on the basis of correlation analysis with the data sets of monthly or weekly means of DOC, discharge, air temperature, humidity, wind speed, and cloudiness at the Pořešín sampling site. This analysis showed that DOC correlated both to air temperature and precipitation (Hejzlar et al. 2003). The DOC values were then converted to DOM for the purpose of the CE-QUAL-W2 input data assuming 40 % carbon content in the aquatic dissolved organic matter (e.g., Thurman 1985).

The STEMP submodel calculated daily water temperature in streams that enter the reservoir. It uses a harmonic function to mimic the annual temperature cycle (Straškraba, Gnauck 1985). This model needed to be calibrated for local conditions as stream water temperature depends on specific morphological conditions, for example size and shape of the channel and canopy cover. Two parametrizations of the model were done in the model of Římov Reservoir: one for the main inflow (Malše-Pořešín) and another for the side tributary BP1 that was considered as a representative for all other side tributaries of Římov Reservoir.
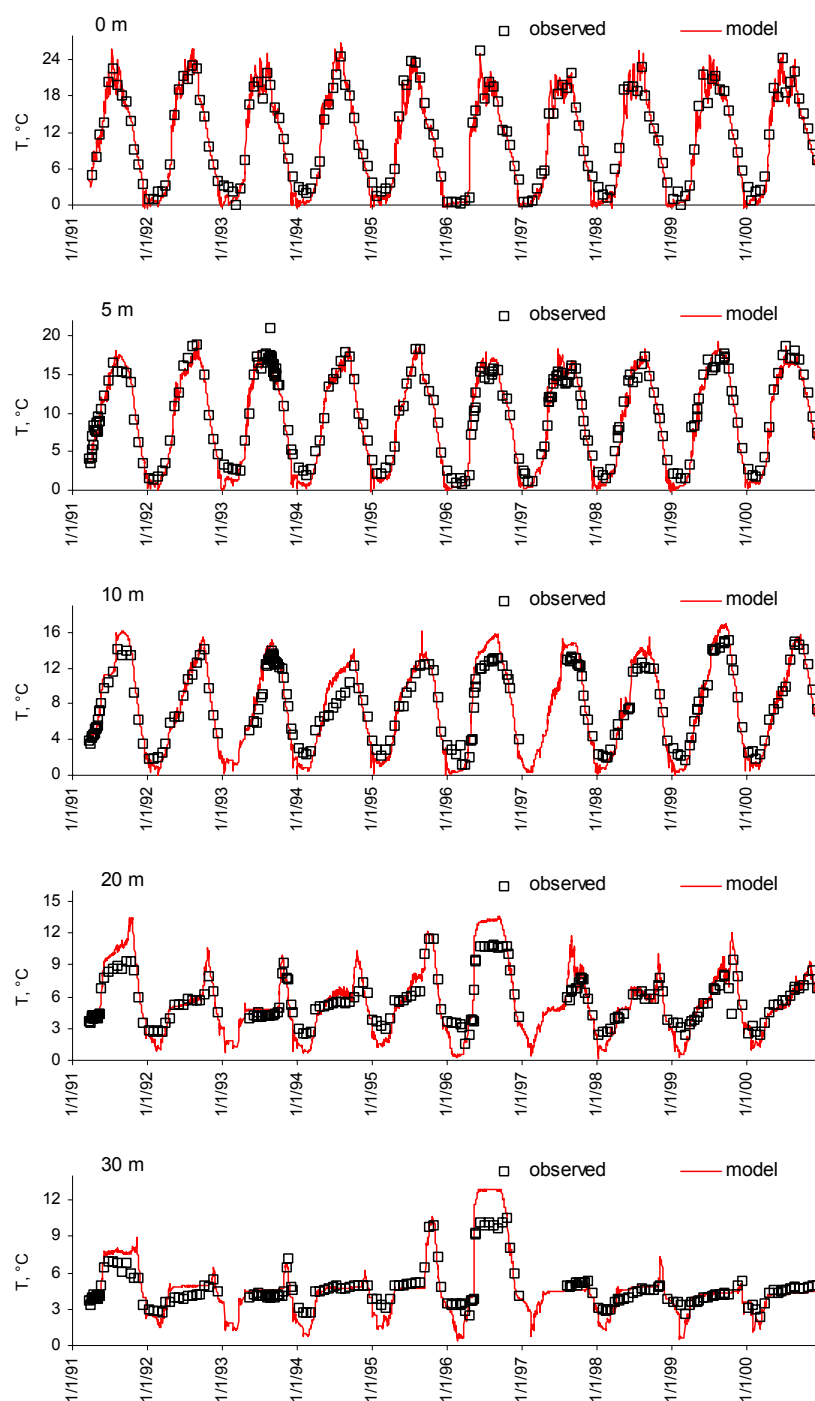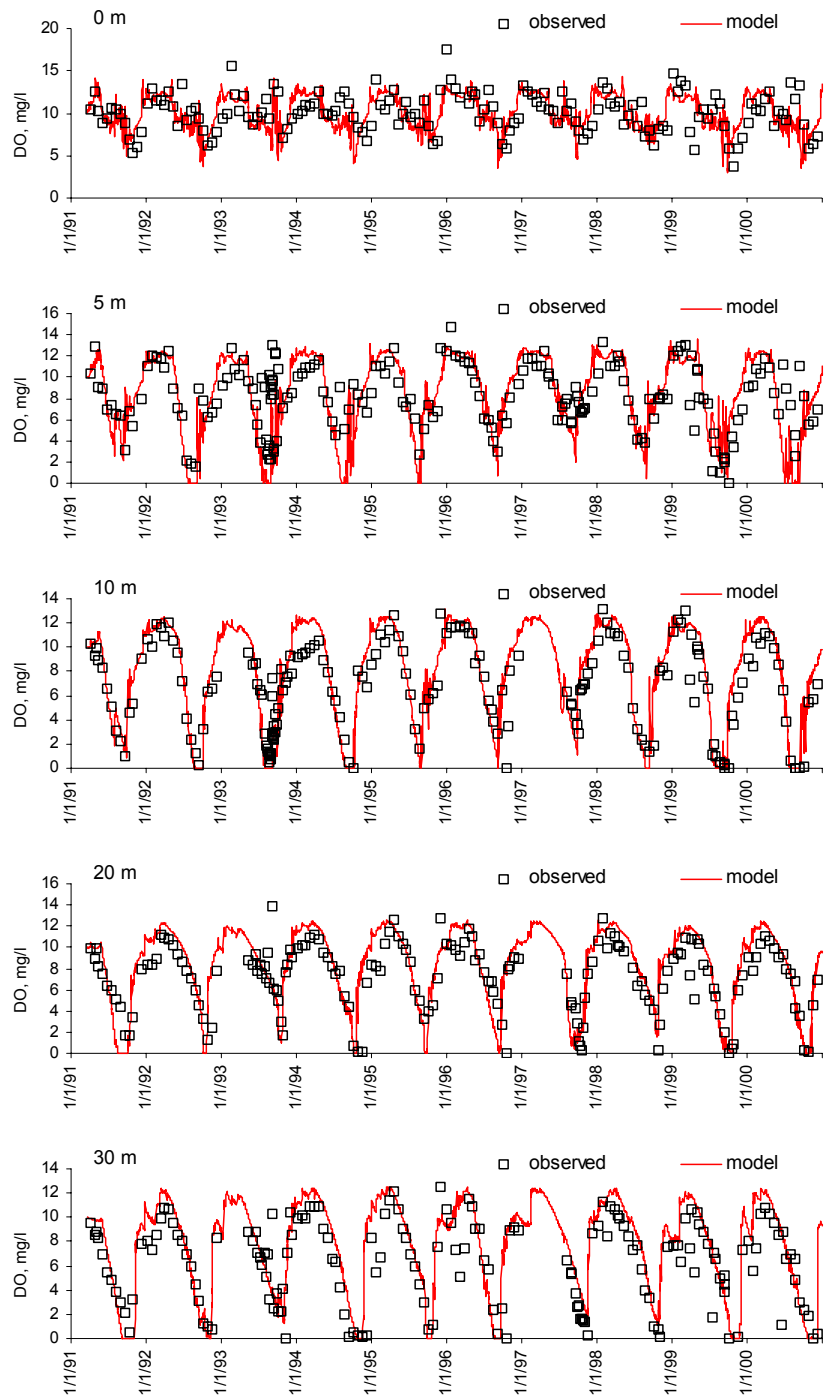
*Figure 9.4. Comparison of CE-QUAL-W2-simulated and observed temperature
in different depths of the water column of Římov Reservoir during
the period 1991-2000*

*Fig. 9.5. Comparison of CE-QUAL-W2-simulated and observed concentrations of dissolved oxygen in different depths of the water column of Římov Reservoir during the period 1991-2000*
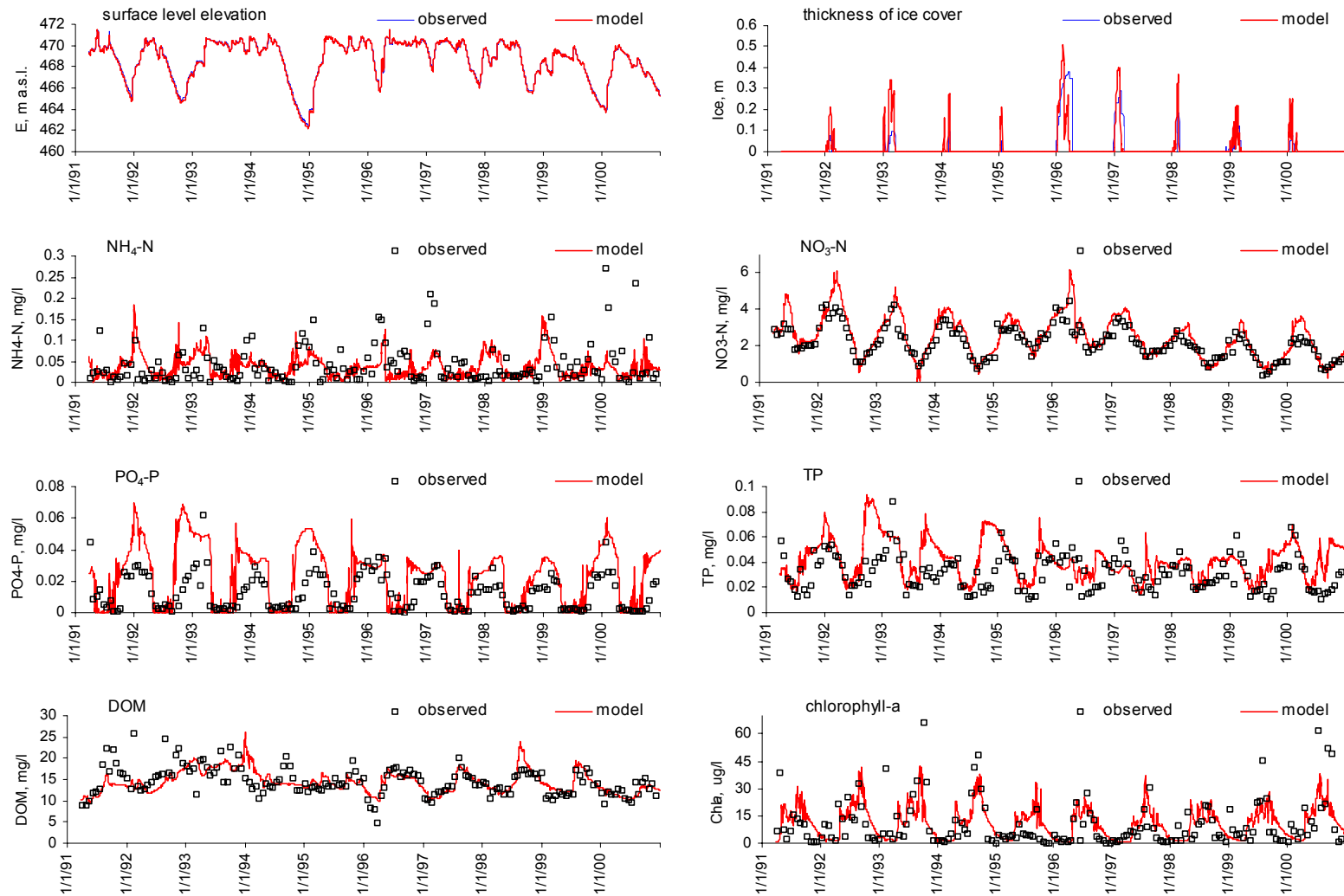
*Figure 9.6. Comparison of CE-QUAL-W2-simulated and observed surface elevation, ice cover thickness, and water quality constituents in the surface layer at the dam of Římov Reservoir for the period 1991-2000*

Table 9.6. Empirical regression models included within the auxiliary model compartments of the HSPF–CE-QUAL-W2 modelling system used for simulation of inflow water quality of Římov Reservoir. N (number of observed data), MAE (mean absolute error), and NS (Nash-Sutcliffe coefficient of model efficiency) refer to the calibration period 1999–2005.

| No. | Equation | Time step | N | MAE | NS |
|---|---|---|---|---|---|
| PHOSP: | | | | | |
| 1 | $PO_4\text{-}P = (DP_{diff} + DP_{point})\,Ret_{DP} - DP_{org}$ | week | 84 | 0.009 | 0.68 |
| 2 | $DP_{diff} = 0.017 + 0.00205 q_s^{0.837AgrL}$ | day | 110 | 0.017 | 0.52 |
| 3 | $DP_{point} = 0.9TP_{point}$ | month | - | - | - |
| 4 | $Ret_{DP} = 1 - 0.325 q_s^{0.326}$ | week | 82 | 0.15 | 0.47 |
| 5 | $DP_{org} = 0.002 + 0.0013DOC$ | any | 572 | 0.003 | 0.41 |
| 6 | $PP = (PP_{diff} + PP_{point})\,Ret_{PP}$ | week | 84 | 0.017 | 0.95 |
| 7 | $PP_{diff} = 0.010 + 0.002AgrL + 2.35\times10^{-6}q_s^{2.163}$ | day | 110 | 0.048 | 0.45 |
| 8 | $PP_{point} = 0.1TP_{point}$ | month | - | - | - |
| 9 | $Ret_{PP} = 1 - 0.263 q_s^{0.433}$ | week | 82 | 0.29 | 0.31 |
| DOM: | | | | | |
| 10 | $DOC = 3.63 + 0.0667\,T_a + 0.198P$ | week | 364 | 0.6 | 0.41 |
| 11 | $DOM = DOC/0.4$ | any | - | 0.07 | - |
| STEMP: | | | | | |
| 12 | $T_{in,i=n}^{Por} = 3.1 - 4.06\cos\left((JD_{i=n} - 17.1)\dfrac{360}{365.25}\right) + 0.55\dfrac{T_{a,i=n} + T_{a,i=n-1}}{2}$ | day | 1722 | 0.85 | 0.97 |
| 13 | $T_{in,i=n}^{BP1} = 4.4 - 4.23\cos\left((JD_{i=n} - 21.7)\dfrac{360}{365.25}\right) + 0.31\dfrac{T_{a,i=n} + T_{a,i=n-1}}{2}$ | day | 793 | 0.61 | 0.97 |

Variables:

$PO_4\text{-}P$ – concentration of orthophosphate in the total catchment runoff [mg/l]

$DP_{diff}$ – concentration of dissolved phosphorus from diffuse sources in the total catchment runoff [mg/l]

$DP_{point}$ – concentration of dissolved phosphorus from point sources in the total catchment runoff [mg/l]

$Ret_{DP}$ – coefficient of retention for dissolved phosphorus in stream network [-]

$DP_{org}$ – concentration of dissolved non-orthophosphate (i.e., organic) P in the total catchment runoff [mg/l]

$q_s$ – specific runoff from catchment [l/s/km$^2$]

$AgrL$ – fraction of the area of agriculture land in the whole catchment area [-]

$TP_{point}$ – concentration of total phosphorus from point sources in total catchment runoff [mg/l]

$DOC$ – concentration of dissolved organic carbon in catchment runoff [mg/l]

$PP$ – concentration of particulate phosphorus in total catchment runoff [mg/l]

$PP_{diff}$ – concentration of particulate phosphorus from diffuse sources in total catchment runoff [mg/l]

$PP_{point}$ – concentration of particulate phosphorus from diffuse sources in total catchment runoff [mg/l]

$Ret_{PP}$ – coefficient of retention for particulate phosphorus in stream network [rel.]

$DOM$ – dissolved organic matter [mg/l]

$T_a$ – air temperature [°C]

$P$ – mean precipitation [mm/d]

$T_{in}$ – water temperature of reservoir inflows (Por – profile Malše-Pořešín, BP1 – tributary PB1)

$JD$ – Julian day

The RESMNG unit was a simple water balance model for simulations of the outflow and withdrawal operation at the reservoir dam according to the current operation manual for any inflow data series. The water balance was calculated with daily time step according to the equation (9.4):

$$V_n = V_{n-1} + Q_{i,n} - Q_{o,n} - Q_{wd,n} \tag{9.4}$$

where: $V_n$ is volume of reservoir on day $n$ [m$^3$], $V_{n-1}$ is volume of reservoir on day $n$-1 [m$^3$], and $Q_{i,n}$, $Q_{o,n}$, and $Q_{wd,n}$ are inflow, total outflow, and withdrawal [m$^3$/d], respectively, on day $n$, The operation rules for the discharged and withdrawn amounts of water and the depths of outflow for different water surface levels were formalised and the system is shown in Table 9.7. This model with the input values of $Q_o$=0.65 m$^3$/s, $Q_{hp}$=1.8 m$^3$/s and $Q_{wd}$=1.2 m$^3$/s automatically generated very similar pattern of water level fluctuation during the modelled period 1991–2000 in comparison with reality (Fig. 9.7).

*Table 9.7. Operation rules for the determination of discharged amount of water and the used outlet and withdrawal structures in the RESMNG model. Symbols: $Q_i$, amount of inflow on the preceding day; $Q_o$, minimum discharge in the river (0.65 m$^3$/s); $Q_{hp}$, discharge used by the hydropower station (1.8 m$^3$/s); $Q_{wd}$, withdrawal of raw water for the treatment plant (1.2 m$^3$/s)*

| Water surface elevation, m a.s.l. | Outflow outlet, m a.s.l. | | | | | Withdrawal outlet, m a.s.l. | | | |
|---|---|---|---|---|---|---|---|---|---|
| | 466.1 | 460.0 | 450.0 | 441.5 | 430.5 | 457.0 | 450.5 | 444.5 | 438.5 |
| >470.65 | $Q_i$ | 0 | 0 | 0 | 0 | $Q_{wd}$ | 0 | 0 | 0 |
| 468.1–470.65 | $Q_o$+$Q_{hp}$ | 0 | 0 | 0 | 0 | $Q_{wd}$ | 0 | 0 | 0 |
| 467.1–468.1 | $Q_o$ | 0 | 0 | 0 | 0 | 0 | $Q_{wd}$ | 0 | 0 |
| 466.1–467.1 | 0 | $Q_o$ | 0 | 0 | 0 | 0 | $Q_{wd}$ | 0 | 0 |
| 461.0–466.1 | 0 | $Q_o$ | 0 | 0 | 0 | 0 | 0 | $Q_{wd}$ | 0 |

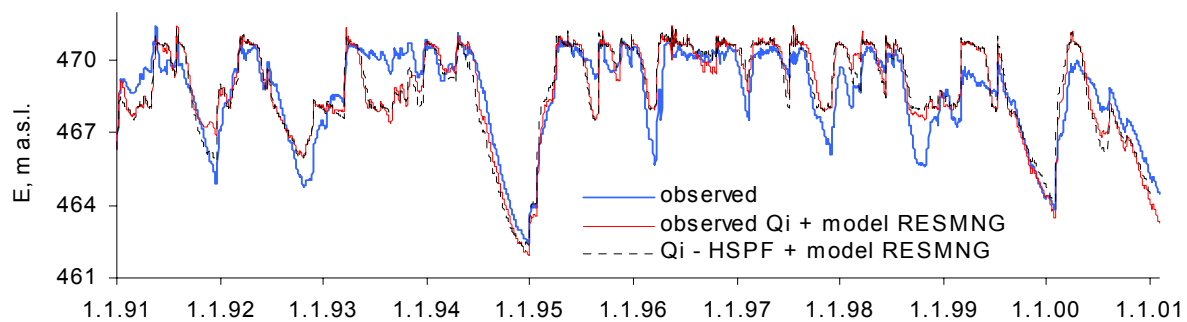| | | | | | | | | |
|---|---|---|---|---|---|---|---|---|
| 457.0–461.0 | 0 | $Q_o$ | 0 | 0 | 0 | 0 | 0 | $Q_{wd}$ | 0 |
| 451.0–457.0 | 0 | 0 | $Q_o$ | 0 | 0 | 0 | 0 | 0 | $Q_{wd}$ |
| 442.1–451.0 | 0 | 0 | 0 | $Q_o$ | 0 | 0 | 0 | 0 | $Q_{wd}$ |
| 441.5–442.1 | 0 | 0 | 0 | 0 | $Q_o$ | 0 | 0 | 0 | $Q_{wd}$ |
| <441.5 | 0 | 0 | 0 | 0 | 0 | 0 | 0 | 0 | 0 |



*Figure 9.7. Comparison of observed and RESMNG simulated water level in Řimov Reservoir*

93

# 10. Sensitivity and uncertainty analysis

Simple sensitivity trials of altering one possible factor a time offer a first step in exploring the importance of various climatic input data for the modelled hydrologic and water quality variables. We conducted this test with the calibrated HSPF/CE-QUAL-W2 modelling system in several steps: (i) with the HSPF model alone, (ii) with the CE-QUAL-W2 model alone, and (iii) with the whole modelling system. The test was done for all meteorological input variables within the validation period 1991-2000. The meteorological input data series were changed one by one by a factor that was derived from the minimum-to-maximum range of mean annual values for each variable (Table 10.1). The data series of temperature were changed using an additive coefficient; the other series (relative humidity, wind speed, cloudiness, precipitation) were changed multiplicatively. The values in Table 10.1 indicate that the most fluctuating input variable was precipitation that changed in the range from –15 % to 19 % and the least fluctuating one was relative humidity that changed in the range from –3 % to +4 %. On the other hand, the mean annual inflow values in Římov Reservoir 1991-2000 fluctuated in the range from –38 % to +76 %. This indicated an important synergistic effect of the meteorological input variables in their impact on the runoff from catchment.

*Table 10.1. Means and ranges of annual mean values of major input variables of the modelling system HSPF–CE-QUAL-W2 at the Římov Reservoir catchment during the period 1991-2000 and ranges of additive or multiplicative coefficients that were used in the sensitivity analysis. Abbrev.: $T_a$, air temperature; RH, relative humidity; WS, wind speed; CL, cloudiness; P, precipitation; $Q_i$, total inflow into Římov Reservoir.*

| Parameter | $T_a$, °C | RH, % | WS, m/s | CL (1/10) | P, mm/yr | $Q_i$, m³/s |
|---|---|---|---|---|---|---|
| average (min-max) | 8.5 (7.1–10) | 76 (73–82) | 2.0 (1.4–2.3) | 6.6 (6.1–7.2) | 585 (440–742) | 4.1 (2.3–7.0) |
| additive coeff. | -1.75–1.17 | - | - | - | - | - |
| multiplicative coeff. | - | 0.97–1.04 | 0.90–1.12 | 0.94–1.07 | 0.85–1.19 | 0.62–1.76 |

## 10.1 HSPF

The sensitivity of the runoff simulated by the HSPF model on the change of meteorological input variables was tested within 11 model runs that are summarised in Table 10.2. The most pronounced impact on the runoff showed the precipitation change followed by temperature.

*Table 10.2. Changes of runoff simulated with the HSPH model in response to the change of input $T_a$, RH, WS, CL, and P from their observed data series 1991-2000 (Sc.0) by using the values of additive ($T_a$) or multiplicative (all other variables) coefficients from Table 10.1.*

| Variable | Sc.0 | +δTa | -δTa | +δRH | -δRH | +δWS | -δWS | +δCL | -δCL | +δP | -δP |
|---|---|---|---|---|---|---|---|---|---|---|---|
| Mean inflow, m³/s | 4.0 | -36% | 24% | 20% | -6% | -12% | 7% | 2% | 0% | 103% | -34% |

*10.2 CE-QUAL-W2*

The sensitivity of the CE-QUAL-W2 model on the change of meteorological input variables was tested within 11 model runs that are summarised in Table 10.3. In all these runs the inflow discharge values corresponded to the measured data, hence the water residence time and the change in storage volume was identical. The inflow phosphorus concentrations were calculated with a constant value for P discharges from point sources (3500 kg/year). The largest impacts on hydrodynamics and water quality exerted the change in air temperature that significantly influenced water temperature in the surface layer of reservoir, duration of ice cover, length of stratification and mixing periods, duration of anoxia in the metalimnion (i.e., 10-m depth) and hypolimnion (i.e., bottom and 20-m depth), and to a smaller extent also water quality.

*Table 10.2. Changes of selected CE-QUAL-W2 output variables in response to the change of the input $T_a$, RH, WS, CL, and P values from their observed data series 1991-2000 (Sc.0) by using the values of additive ($T_a$) or multiplicative (all other variables) coefficients from Table 10.1.*

| Variable | Sc.0 | +δT$_a$ | -δT$_a$ | +δRH | -δRH | +δWS | -δWS | +δCL | -δCL | +δP | -δP |
|---|---|---|---|---|---|---|---|---|---|---|---|
| T$_{in}$, °C | 8.4 | 0.5 | -0.8 | 0.0 | 0.0 | 0.0 | 0.0 | 0.0 | 0.0 | 0.0 | 0.0 |
| T$_{0m}$, °C | 10.5 | 0.8 | -1.1 | 0.1 | -0.1 | 0.0 | 0.0 | -0.1 | 0.2 | 0.0 | 0.0 |
| T$_{5m}$, °C | 9.0 | 0.7 | -1.0 | 0.1 | -0.1 | 0.1 | 0.0 | -0.1 | 0.2 | 0.0 | 0.0 |
| T$_{10m}$, °C | 7.2 | 0.6 | -0.8 | 0.0 | 0.0 | 0.2 | -0.1 | -0.1 | 0.1 | 0.0 | 0.0 |
| T$_{20m}$, °C | 4.8 | 0.3 | -0.4 | 0.0 | 0.0 | 0.1 | -0.1 | 0.0 | 0.1 | 0.0 | 0.0 |
| T$_{30m}$, °C | 4.0 | 0.1 | -0.2 | 0.0 | 0.0 | 0.0 | 0.0 | 0.0 | 0.0 | 0.0 | 0.0 |
| T$_{bottom}$, °C | 4.0 | 0.0 | -0.1 | 0.0 | 0.0 | 0.0 | 0.0 | 0.0 | 0.0 | 0.0 | 0.0 |
| Ice cover duration, d/yr | 45 | -14% | 39% | 0% | 0% | -1% | 4% | 0% | -1% | 0% | 0% |
| Summer stratification period, d/yr | 223 | 5% | -6% | 0% | 0% | -1% | 1% | 0% | 1% | 0% | 0% |
| Winter stratification period, d/yr | 60 | -18% | 33% | -2% | 2% | -21% | 14% | 1% | -4% | 0% | 0% |
| Mixing periods, d/yr | 82 | -1% | -7% | 0% | -1% | 18% | -13% | 0% | -1% | 0% | 0% |
| Duration of anoxia at 10 m, d/yr | 13 | 40% | -44% | 4% | -5% | -20% | 5% | -6% | 6% | 0% | 0% |
| Duration of anoxia at 20 m, d/yr | 3 | 144% | -91% | 3% | -18% | 38% | 44% | -12% | 12% | 0% | 0% |
| Duration of anoxia at bottom, d/yr | 17 | 71% | -70% | 28% | -8% | 86% | 64% | -8% | 136% | 0% | 0% |
| Inflow mean PO$_4$-P, µg/l | 26 | 7% | -5% | 0% | 0% | 0% | 0% | 0% | 0% | 0% | 0% |
| Inflow max. PO$_4$-P, µg/l | 39 | 3% | -4% | 0% | 0% | 0% | 0% | 0% | 0% | 0% | 0% |
| Inflow mean TP, µg/l | 46 | 4% | -3% | 0% | 0% | 0% | 0% | 0% | 0% | 0% | 0% |
| Inflow max. TP, µg/l | 340 | 0% | 0% | 0% | 0% | 0% | 0% | 0% | 0% | 0% | 0% |
| Inflow mean DOC, mg/l | 4.6 | 2% | -3% | 0% | 0% | 0% | 0% | 0% | 0% | 1% | -1% |
| Inflow max. DOC, mg/l | 7.0 | 1% | -2% | 0% | 0% | 0% | 0% | 0% | 0% | 6% | -5% |
| Reservoir mean PO$_4$-P, µg/l | 12 | -1% | 4% | 0% | 0% | 1% | 0% | 1% | -2% | 0% | 0% |
| Reservoir max. PO$_4$-P, µg/l | 28 | -4% | -4% | 0% | 0% | -4% | 0% | 0% | 0% | 0% | 0% |
| Reservoir mean TP, µg/l | 25 | 0% | 1% | 0% | 0% | 1% | -1% | 0% | 0% | 0% | 0% |
| Reservoir max. TP, µg/l | 34 | 0% | 4% | 0% | 1% | 1% | -1% | 1% | -1% | 0% | 0% |
| Reservoir mean DOC, mg/l | 4.6 | 2% | -2% | 0% | 0% | 0% | 0% | 0% | 0% | 0% | 0% |
| Reservoir max. DOC, mg/l | 5.7 | 2% | -2% | 0% | 0% | 0% | 0% | 0% | 0% | 0% | 0% |
| Reservoir mean Chl*a*, µg/l | 7 | 1% | -2% | 0% | 0% | 2% | -2% | 0% | 1% | 0% | 0% |
| Reservoir max. Chl*a*, µg/l | 23 | 2% | 1% | 0% | 0% | -1% | 1% | 0% | 1% | 0% | 0% |

*10.3 HSPF/CE-QUAL-W2*

The response of the whole HSPF/CE-QUAL-W2 modelling system on the changes of input meteorological variables is summarised in Table 10.3. In comparison with the sensitivity of the sole CE-QUAL-W2 model, the impacts on temperature, anoxic conditions in the reservoir metalimnion and hypolimnion, and water quality were amplified. In addition to the dominant effect of temperature change, also changes in wind speed and precipitation showed important impacts on oxic conditions and maximum concentrations of phosphorus and chlorophyll-*a*.

*Table 10.3. Changes of selected HSPH and CE-QUAL-W2 output variables in response to the change of input $T_a$, RH, WS, CL, and P from their observed data series 1991–2000 (Sc.0) by using the values of additive ($T_a$) or multiplicative (all other variables) coefficients from Table 10.1.*

| Variable | Sc.0 | +δTa | -δTa | +δRH | -δRH | +δWS | -δWS | +δCL | -δCL | +δP | -δP |
|---|---|---|---|---|---|---|---|---|---|---|---|
| Mean inflow, $m^3$/s | 4.0 | -36% | 24% | 20% | -6% | -12% | 7% | 2% | 0% | 103% | -34% |
| Mean total volume, mil.$m^3$ | 28.8 | -26% | 7% | 16% | -3% | -7% | 2% | 1% | 0% | 17% | -20% |
| TRT, d | 83.8 | 17% | -14% | -3% | 3% | 7% | -5% | -1% | 0% | -42% | 21% |
| $T_{0m}$, °C | 10.5 | 0.7 | -1.1 | 0.2 | -0.1 | 0.0 | 0.0 | -0.1 | 0.0 | -0.1 | 0.0 |
| $T_{5m}$, °C | 9.1 | 0.6 | -0.7 | 0.5 | -0.1 | 0.0 | 0.0 | -0.1 | 0.0 | 0.3 | -0.1 |
| $T_{10m}$, °C | 7.1 | 0.6 | -0.3 | 0.6 | -0.1 | 0.0 | 0.0 | 0.0 | 0.0 | 1.0 | -0.2 |
| $T_{20m}$, °C | 4.7 | 0.2 | -0.3 | 0.2 | 0.0 | 0.1 | 0.0 | 0.0 | 0.0 | 0.2 | -0.1 |
| $T_{30m}$, °C | 4.0 | -0.6 | -0.1 | 0.0 | 0.0 | -0.1 | 0.1 | 0.0 | 0.0 | 0.3 | -0.5 |
| $T_{bottom}$, °C | 4.0 | 0.0 | -0.1 | 0.0 | 0.0 | 0.0 | 0.0 | 0.0 | 0.0 | 0.2 | -0.1 |
| Ice cover duration, d/yr | 45 | -7% | 37% | 2% | 3% | 2% | 3% | 0% | 0% | 3% | 2% |
| Summer stratification period, d/yr | 222 | 2% | -6% | 1% | 0% | -2% | 1% | 0% | 0% | 1% | -1% |
| Winter stratification period, d/yr | 61 | -21% | 27% | -4% | 1% | -15% | 13% | 1% | 0% | 13% | -9% |
| Mixing periods, d/yr | 81 | 11% | -5% | 0% | 0% | 17% | -13% | 1% | 0% | -13% | 10% |
| Duration of anoxia at 10 m, d/yr | 13 | 123% | -38% | -13% | 13% | 16% | 4% | -3% | 0% | -34% | 76% |
| Duration of anoxia at 20 m, d/yr | 3 | 845% | -67% | 164% | 73% | 103% | 18% | -9% | 0% | 252% | 185% |
| Duration of anoxia at bottom, d/yr | 19 | 215% | -39% | -17% | 21% | 104% | 60% | -3% | 0% | 205% | 84% |
| Reservoir mean $PO_4$-P, µg/l | 12 | 1% | 4% | -2% | 0% | 0% | 0% | 0% | 0% | 5% | 1% |
| Reservoir max. $PO_4$-P, µg/l | 26 | 27% | 0% | -4% | 0% | 0% | 0% | 0% | 0% | 42% | 15% |
| Reservoir mean TP, µg/l | 24 | 0% | 2% | -1% | 0% | 1% | -1% | 0% | 0% | 4% | 0% |
| Reservoir max. TP, µg/l | 34 | 16% | 15% | 4% | 0% | 0% | 1% | 1% | 0% | 40% | 5% |
| Reservoir mean DOC, µg/l | 4.6 | 0% | -2% | 0% | 0% | 0% | 0% | 0% | 0% | 1% | -2% |
| Reservoir max. DOC, µg/l | 5.7 | -2% | 0% | 2% | 0% | -1% | 1% | 0% | 0% | 13% | -5% |
| Reservoir mean Chl*a*, µg/l | 7 | -1% | -1% | -1% | 1% | 2% | -2% | 0% | 0% | 2% | 1% |
| Reservoir max. Chl*a*, µg/l | 24 | -12% | 8% | 6% | 0% | 2% | -1% | -1% | 0% | 14% | -15% |

## 11. Summary

The testing of the atmosphere-river network-reservoir modelling system for the simulations of hydrology and water quality was done at the catchment of Římov Reservoir (Vltava River basin, Czech) with the modelling setup that consisted of the HSPF catchment precipitation-runoff model and the CE-QUAL-W2 reservoir hydrodynamics and water quality model. The aim of the testing was to evaluate reliability of modelling system by a sensitivity and uncertainty analysis.

The sensitivity analysis was designed to reveal the effects of changes in the main climatic input variables on the runoff from the catchment and selected water quality variables in the reservoir. The aim of the sensitivity analysis was to reveal the extent of effects that the input variable fluctuations exert on the runoff from the catchment, reservoir hydrodynamics, and reservoir water quality. The input variables were changed one by one from the original state by a increment to cover the range of minimum and maximum mean annual values of the given variable and the response of selected model output variables were recorded and evaluated for annual and monthly mean values. The HSPF model showed the highest sensitivity of the modelled runoff towards the changes in precipitation, temperature, and relative humidity. The CE-QUAL-W2 model was most sensible on the change of climatic conditions for the variables representing the seasonal pattern of stratification in the reservoir, i.e. duration of ice cover and length of summer stratification conditions. Reservoir water quality variables like P and chlorophyll-a concentrations were less significantly affected by the used changes of input meteorological variables but largely were influenced by the change of river flow.

The uncertainty analysis of the modelling system was used to describe main uncertainty sources that included uncertainty of model parameterisation and uncertainty due to measurement errors of input meteorological and hydrological data. The study was done for the whole modelling HSPF–CE-QUAL-W2 system and showed approximately equal shares of uncertainties from both sources of errors.

## 12. References

Bicknell B.R., Imhoff J.C., Kittle J.L., Jr., Jobes T.H., Donigian A.S., Jr. (2001): Hydrological Simulation Program–Fortran (HSPF). User's Manual for Release 12. U.S. EPA National Exposure Research Laboratory, Athens, GA, in cooperation with U.S. Geological Survey, Water Resources Division, Reston, VA.

Cole T. M., Wells S. C. (2006): CE-QUAL-W2: A Two-Dimensional, Laterally Averaged, Hydrodynamic and Water Quality Model, Version 3.5. User Manual. Instruction Report EL-06-1. US Army Engineering and Research Development Center, Vicksburg, MS.

Hejzlar J., Dubrovský M., Buchtele J., Růžička M. (2003): The effect of climate change on the concentration of dissolved organic matter in a temperate stream (the Malše River, South Bohemia). Science of Total Environment 310, 143–152.

Nash J. E., Suttcliffe J. V. (1970): River forecasting thought conceptual models: Part I, A discussion of principles. Journal of Hydrology 10, 282–290, 1970.

Straškraba M., Gnauck A. H. (1985): Freshwater Ecosystems: Modelling and Simulation. Elsevier, Amsterdam, the Netherlands.

Thurman E. M. (1985): Organic Geochemistry of Natural Waters. Nijhoff Publishers, Dordrecht, the Netherlands.